

Review

# Water Cleaning Adsorptive Membranes for Efficient Removal of Heavy Metals and Metalloids

Maria Giovanna Buonomenna <sup>1,\*</sup>, Seyyed Mojtaba Mousavi <sup>2</sup>, Seyyed Alireza Hashemi <sup>3</sup>  
and Chin Wei Lai <sup>4</sup>

- <sup>1</sup> Ordine dei Chimici e dei Fisici della Campania (OCF) and MIUR, 80134 Naples, Italy  
<sup>2</sup> Department of Chemical Engineering, National Taiwan University of Science and Technology, Taipei City 10607, Taiwan  
<sup>3</sup> Nanomaterials and Polymer Nanocomposites Laboratory, School of Engineering, University of British Columbia, Kelowna, BC V1V 1V7, Canada  
<sup>4</sup> Nanotechnology & Catalysis Research Center (NANOCAT), Institute for Advanced Studies, University of Malaya, Kuala Lumpur 50603, Malaysia  
\* Correspondence: mg.buonomenna@chimici.it

**Abstract:** Heavy metal pollution represents an urgent worldwide problem due to the increasing number of its sources; it derives both from industrial, e.g., mining, metallurgical, incineration, etc., and agricultural sources, e.g., pesticide and fertilizer use. Features of membrane technology are the absence of phase change or chemical additives, modularity and easy scale-up, simplicity in concept and operation, energy efficiency, and small process footprint. Therefore, if membrane technology is coupled to adsorption technology, one of the most effective treatment strategies to remove heavy metals, namely, Adsorptive Membrane Technology, many typical disadvantages of traditional processes to remove heavy metals, such as low-quality treated water, excessive toxic sludge production, which requires further treatment, can be overcome. In this review, after a broad introduction on the relevance of heavy metal removal and the methods used, a thorough analysis of adsorptive membrane technology is given in terms of strategies to immobilize the adsorbents onto/into membranes and materials used. Regarding this latter aspect, the impressive number of papers present in the literature on the topic has been categorized into five types of adsorptive membranes, i.e., bio-based, bio-inspired, inorganic, functionalized, and MMMs.

**Keywords:** heavy metals; metalloids; water cleaning; adsorptive membranes; multifunctional membrane separation processes; process intensification



**Citation:** Buonomenna, M.G.; Mousavi, S.M.; Hashemi, S.A.; Lai, C.W. Water Cleaning Adsorptive Membranes for Efficient Removal of Heavy Metals and Metalloids. *Water* **2022**, *14*, 2718. <https://doi.org/10.3390/w14172718>

Received: 9 August 2022

Accepted: 26 August 2022

Published: 31 August 2022

**Publisher's Note:** MDPI stays neutral with regard to jurisdictional claims in published maps and institutional affiliations.



**Copyright:** © 2022 by the authors. Licensee MDPI, Basel, Switzerland. This article is an open access article distributed under the terms and conditions of the Creative Commons Attribution (CC BY) license (<https://creativecommons.org/licenses/by/4.0/>).

## 1. Introduction: A Broader Context

### 1.1. The Problem of Heavy Metals and Metalloids

With the rapid development of industrial fields related to metallurgy, electroplating, machinery manufacturing, and electronics, a large amount of wastewater containing heavy metals is discharged into bodies of water [1]. In particular, heavy metals, along with almost all pollutants, find their way finally to the sea as the ultimate sink. Moreover, not only sea water but also other sources of drinking water, e.g., surface water and groundwater, are likely to be polluted by heavy metals [2,3]. Although metals are removed during the desalination of seawater, desalinated drinking water still might contain various metals and metalloids (i.e., the elements such as boron, arsenic, antimony, and tellurium, located along a diagonal line separating metals from non-metals on the periodic table) possibly due to treatment and stabilization, blending with treated groundwater, and leaching of metal components from pipes of the water distribution system (WDS) [4]. Unlike other toxic substances, heavy metal ions cannot be biodegraded in nature and accumulate in living organisms. Some of them can cause serious damage to the central nervous system (lead, mercury), kidney (copper, lead, and mercury), skin (arsenic, chromium), and liver

or lung (nickel, mercury, lead, and copper) [5,6]. Boron, a metalloid or semimetal, is an essential element for plants and animals as well as human beings [7,8]. As a major solution for water scarcity in this century, seawater desalination has attracted increasing attention in recent years [9,10]. The concentration of boron in seawater is usually between 4 and 6 mg L<sup>-1</sup> [11,12], but much higher values (>100 mg L<sup>-1</sup>) can be found in some groundwater and wastewater sources [13]. The World Health Organization has imposed a boron concentration limit of 2.4 mg L<sup>-1</sup> [14] for drinking water, but many countries have implemented stricter limits (<1 mg L<sup>-1</sup>) [15]. The boron concentration limit for irrigation water can be much lower than that for drinking water (<0.5 ppm), which poses a significant technological challenge [15–17]. The environmental regulations on heavy metals are increasingly stringent as the guideline values of acceptability demonstrate (Table 1), whereas the global needs for most heavy metals continue to increase due to the rapid development of modern industrial activities [18,19].

**Table 1.** Heavy metals and metalloids in drinking water.

Element to Be Removed	Element Type	Source	Limit of Acceptability (mg/L)	Effect on Public Health [18,19]	Refs.
Arsenic	Metalloid	In groundwater, where there are sulfide mineral deposits and sedimentary deposits deriving from volcanic rocks, the concentrations can be significantly elevated.	10	Long-term exposure to arsenic in drinking water is causally related to increased risks of cancer in the skin, lungs, bladder, and kidney, as well as other skin changes, such as hyperkeratosis and pigmentation changes.	[20]
Boron	Metalloid	Groundwaters, seawater, wastewaters	2400	Animals suffer from kidney failure and reproductive system and nervous system diseases while plants can wither and eventually die when exposed to excess amounts of boron.	[21,22]
Cadmium	(Heavy) metal	Cadmium is released to the environment in wastewater from steel and plastic industries, batteries, impurities in the zinc of galvanized pipes and solders and some metal fittings, etc. Diffuse pollution is caused by contamination from fertilizers and local air pollution. Food is the main source of daily exposure to cadmium.	3	The kidney is the main target organ for cadmium toxicity. Cadmium has a long biological half-life in humans of 10–35 years. There is evidence that cadmium is carcinogenic by the inhalation route. However, there is no evidence of carcinogenicity by the oral route and no clear evidence for the genotoxicity of cadmium.	[20]
Copper	(heavy) metal	Copper is used to make pipes, valves, and fittings and is present in alloys and coatings. The primary source most often is the corrosion of interior copper plumbing.	2	Gastrointestinal effects	[20]
Iron	(heavy) metal	Anaerobic groundwater may contain ferrous iron at concentrations up to several milligrams per liter. Iron may also be present in drinking water as a result of the use of iron coagulants or the corrosion of steel and cast iron pipes during water distribution.	No health-based guideline value is proposed	Iron is an essential element in human nutrition, particularly in the (II) oxidation state.	[20]
Lead	(heavy) metal	Lead is rarely present in tap water as a result of its dissolution from natural sources. Rather, its presence is primarily from corrosive water effects on household plumbing systems containing lead in pipes, solder, fittings, or the service connections to homes.	10	Exposure to lead is associated with a wide range of effects, including various neurodevelopmental effects, mortality, impaired renal function, hypertension, impaired fertility, and adverse pregnancy outcomes.	[20]
Manganese	(heavy) metal	Manganese is naturally occurring in many surface water and groundwater sources, particularly in anaerobic or low oxidation conditions, and this is the most important source of drinking water.	At levels exceeding 100 mg L <sup>-1</sup> , it causes an undesirable taste	Not of health concern at levels found in drinking water	[20]

Table 1. Cont.

Element to Be Removed	Element Type	Source	Limit of Acceptability (mg/L)	Effect on Public Health [18,19]	Refs.
Mercury	(heavy) metal	Electrolytic production of chlorine, in electrical appliances, in dental amalgams and as a raw material for various mercury compounds.	6	Hemorrhagic gastritis and colitis with the ultimate damage to the kidney.	[20]
Molybdenum	(heavy) metal	Molybdenum is found naturally in soil and is used in the manufacture of special steels and in the production of tungsten and pigments. Molybdenum compounds are used as lubricant additives and in agriculture to prevent molybdenum deficiency in crops.	Although Mo is an essential element in the human body, WHO standards recommend that it does not exceed 70 mg L <sup>-1</sup> in potable water	-	
Nickel	(heavy) metal	Where there is heavy pollution, areas in which nickel that occurs naturally in groundwater is mobilized or where there is use of certain types of kettles, of non-resistant material in wells, or of water that has come into contact with nickel or chromium-plated taps, the nickel contribution from water may be significant.	70	Possibly carcinogenic	[20]
Zinc	(heavy) metal	High concentrations in tap water can be observed as a result of dissolution of zinc from pipes.	Not of health concern at levels found in drinking-water	May affect acceptability of drinking-water	

### 1.2. General Removal Methods of Heavy Metals and Metalloids

Several methods exist to remove heavy metal ions and metalloids from wastewater, and all come with their advantages and disadvantages, as listed in Table 2. The efficiency of chemical precipitation (Table 2, entry 1) under idealized conditions can be as high as ~99% [23,24]. However, the technique can produce secondary pollution in the form of high quantities of sludge and toxic fumes. Furthermore, it is only suitable for treating water contaminated with high concentrations of heavy metals [5]. Adsorbents or ion-exchange resins (Table 2, entries 2 and 3, respectively) can also be used to remove heavy metal ions and other pollutants [25,26]. Adsorption is the most widely used method for heavy metal removal because of its low cost, simplicity, adaptability, and ecofriendly nature, but it has certain limitations such as a slow rate and a high internal diffusion resistance [27]. Moreover, the adsorption technology typically offers efficiencies that tend to decrease with prolonged use [28,29]. The advancement in nanotechnology has allowed the design of novel adsorbents based on nanomaterials.

Regarding ion-exchange, fully saturated ion-exchange resins must be converted by chemical reactions, which can also cause uncontrolled secondary pollution. Flotation (Table 2, entry 4) can be very efficient in treating specific heavy metal ions [30], but they are demanding in terms of resources and thus they are cost-effective only in large-scale processing and are not suitable for decontamination at smaller scales.

Membrane processes have in general several advantages (Table 2, entry 5) such as high separation efficiency, ease to scale up, being environmentally friendly, and energy saving compared to other processes with phase changes such as distillation. There are several membrane processes that can be used for metal removal, as discussed below.

**Table 2.** Overview of various processes for heavy metal and metalloid removal.

Entry #	Process	Description	Advantages	Disadvantages
1	Chemical precipitation	Chemicals (calcium hydroxide and sodium hydroxide in hydroxide precipitation, iron sulfide in sulfide precipitation) react with heavy metals ions to form insoluble precipitates, which can be separated from the water by sedimentation or filtration	Relatively simple and inexpensive	<ul style="list-style-type: none"> <li>• Large volumes of relatively low-density sludge with possible problems of dewatering and disposal.</li> <li>• amphoteric characteristics of metals hydroxides.</li> <li>• inhibition of metal hydroxide precipitation due to possible presence of complexing agents in the wastewater.</li> </ul> Moreover, in the case of sulfide precipitation, evolution of toxic H <sub>2</sub> S fumes in acidic conditions can occur and formation of colloidal precipitates can cause problems in either settling or filtration processes.
2	Adsorption	Heavy metal ions are directly separated from wastewater by adsorption on activated carbon, low-cost adsorbents, bio-adsorbents	Effective, economic, flexible in design and operation	Weak selectivity, waste product
3	Ion exchange	Solution containing heavy metals ions passes through a cation column allowing the exchange with the hydrogen ions on the resin	High treatment capacity, high removal efficiency	Careful control of variables such as pH, temperature, initial metal concentration, contact time, and ionic charge of the wastewater is mandatory
4	Ion flotation	Metal ions made hydrophobic by use of surfactants are removed by air bubbles	Ease of operation, low cost, and suitable for treating large volumes of dilute aqueous solutions	Careful control of variables such as pH, temperature, and initial metal concentration
5	Membrane processes	A membrane acts as a selective barrier in pressure-driven membrane operations and electrodialysis or only as barrier in liquid membranes operations allowing the separation of metal ions	High separation efficiency, easy to scale up, environmentally friendly, energy saving, no phase changing, and easy integration with other traditional processes	Careful selection of the membrane materials to address the challenges related to membrane lifetime, fouling, and selectivity reduction in the case of strong acidic, alkaline, and/or oxidizing feed solutions

### 1.3. A Glimpse at Membrane Processes for Heavy Metals and Metalloids Removal

The hardware of a membrane process, i.e., the membrane, is a selective barrier that can be classified on the basis of its pore size and retained substances, which do not pass through the pores (Figure 1).

As evidenced in Figure 1, metal ions (and metalloids) can be directly separated by two pressure-driven membrane processes, i.e., reverse osmosis (RO) and nanofiltration (NF) (Table 3, entries 1 and 2, respectively). Several successful studies have been reported that have used NF membranes as tools for heavy metal removal [32–34]. Even though the separation in NF occurs due to solution-diffusion as well as sieving mechanisms and the Donnan effect, dielectric exclusion and electromigration also make NF useful in the separation of both charged and uncharged organic solutes [35]. Converting produced water from a pollution source into a new water resource is achievable through the use of a combined NF as a pretreatment and RO system [36] or multistage RO rather than a single membrane (NF or RO alone) (Figure 2).

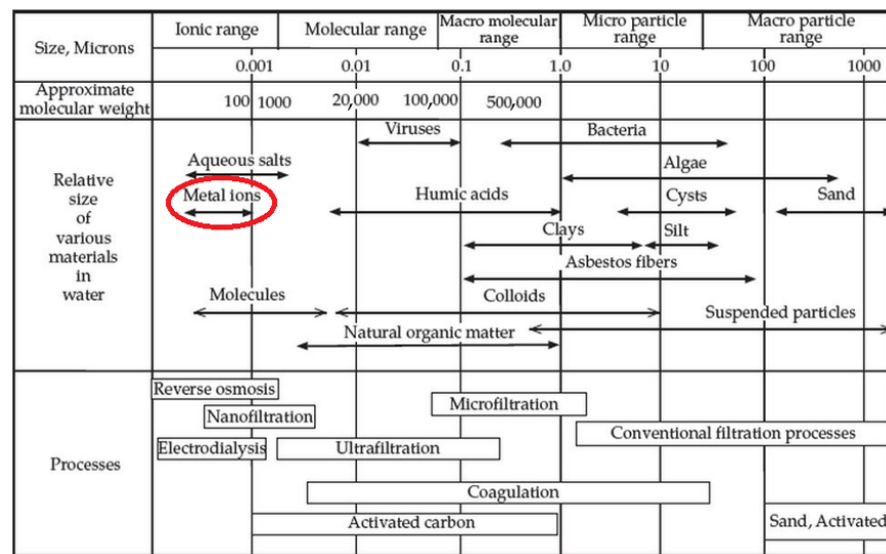


Figure 1. Membrane filtration spectrum. Adapted with permission from [31], copyright of Elsevier.

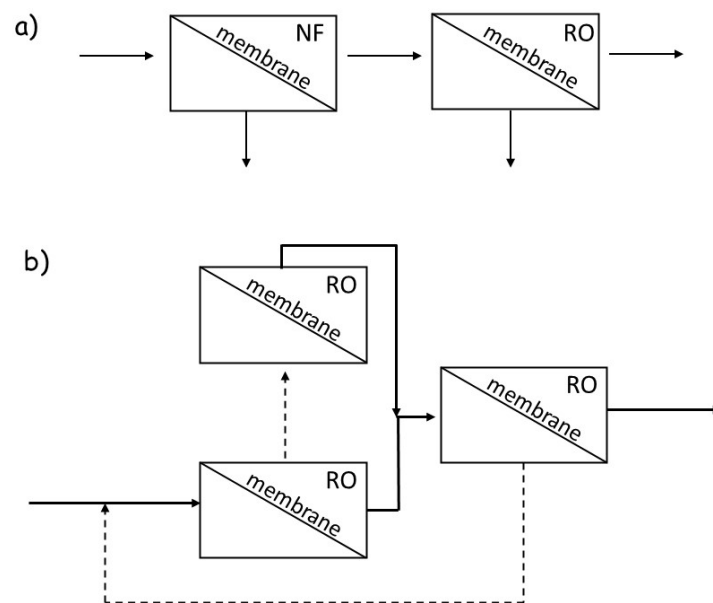


Figure 2. (a) NF as pretreatment for RO; (b) multistage RO scheme used in [37]. Adapted with permission from [37], copyright of Elsevier.

Indeed, a current challenge for RO and NF membranes is the removal of neutral and low molecular weight solutes as electrostatic repulsion and size exclusion mechanisms are weak for these solutes. For example, in natural waters, the removal of the toxic metalloid As(III), which has a pKa of 9.1 and Stokes radius of 0.24 nm [38], varies from 25% to 75% depending on operating conditions [39]. Therefore, pH adjustments and oxidation of As(III) to As(V), which is charged at a neutral pH and has a slightly larger Stokes radius (0.26 nm) [38], are the prevalent strategies to improve arsenic rejection [39]. Boron is another small, neutral solute (metalloid) of concern, as it is present in seawater at an average concentration of 5 mg L<sup>-1</sup> [40]. In water, boron is present as boric acid (Stokes radius of 0.16 nm and pKa of 9.2 in freshwater, 8.6 in saltwater) [41] and tends to diffuse rapidly through RO membranes via hydrogen bonding between the hydroxyl groups in boric acid and bound water in the membrane [42]. Conventional seawater and brackish water RO membranes exhibit varying levels of single-pass boron rejection, which depend on factors such as solution pH and membrane choice [43]. Consequently, desalination

plants often deploy multistage RO (Figure 2b) to reduce boron concentrations to desired levels: as mentioned above, maximum boron concentrations in the range of 0.5–1.0 mg L<sup>-1</sup> are common for irrigation of several sensitive crops. At the Ashkelon plant in Israel, the boron polishing system has been estimated to account for 10% of the overall energy cost [44]. Therefore, improving boron rejection will significantly benefit overall water purification membrane performance. In general, RO membranes are designed to separate all ions from water in a pressure-driven process that leads to highly efficient desalination, but nonselective ion isolation [45].

In forward osmosis (FO) (Table 3, entry 3) as in RO and NF, a dense membrane is used, but without applying any external pressure: the natural energy of osmotic pressure is used to transport water through the membrane while retaining all the dissolved solutes on the other side. In recent years, FO received interest from the scientific community for heavy metal ion removal [46,47] due to its low polluted tendency, reduced energy cost, and it being environmentally friendly. The membranes used are thin film composite (TFC) membranes, typical of RO and NF, but further exploration before the process is effective by these membranes is necessary.

Two other membrane operations that can be used directly for the removal of metals are electrodialysis (ED) (Table 3, entry 4) and membrane capacitive deionization (MCDI) (Table 3, entry 5).

ED, differently from RO and NF, is not pressure-driven, with its driving force an electrical potential difference. Conventional ED membranes, which are ion-exchange membranes, are highly selective for counterions over co-ions, but do not exhibit high counterion–counterion selectivity needed for target ion isolation [48,49]. So, they are capable of water desalination, but not selective transport behavior. A low-resistance membrane is essential to achieve a high removal efficiency at low energy consumption.

MCDI (Table 3, entry 5) has emerged in the past 15 years (Figure 3) as an alternative desalination technique and since then has received extensive research attention.

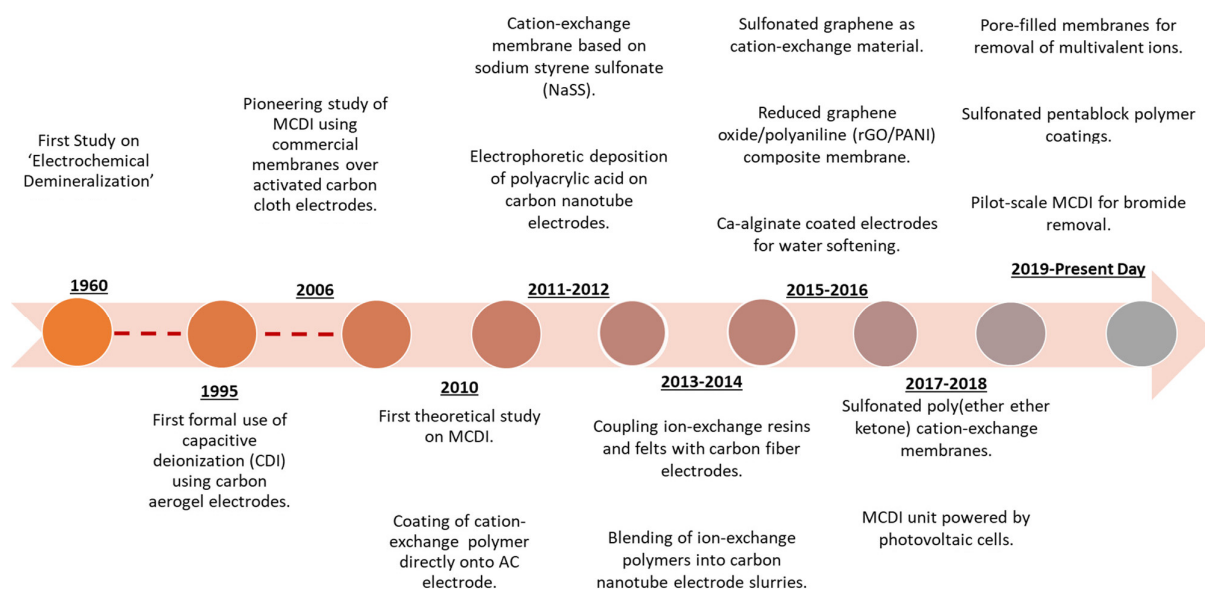


**Figure 3.** Timeline displaying selected key developments and advances of ion-exchange materials for MCDI. Reproduced from [50], used under CC-BY 4.0.

MCDI removes salts by application of a voltage between two electrodes covered with ion-exchange membranes (Figure 4), which maximizes the desalination performance in terms of salt removal and energy efficiency [50].

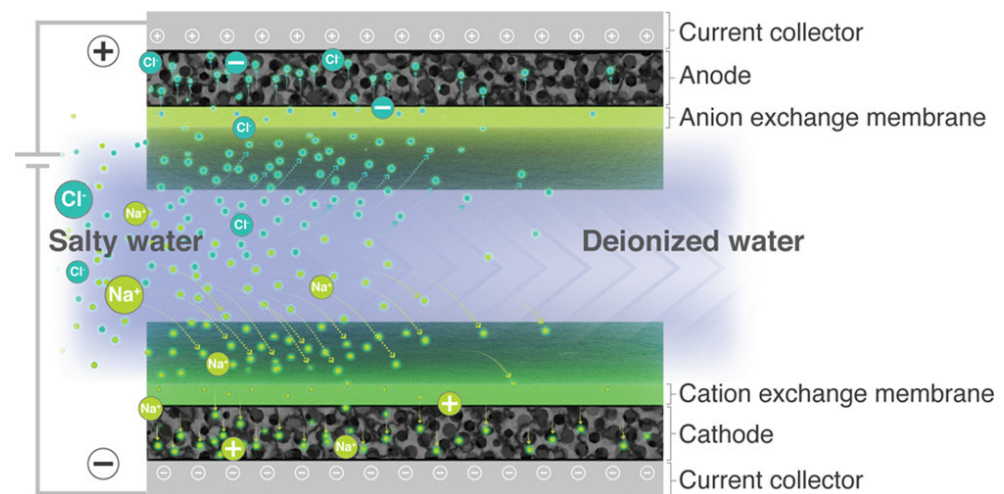


**Figure 4.** Schematic representation of the typical symmetric MCDI cell configuration: anode, positively polarized electrode; cathode, and negatively polarized electrode. Reproduced with permission from [50], used under CC-BY 4.0.

MCDI can be defined as an adsorption-based water desalination process wherein ions are collected capacitively in the electrical double layer of polarized electrodes. During adsorption in MCDI, co-ions are expelled from the micropores as counterions are adsorbed: the presence of a selective ion-exchange membrane prevents co-ions from exiting into the spacer channel.

However, this electrostatic adsorption mechanism leads to low adsorption selectivities between different ion types with a similar charge [51].

As shown in Figure 1, the pore size of microfiltration (MF) and ultrafiltration (UF) membranes are too large for metal ions and MF and UF can be used for their removal only integrated into the hybrid processes. In so-called polymer-enhanced ultrafiltration (PEUF) (Table 3, entry 6), water-soluble polymers (added in the feed stream) form macromolecular complex compounds with the metal ions to be removed, thereby exceeding the molecular weight-cut-off (MWCO) of the membrane.

In membrane bioreactors (MBR) (Table 3, entry 7) and osmotic membrane bioreactors (OMBRs) (Table 3, entry 8), a macroporous and dense membrane, respectively, acts like a barrier for the suspended and colloidal particles contributing to the effective removal of heavy metals attached to the sludge suspended solids [52]. MBR, which is the combination of the conventional activated sludge process followed by membrane separation, has proved to be an effective technology in treating industrial wastewater streams contaminated with insistent heavy metals [53]. Various mechanisms are at the basis of heavy metal ions removal in both physical, such as their entrapment within sludge floc, adsorption onto the flocs/vermiculates surface, diffusions into the flocs structure, and biosorption onto the cell walls of consortia, and chemical, such as metals precipitation by changing pH in the bio-tank [54,55]. OMBR is a combination of the FO process (mentioned above) and a bioreactor [55]. It is known for its low membrane fouling propensity and higher removal of nutrients and suspended solids with its increasing applications for direct and indirect portable reuse. One of the drawbacks of this technology is the accumulation of salts in the feed side of the membrane not only due to the reverse draw solute movement, i.e., “leakage” of salts from the draw solution toward the feed side, but also due to the accumulation of salts in the bioreactor originating from the feed that is totally rejected by the FO membrane salts accumulation and has negative impacts on the treatment performances and the bacterial consortia as well [55].

**Table 3.** Membrane processes for heavy metal ion removal.

Entry #	Membrane Process	Membrane Type	Driving Force	Mechanism of Separation	Remarks	Selected Studies
1	Reverse Osmosis (RO)	dense	Pressure difference	solution-diffusion	The process can be performed in removing low levels of heavy metals. Usually, it is coupled to other removal operations in a hybrid-integrated process.	[56–66]
2	Nanofiltration (NF)	porous charged (1–10 nm)	Pressure difference	Donnan exclusion	Compared to RO, NF is an energy-saving process and is very attractive for effective removal of heavy metal ions.	[67–69]
3	Forward osmosis (FO)	dense	Osmotic pressure difference	solution-diffusion	Differently, from RO, FO can be applied to treat high-salinity wastewater with the challenging objective to eliminate heavy metals here contained. However, FO suffers from concentration polarization.	[70,71]
4	Electrodialysis (ED)	ion-exchange membranes	Electric potential difference	Ion exclusion	ED can only be cost-effective if applied integrated with other treatment processes. Electrodeionization (EDI) can be effectively used in removal of metal ions from dilute solutions.	[72–80]
5	Membrane Capacitive Deionization (MCDI)	ion-exchange membranes	Electrical potential	Ion exclusion	The electrostatic adsorption mechanism leads to low adsorption selectivities between different ion types with a similar charge.	[81,82]
6	Polymer-enhanced ultrafiltration (PEUF)	porous (0.01–0.1 $\mu\text{m}$ )	Pressure difference	size exclusion	PEUF is a combination of selective binding of target metal ions to a water-soluble polymer followed by ultrafiltration.	[83–89]
7	Membrane bioreactors employing UF membranes (MBRs)	porous (0.01–0.1 $\mu\text{m}$ )	Pressure difference	size exclusion	Removal efficiencies are lower than other membrane processes and depend on Mixed Liquor Suspended Solids (MLSS) concentration. Therefore, new concepts such as the ion-exchange membrane bioreactor (IEMB) process were developed to achieve high metal ions removal.	[90–92]
8	Osmotic membrane bioreactors (OMBRs)	dense	Osmotic pressure difference	solution-diffusion	OMBR is a low membrane fouling technology with high capability of nutrient removals and rejections of monovalent ions and thus can be considered promising for industrial wastewater containing heavy metals.	[93]
9	Liquid membranes (LMs)	porous (0.1–10 $\mu\text{m}$ )	Concentration difference	solution-diffusion	LMs can be efficiently used for wastewater treatment. However, instability problems over time are one of the main shortcomings.	[94–96]
10	Membrane distillation (MD)	porous (0.1–10 $\mu\text{m}$ )	Partial vapor pressure difference due to a temperature difference	vapor/liquid equilibrium of a liquid mixture occurs, therefore, the permeate composition is dependent on the partial pressure of respective components of the feed.	Comparison with pressure-driven membrane processes such as RO or NF suggests that with direct contact MD high metal ion removal efficiencies can be obtained.	[97,98]
11	Adsorptive membrane	Porous/dense	Pressure difference/Electrical potential	Adsorption (coordinative interactions, ion exchange, electrostatic adsorption, hydrogen bonding, specific surface bonding, and chelation).	All the advantages of adsorption (see Table 2) are combined with the ones of the membrane processes.	This review and references herein

In addition to the pressure-driven membrane processes mentioned above, two other different membrane operations using porous membranes and have traditionally been applied in the field of heavy metal and metalloid removal: membrane distillation (MD) and liquid membranes (LM) (Table 3, entry 9 and 10, respectively). Even though the membranes used in both these two membrane processes are macroporous (i.e., with pores > 50 nm) as in MF and UF, the driving forces and the membrane role are different, and both MD

and LM can also be used not integrated with other membrane processes to remove metal ions [94–98]. More specifically, MD is a thermally driven separation process, in which only vapor molecules are able to pass through a porous hydrophobic membrane. In LM, the membrane is not as selective as in other membrane processes, but it, containing an organic phase, acts as a barrier between two aqueous solutions where the driving force for mass transfer is due to a concentration gradient. LMs offer the possibility to operate highly selective separation and recovery from dilute aqueous leading to extraction and subsequent stripping operations in a single step. However, instability problems over time are one of the main drawbacks.

All of the above membrane processes suffer from one main problem: specificity in heavy ion removal. In other words, although they can perform very well with a given heavy metal ion, they are highly inefficient in treating other metal contaminants, which makes their use very limited. More importantly, the removal of several ions simultaneously is highly inefficient. For example, using commercial NF membranes, it has been shown that while the removal efficiency of nickel ions alone can reach 98% [99], the specific ion removal of nickel and cadmium together decreases to ~83% [100]. This hampers the use of NF in treating environmentally polluted waters, in which several heavy metal ion pollutants typically coexist together. Finally, in all cases, the efficiency of the above membrane processes drops rapidly as soon as the feeding conditions depart from optimized pH and concentrations. An extensive treatise of all the membrane processes for metal ions removal is far beyond the scope of this review and further reading of the relevant publications on each subject as reported in Table 3 (entries 1–10) and recent reviews [101–103] are recommended. Among the various membrane processes for heavy metal removal, adsorptive membrane technology so-called also membrane adsorbers (Table 3, entry 11) has gained great attention [104–107] thanks to lower pressure demands and lower energy of membrane operation without compromising the adsorption selectivity. Below, an overview of adsorptive membrane technology as well as adsorptive membranes is given.

## 2. Adsorptive Membrane Technology

Adsorptive membrane technology is the integration of adsorption and membrane technology as the name itself suggests. Adsorptive membranes are a whole emerging class of materials shaped as membranes that exhibit improved performance compared to conventional membranes [104,105,108,109].

Traditional adsorption is operated using packed beds filled with microporous beads in order to maximize the active surface area. However, the convective flow, which drives the feed through the packed bed, occurs around the microporous beads bypassing the active pores within them. In order to optimize the process via a diffusive transport mechanism from the exterior surface of the bead to the active sites within the beads, long residence times to ensure that the active sites saturate with the feed are necessary and realized thanks to the increased size of the equipment, which in turn increases capital and operating costs [110]. Conventional adsorptive membranes (Figure 5A) are usually prepared by surface modification of porous UF/MF polymeric membranes, e.g., pore diameters,  $d_p \approx 10\text{--}1000$  nm (see Figure 1), with specific functional groups or the addition of nanoparticles onto the membrane surface, which can bind the metal ions through ion exchange or surface complexation, even though the pore sizes of these membranes (MF/UF) are larger than the size of metal ions. They offer shorter diffusion distances between the solutes and binding moieties on the sorbent surface [111–117]. Such an approach follows the paradigm of traditional membrane filtration (MF, UF, coarse NF) (Figure 5A). This configuration reduces mass transfer resistance and, consequently, affords higher throughput operation while utilizing available binding sites more efficiently. The separation by adsorptive membranes typically can be operated with lower pressure drop compared to packed beds and requires a smaller capital footprint. Moreover, because the feed flows through the membrane containing the active sites, the metal ions capture relies on diffusion lengths on the scale of nanometers rather than micrometers, shortening the time required for the

metal ions to bind with active sites compared to fixed bed filters and increasing the overall throughput capabilities of the process [118–120]. However, despite the advantageous mass transfer associated with membranes, the performance of many state-of-the-art conventional adsorptive membranes is hindered by low binding affinities and limited saturation capacities, which have been the main hurdle in their commercialization. Advanced adsorptive membranes (Figure 5B) are based on the incorporation of: (1) single-digit nanopores (i.e., pores with diameters < 10 nm) into the polymer matrix through carbon nanotubes (CNTs), porous metal-framework (MOFs), porous aromatic frameworks (PAFs), and covalent organic frameworks (COFs); and (2) solute-selective ligands grafted to membrane polymer chains [121]. More specifically, this second approach to design advanced adsorptive membranes refers to tuning the coordinative interactions between the solute and the polymer matrix, a key feature at the basis of the remarkable selectivity of biological membranes [122], and the resulting adsorptive membranes are named [121] chelating membranes. These new advanced adsorptive membranes can be used in multifunctional membrane separation processes such as ion-capture-ED (IC-ED) and solute-capture diffusion dialysis (SC-DD) [123] where the driving forces are electrical potential and concentration gradients, respectively, but also NF. Regarding NF, the development of a systematic synthetic platform that allows the functionalization of polymers with solute (metal ions)-selective ligands with controlled water swelling is highly required. In fact, water swelling could ensure enough mobility for the transport of the solutes through the membrane matrix as well as long-term stability without the risk of leaching of metal ions-complexes (ionophores), a typical issue of LMs in general and supported liquid membranes, in particular.

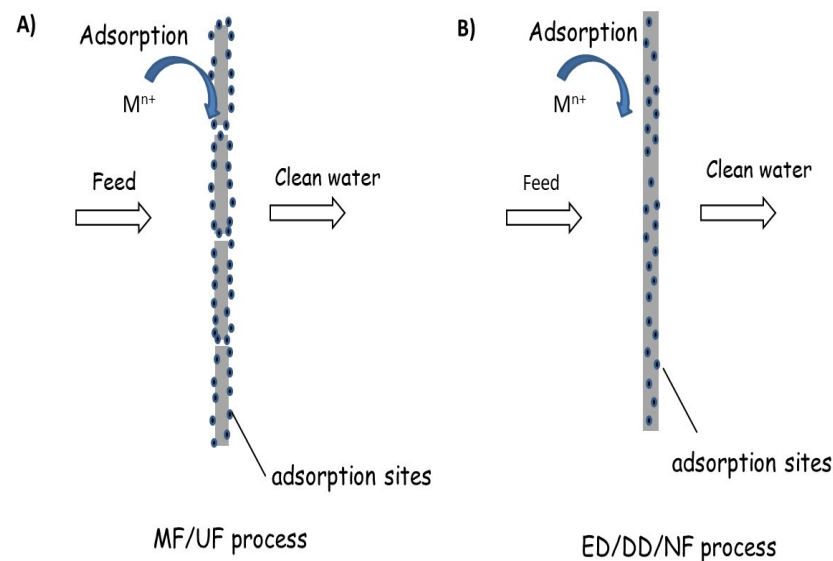


**Figure 5.** Classification of adsorptive membranes and corresponding separation processes: (A) membranes with functionalized pores and (B) dense/nanoporous membranes with entrapped adsorption sites.

## 2.1. Adsorptive Membranes

### 2.1.1. Ways to Introduce Adsorbents into/onto Separation Membranes

The method of preparation of adsorptive membranes plays a fundamental role in their performance. Overall, there are two main methods to give a membrane adsorptive function.

The first is to entrap the adsorbent into/onto the membrane matrix during its preparation by mixing it with the other components. For example, in the case of polymer-based membranes, the adsorbent is added to the polymer casting solution giving intrinsic asymmetric membranes. Another possibility is to add the adsorbent to the solution, which forms the thin film onto a porous asymmetric membrane (support), giving thin film composite membranes. Both variants of this method are used in the many studies discussed in this

review. A fine tuning of the adsorbent quantity is necessary. Usually, the ratio of adsorbent in the membrane is low to avoid the formation of agglomerates and then of defects, which could compromise the membrane performance. To overcome this drawback, adsorbents were made more compatible with the hosting membrane matrix by their fine functionalization as in the case of MOF nanofibers-based adsorbents [124] used to prepare mixed matrix membranes (MMMs) discussed below in the related subparagraph.

The second method refers to the so-called “formed-in-place membrane” or “dynamic membrane (DM)”. The two terms have been used interchangeably [125]. DM is a layer of particles deposited via permeate drag on a conventional membrane, with the deposited particles acting as a secondary membrane [126–129]. Based on whether the DM is composed of feed constituents deposited during filtration or intentionally pre-deposited particles with desired properties on the primary membrane [126], DMs can be divided into two types, namely, (1) self-formed DMs, whereby the solid particles from wastewater form the DM and aid in improving permeate quality [130]; and (2) pre-deposited DMs, formed via deposition of materials such as metallic compounds (especially oxides), polymers, activated carbon, soil-based compounds, and nanoparticles onto UF, MF, NF, or RO membranes. The first report on DMs was in 1966 by the Oakridge National Laboratory [131], whereby hydrous zirconium [Zr(IV)] oxide served as a DM on a RO membrane for salt rejection. Since then, numerous papers on DMs for various applications have been published [125].

The characteristics of some studies on adsorptive DMs applied in the field of heavy metals removal are reported in Table 4.

**Table 4.** Characteristics of some studies on adsorptive DMs.

Entry #	Adsorbent	Membrane	DM Type	Heavy Metals	Remarks	Ref.
1	Micro-sized granular ferric hydroxide (Fe(OH) <sub>3</sub> ) (mGFH)	MF	Pre-deposited	As(V)	μGFH proved to be promising as emerging pre-depositing material for a DM filter	[132]
2	Micro-sized tetravalent manganese ferrioxhyte (δ-Mn(IV) FeOOH) (mTMF)	MF	Pre-deposited	As(V)	μTMF proved to be promising as emerging pre-depositing material for a DM filter.	[132]
3	Polydopamine (PDA) nanoparticles	UF	Pre-deposited	Pb(II), Cd(II), Cu(II)	Significant enhancement of adsorption capacity is derived from the three-dimensional distribution of the adsorbent PDA on the cross section of UF membrane.	[133]
4	Hollow porous Zr(OH) <sub>x</sub> nanospheres (HPZNS) coated with PDA	UF	Pre-deposited	Pb(II)	Compared to the blend membrane, the pre-deposited DM showed 2.1-fold increase in the effective treatment volume for the treatment of Pb(II)-contaminated water from 100 ppb to below 10 ppb (WHO drinking water standard).	[134]
5	Graphene oxide/ PDA	UF	Pre-deposited	Pb(II)	Outstanding Pb(II) rejection can be attributed to chelation of amino groups on the PDA layer.	[135]
6	UiO-66-NH <sub>2</sub>	UF	Pre-deposited	Cr(III)/Cr(VI)	Negligible leakage of the adsorbent UiO-66-NH <sub>2</sub> owing to the successful cross-link of PEI. The membrane can be easily regenerated and reused.	[136]

The common advantage emphasized in the studies of the pre-deposited DMs listed in Table 4 is that the polymer matrix does not cover the surface of adsorbents reducing the number of effective adsorption active sites and thus decreasing the adsorption performance as it occurs with blend membranes [137]. The advantage of this strategy is that the UF membranes can be endowed with adsorption ability, while the inherent ultrafiltration properties were well maintained. As shown in Figure 6, the pre-deposited DM membrane (Table 4, entry 4) not only allows the removal of multiple pollutants from water, such as colloidal gold and polyethylene glycol, as a conventional UF membrane, but also toxic pollutants (Pb(II) as one example).

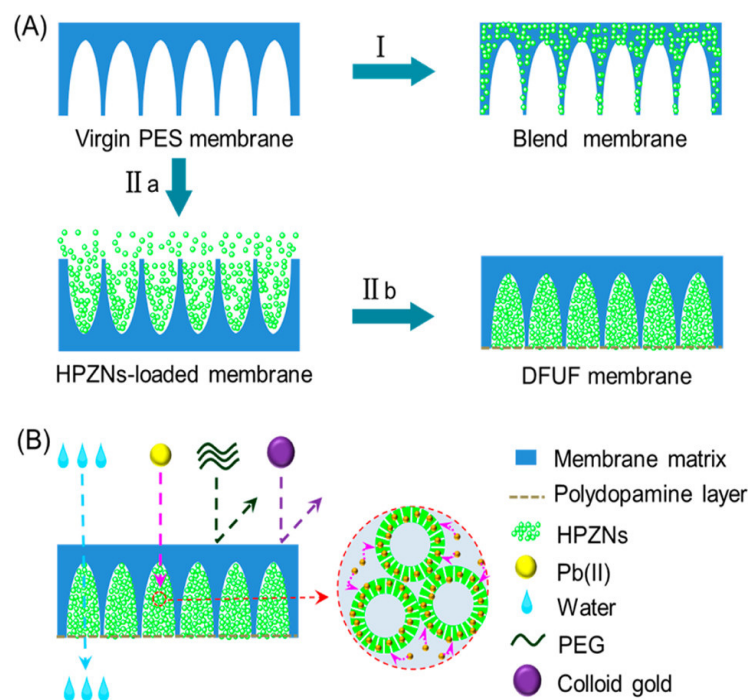
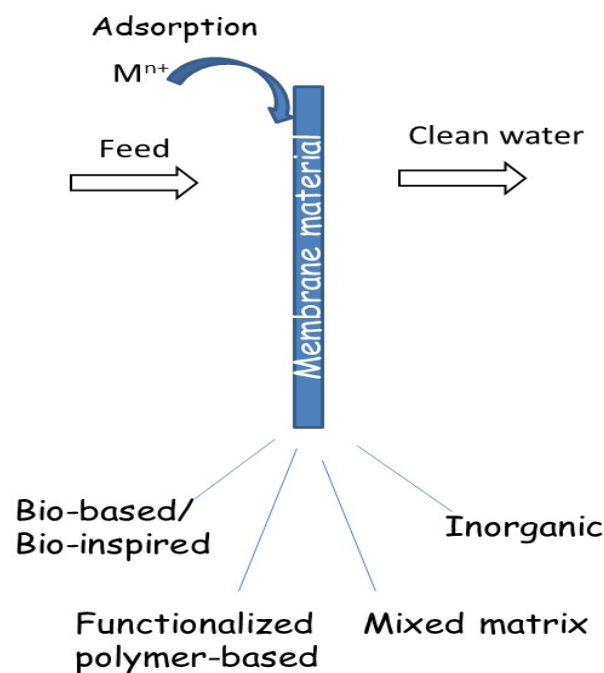


**Figure 6.** Schematic representation of UF membrane designs: (A) Virgin polymer UF membrane and a traditional blend membrane are both synthesized through a one-step casting method (I). A new 2-step method to form pre-deposited DM (Dual Function UF membrane) (II); (B) the purification process for polluted water by pre-deposited DM. Reproduced with permission from [134], copyright of the American Chemical Society.

### 2.1.2. Types of Adsorptive Membranes

Depending on the membrane materials, adsorptive membranes can be classified into four main groups: bio-based/bio-inspired, functionalized polymer-based, inorganic, and mixed matrix membranes (Scheme 1).



**Scheme 1.** Classification of adsorptive membranes in terms of membrane materials.

### Bio-Based Adsorptive Membranes

In this paragraph, membranes based on natural and renewable polymeric materials such as cellulose are reviewed. Chitosan-based adsorptive membranes have been reviewed by Salehi et al. [138] and therefore are not discussed in this review. Cellulose is the most abundant natural and renewable polymeric material. Its biocompatibility, hydrophilicity, and non-toxicity represent an interesting ecofriendly membrane material for metal ion removal. Moreover, its potential functional ability allows the selective removal of various metal ions [139,140]. Membranes based on cellulose capable of removing metal ions have been prepared using various strategies. Wang et al. [141] (Table 5, entries 1, 2) prepared an MF nanofibrous membrane where ultra-fine cellulose nanofibers (CNFs) (diameter 5 nm) were infused into an electrospun polyacrylonitrile (PAN) nanofibrous scaffold deposited onto a non-woven PET support (Figure 7).

**Table 5.** Performance of recent cellulose-based adsorptive membranes.

Entry #	Type of Membrane	Heavy Metal Ions	Optimum Conditions/ Experimental Conditions	Adsorption	Ref.
				mg g <sup>-1</sup>	
1	Microfiltration nanofibrous (PVAm-CNF)	Cr(VI)	pH 4; initial conc. 50 ppm	100	[141]
2	Microfiltration nanofibrous (CNF)	Pb(II)	pH 6; initial conc. 50 ppm	260	[141]
3	Fully bio-based nanocellulose membrane (CNC <sub>SL</sub> )	Cu(II) *	pH 2.3; initial conc. 330 ppm	9.6	[142]
4	Fully bio-based nanocellulose membrane (CNC <sub>BE</sub> )	Cu(II) *	pH 2.3; initial conc. 330 ppm	24	[142]
5	Fully bio-based phosphorylated Nanocellulose membrane (PCNC <sub>SL</sub> )	Cu(II) *	pH 2.3; initial conc. 330 ppm	79	[142]
6	Fully bio-based nanocellulose membrane (CNC <sub>BE</sub> )_acetone treatment	Cu(II) *	pH 2.3 Initial conc. 330 pm	33	[143]
7	Fully bio-based nanocellulose membrane (CNC <sub>SL</sub> )_acetone treatment	Cu(II) *	pH 2.3; Initial conc. 330 ppm	33	[144]
8	Regenerated cellulose membrane grafted with PDMAEMA	Cu(II)	pH-; Initial conc. 25.6 ppm	41.9	[144]
9	Regenerated cellulose membrane grafted with PDMAEMA	Cu(II)	pH-; Initial conc. 76.8 ppm	150	[144]
10	Regenerated cellulose membrane grafted with PDMAEMA	Cu(II)	pH-; Initial conc. 128 ppm	225	[144]

\* Not only Cu(II), but also Fe(III) and Ag(I) have been investigated in [142], but in the present review only heavy metal ions, dangerous as reported in Table 2, were considered.

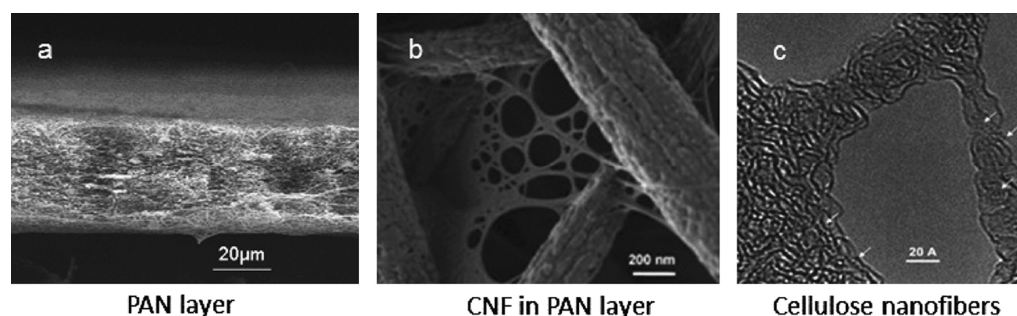


**Figure 7.** SEM images of electrospun PAN/PET membrane ((a) cross-section view), and PAN/PET membrane infused with PVAm-CNF ((b) top view). TEM image (c) taken at a small section of the cellulose network containing pores and individual polymer chains with a spaghetti-like configuration. Reproduced with permission from [141], copyright of Elsevier B.V.

The nanofibrous structure assures high surface area per unit mass resulting in high adsorption capability and good permeation flux. CNFs were prepared according to the method of Isogai and co-workers [145], which led to large surface area and significant amounts of C6 carboxylate groups on the fiber surface. The amidation process was used to introduce functional groups able to efficiently interact with the metal ions and adsorb them. The scheme of the chemical procedure, i.e., TEMPO (2,2,6,6-tetramethylpiperidine-1-oxylradical) oxidation in water and subsequent amidation is given in Figure 8. After the TEMPO oxidation procedure at pH 10–11 (Figure 8), carboxylated CNFs with diameters of ca 5 nm were obtained. Amino-modified cellulose nanofibers (mCNF) were prepared using EDC and NHS as catalysts and PVAm, PEI, or EA as grafting agents. The suspension of aminated CNFs was infused into the PAN nanofibrous layer by applying an external pressure of about 2 psi. Finally, the composite membrane was heated at 50 °C to initiate cross-linking reaction to immobilize the CNF network. Two different membrane types have been used for Cr(VI) and Pb(II) adsorption: a membrane based on CNFs amino-modified by PVAm (PVAm-CNF, Table 5, entry 1) and a membrane based on as-made CNFs without amino-modification (CNF, Table 5, entry 2). The adsorption maximum for the two metal ions was observed at different pHs: pH 4 and 7 for Cr(VI) and Pb(II), respectively. The different pH depends on the different species involved in the adsorption process.

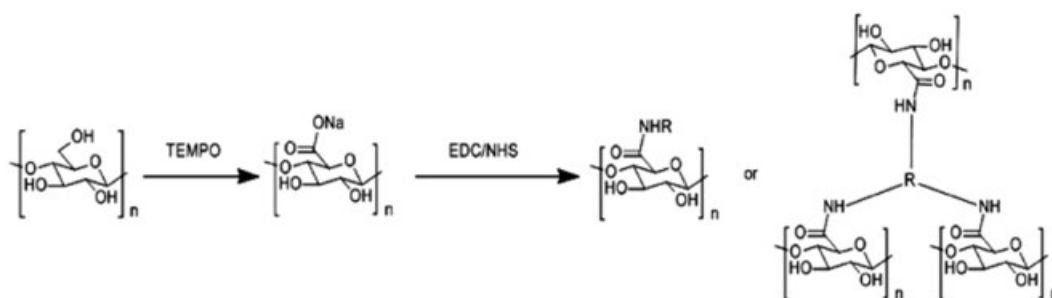


**Figure 8.** Oxidation and amidation of ultra-fine cellulose nanofibers. Reproduced with permission from [141], copyright of Elsevier B.V.

In particular, for Cr(VI), as the pH increased from 1 to 4, the main species is  $\text{HCrO}_4^-$ , which could be attracted by positively charged amino groups on the PVAm-CNF surface; in the case of Pb(II), as the pH value increased from 2 to 6, the carboxylate groups on the surface of CNF start to deprotonate increasing their ability to adsorb Pb(II) ions.

In the fully bio-based approach by Karim et al. [142], not only the selective layer but also the support is made of cellulose: a thin layer of native and modified cellulose nanocrystals was used as a functional entity on a support layer of a microsized cellulose fibers (Figure 9).

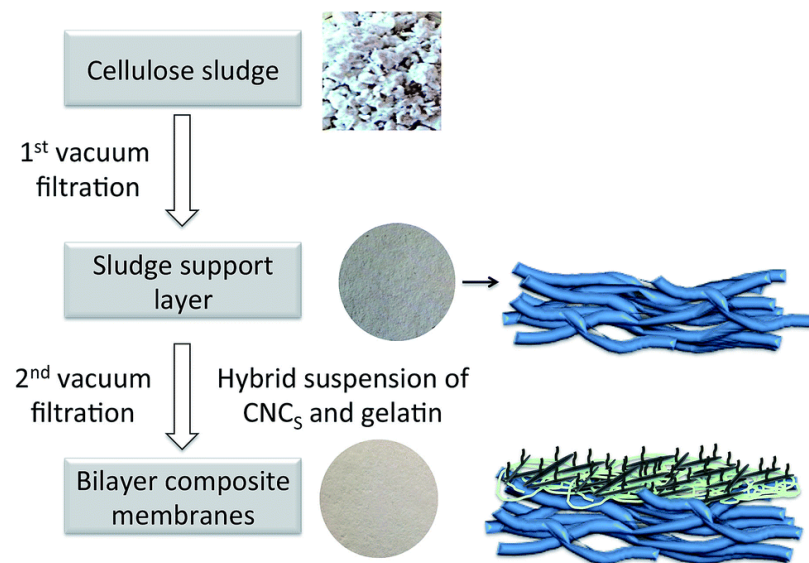


**Figure 9.** Schematization of the fabrication process of layered cellulose nanocomposite membranes using vacuum-filtration process [142]. Used under CC BY 3.0.

The cellulose nanocrystals (CNCs) were prepared by two routes, both different from that one used by Wang et al. [141] (Table 5, entries 1, 2): the first one by using sulfuric acid hydrolysis (CNC<sub>SL</sub>) as reported in previous work by Karim et al. [146]; the second by bioethanol pilot plant process in dilute acid (CNC<sub>BE</sub>) [147]. The CNC<sub>SL</sub> were enzymatically functionalized with phosphoryl groups (PCNC<sub>SL</sub>) according to Božič et al. [148]. Both CNC<sub>SL</sub> and CNC<sub>BE</sub> show typical cellulose nanocrystal structures with diameters in the range of 5–10 nm.

The heavy metal removal process is the result of the high surface area of these nanomaterials based on nanocellulose and the nature and density of functional groups on the nanocellulose surface with the order PCNC<sub>SL</sub> > CNC<sub>BE</sub> > CNC<sub>SL</sub> (Table 5, entries 3–5). PCNC<sub>SL</sub> was highly effective for Cu(II) removal compared to CNC<sub>SL</sub> and CNC<sub>BE</sub> due to the presence of the two negative charges of phosphate groups ( $\text{PO}_4^{2-}$ ) (Figure 10).

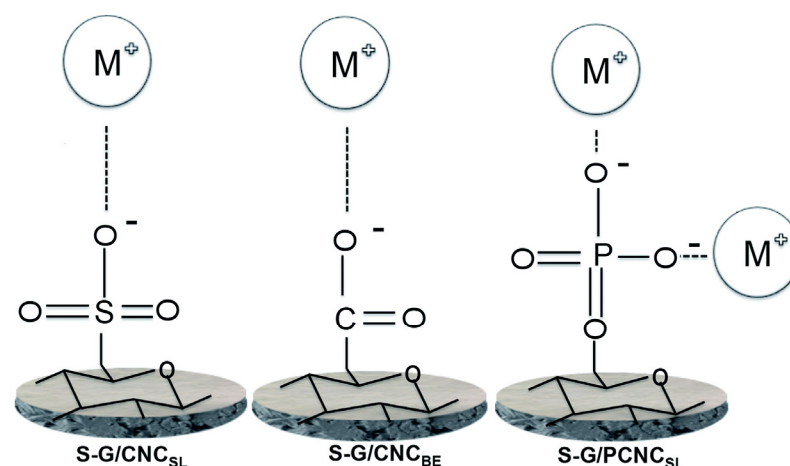


**Figure 10.** Proposed mechanism for the metal ion adsorption by cellulose nanocomposites investigated in [142]. Used under CC BY 3.0.

In a subsequent paper [143], the same research group explored the effect of processing routes on the structure and performance of the nanocellulose membranes, i.e., CNC<sub>SL</sub> and CNC<sub>BE</sub>. In particular, acetone treatment prior to air drying was employed to tailor the surface area and porosity (Figure 11).

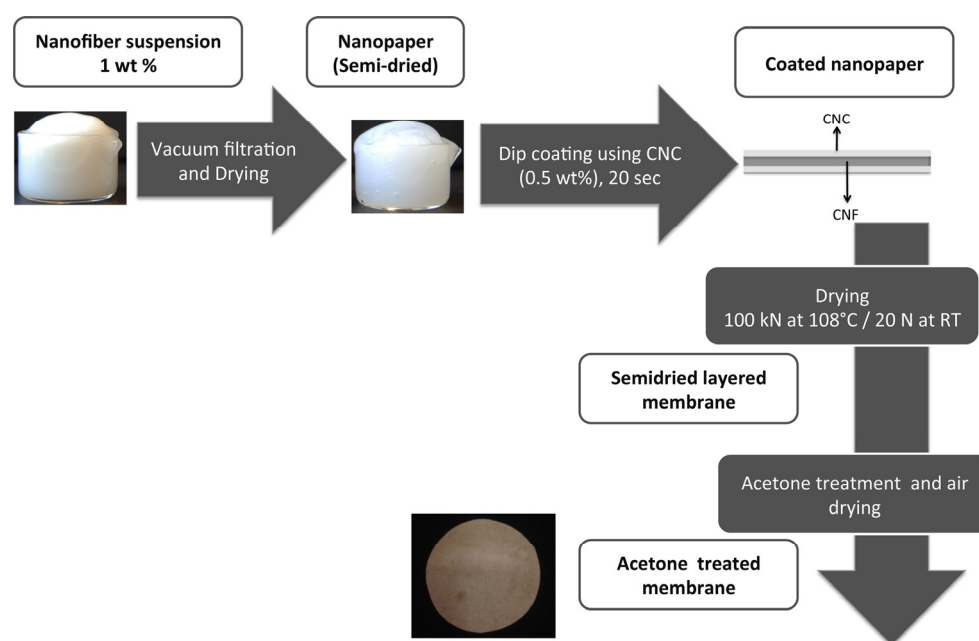


**Figure 11.** Schematic representation of membranes processing by Karim et al. [144]. Reproduced with permission from [143], copyright of Elsevier.

Even though the acetone treatment introduces higher porosity and a higher surface area, the observed adsorption capability was lower than that of PCNCSL explored in the previous study, i.e. [142]:  $33 \text{ mg g}^{-1}$  (Table 5, entry 6) vs.  $79 \text{ mg g}^{-1}$  (Table 5, entry 5). However, the authors of [143] claimed as the main advantage of the acetone treatment, irrespective of the relatively lower adsorption capability, the higher mechanical stability of the membranes compared to those described in [142].

The approach proposed by Algarra et al. [149] and Jiang et al. [144] is different: no single cellulose nanocrystals are assembled in a membrane as reported above, but suitable groups to form complexes with heavy metal ions were introduced into a commercial regenerated cellulose membrane.

In particular, Algarra et al. [149] impregnated a regenerated cellulose support with a diaminobutane-based poly(propyleneimine) dendrimer functionalized with sixteen thiol groups (DAB-3-(SH)16 to enhance the complexation of Hg(II), Cd(II), and Pb(II) (Figure 12).

However, the authors in [149] did not report concentration data for the adsorbed metal ions, rather they only observed the time evolution of the concentration ratio for each different membrane and metal ion studied. A decrease in diffusive permeability through the membrane loaded with the dendrimer compared to the original sample of regenerated cellulose membrane was observed for all the electrolytes, but with different percentages: CdCl<sub>2</sub> (~20%) and HgCl<sub>2</sub> and PbCl<sub>2</sub> (~45%).

In the study by Jiang et al. [144], a regenerated cellulose membrane was functionalized with poly(*N,N*-dimethylaminoethyl methacrylate) (PDMAEMA) via an atom transfer radical polymerization method to remove Cu<sup>2+</sup> ions from an aqueous solution. The PDMAEMA grafting degree, which can be controlled by a variation in grafting time, influences the Cu<sup>2+</sup> ion adsorption: adsorption results indicated that the adsorption capacity increased as the grafting time changed from 5 to 50 min. Moreover, the effect of initial Cu<sup>2+</sup> concentration on the adsorption capacity has been also studied. The adsorption capacity increased from 41.94 to 225.36  $\text{mg g}^{-1}$  (Table 5, entries 8–10) with an increase in initial Cu<sup>2+</sup> concentration from 25.6 to 128  $\text{mg L}^{-1}$ .

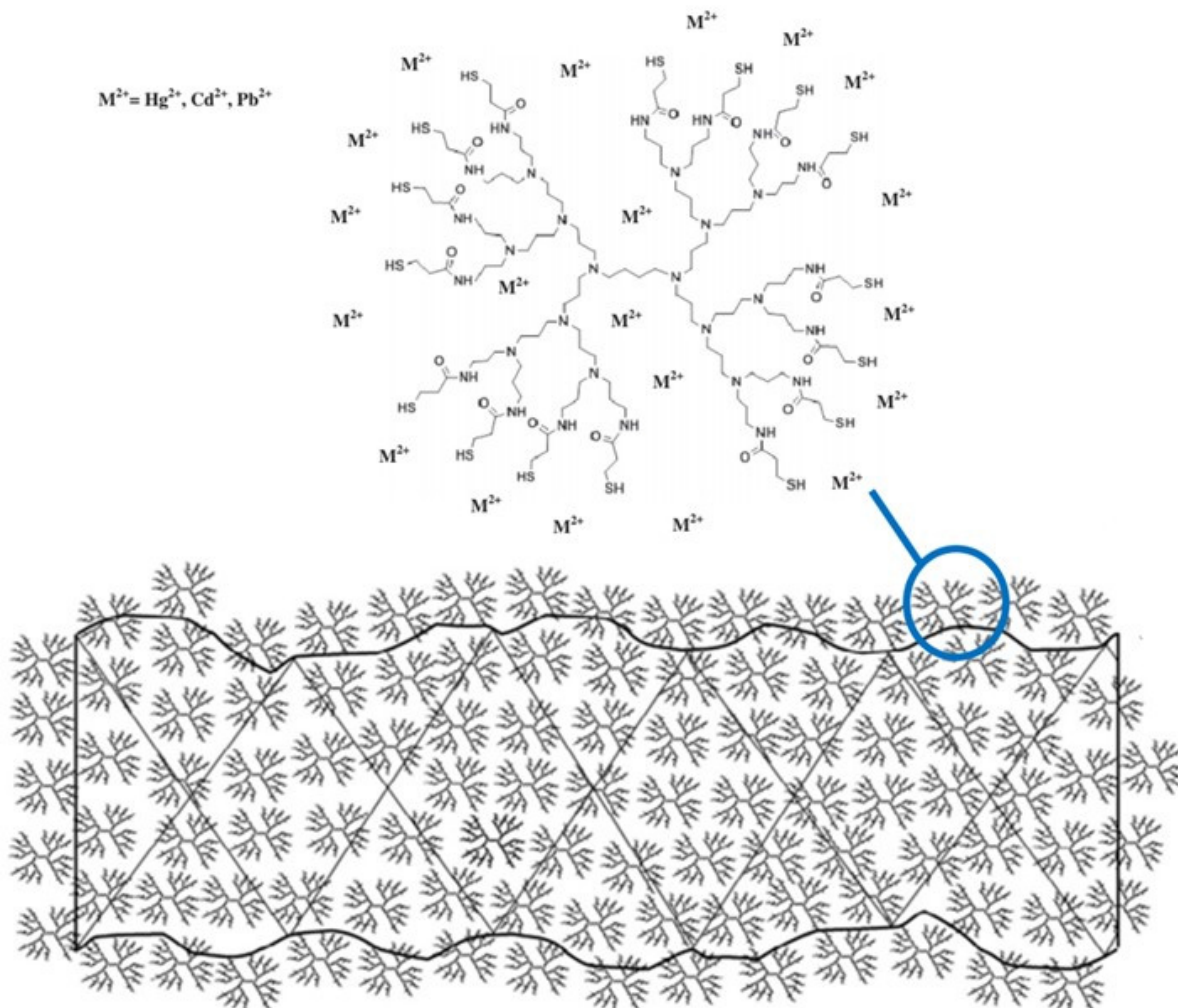


**Figure 12.** Schematic representation of the coated regenerated cellulose membrane by DAB-3-(SH)16 dendrimer. The detail (top, right) illustrates the dendrimer's ability to adsorb cations. Adapted with permission from [149], copyright of Elsevier.

### Bio-Inspired Adsorptive Membranes

Nature gives examples of membranes with higher separation rates than man-made equivalents. In this respect, aquaporin-based biomimetic membranes fabricated by combining the aquaporin protein (embedded within amphiphilic molecules, such as lipids) with a polymer support structure have attracted great interest [150]. The role of aquaporins has been replicated with artificial channels such as carbon nanotubes (CNTs) (~1 nm), self-assembled block copolymers, and membranes designed with coordination chemistry and subnanometer pores.

Subnanometer biological ion channels are well known for their outstanding selectivity [151,152]. A remarkable example is given by the potassium ions channel, which shows an unusual selectivity allowing the passage of larger  $K^+$  ions (1.3 Å) over smaller  $Na^+$  ions (1.0 Å) due to different paths and interactions in the pore of the potassium channel [153].

Interesting studies are reported in the literature regarding the design of engineered artificial pores for metal ions separations.

Wen et al. [154] reported on polyethylene terephthalate (PET) membranes with synthetic subnanometer pores obtained via irradiation with swift heavy ions and subsequent UV illumination. The track in PET membranes is a nanostructure with a core of 0.3 nm radius. The observed selectivity of metal ions transport, i.e.,  $Li^+ > Na^+ > K^+ > Cs^+ \gg Mg^{2+} > Ca^{2+} > Ba^{2+}$ , gives strong evidence that the ionic transport proceeds through subnanome-

ter pores. Molecular dynamics simulations reproduced the ionic transport selectivity and showed that it is associated with the dehydration of ions. Dehydration effects represent a key factor in the transport through subnanometer biological ion channels [155] and are also the basis of ultrafast and selective ion transport in other subnanostructured membranes, i.e., ZIF-8 membranes prepared and investigated by Zhang et al. for the selective transport of alkali metal ions ( $\text{Li}^+/\text{Rb}^+$ ) [156].

Two recent studies are strictly focused on coordinative interactions between the metal ions and membrane matrix, i.e., host–guest interactions. The first by Warnock et al. [122] involved incorporating 12-crown-4 ether in polynorbornene networks to give outstanding performance membranes with water content tunable over a relevant range to promote the selective transport of  $\text{Li}^+$  over  $\text{Na}^+$  and  $\text{Mg}^{2+}$ . Crown ethers are a class of ligands known to bind various cations depending on the relative size of their cavity and the size of the target ion [157]. In polymeric membranes without any polymer-ion specific interactions, the diffusivity selectivity depends on the solvated size of each ion in the membrane; therefore, even though the ionic radius of  $\text{Li}^+$  is smaller than that of  $\text{Na}^+$ , its hydrated radius is larger, i.e.,  $3.8\text{\AA}$  ( $\text{Li}^+$ ) vs.  $3.68\text{\AA}$  ( $\text{Na}^+$ ), leading to a diffusivity selectivity that favors  $\text{Na}^+$  over  $\text{Li}^+$ . Warnock et al. [122] reversed this trend observing  $\text{Li}^+/\text{Na}^+$  selectivity due to the significant ion–pore wall interactions between  $\text{Na}^+$  and 12-crown-4 ether, which hinders the diffusion of  $\text{Na}^+$  relative to  $\text{Li}^+$ .

The second study by DuChanois et al. [158] is about polyelectrolyte multilayer membranes with iminodiacetate (IDA) functional groups able to coordinate strongly  $\text{Cu}^{2+}$  (higher binding energy) compared to  $\text{Ni}^{2+}$ ,  $\text{Co}^{2+}$ , and  $\text{Mg}^{2+}$  (lower binding energy). Therefore,  $\text{Cu}^{2+}$  ions permeate more selectively through the membrane than ions with lower binding energy.

The manufacture of self-assembled block copolymers-based materials is another bio-inspired synthetic membrane production strategy suited to scale-up and easily applied to conventional porous supports [159].

Self-assembly of block copolymers occurs due to inherent differences between the constituent blocks, leading to phase separation. The selection of appropriate conditions (concentration, solvent, drying times, etc.) can dictate this separation, resulting in various structures, including hexagonally packed cylindrical phases [160,161]. Weidman et al. [117] used a polyisoprene-*b*-polystyrene-*b*-poly(*N,N*-dimethylacrylamide) (PI-PS-PDMA) triblock polymer as a precursor for the formation of a copper-selective adsorber. The adsorptive membranes were fabricated from self-assembled block polymers using the self-assembly and non-solvent induced phase casting (NIPS) method [162–164]. Then, the conversion of the PDMA block of the resulting membrane to a poly(acrylic acid) (PAA) moiety results in pore walls that can adsorb copper ions reversibly. As such, the nanoporous membranes have a relatively high copper binding capacity of  $260\text{ mg g}^{-1}$  membrane (see for comparison the data reported in Table 5). Moreover, the PAA moieties can be further functionalized, creating high capacity adsorbers tailored for the separation of specific similarly sized and similarly charged solute molecules [165].

The strategy of blending block copolymers with another polymer allows the tune sieving and adsorption properties of so-called tunable sieving and adsorption (TSA) membranes. This strategy has been explored by Yao et al. [166], Kausar [167], and Zhang et al. [168]. In more detail, Yao et al. [166] fabricated TSA membranes via non-solvent-induced phase separation by blending amphiphilic block copolymers P(MMA-*b*-DMAEMA) and polyvinylidene fluoride (PVDF). The two blocks of the amphiphilic copolymers were selected for their specific properties: PMMA has been proved as a proper hydrophobic component due to good compatibility with PVDF; and DMAEMA is a tertiary amine-containing monomer frequently used to synthesize hydrophilic and multifunctional polymers. The adsorption capacity of the TSA membranes was tested with Cr(VI) solutions at different pH values. Pure PVDF membrane does not adsorb Cr(VI) ions, while the P(MMA-*b*-DMAEMA)-containing PVDF membranes show excellent pH-dependent adsorption properties. In particular, the membrane blended with the longer PDMAEMA

block-containing copolymer achieved a higher equilibrium adsorption amount of Cr (VI) ions due to the higher content of PDMAEMA, which, with its chains hanging on the membrane surface and pore walls, facilitates the ions adsorption more or less depending on pH. The mechanism of the pH-dependent Cr(VI) adsorption capacity is illustrated in Figures 13 and 14.

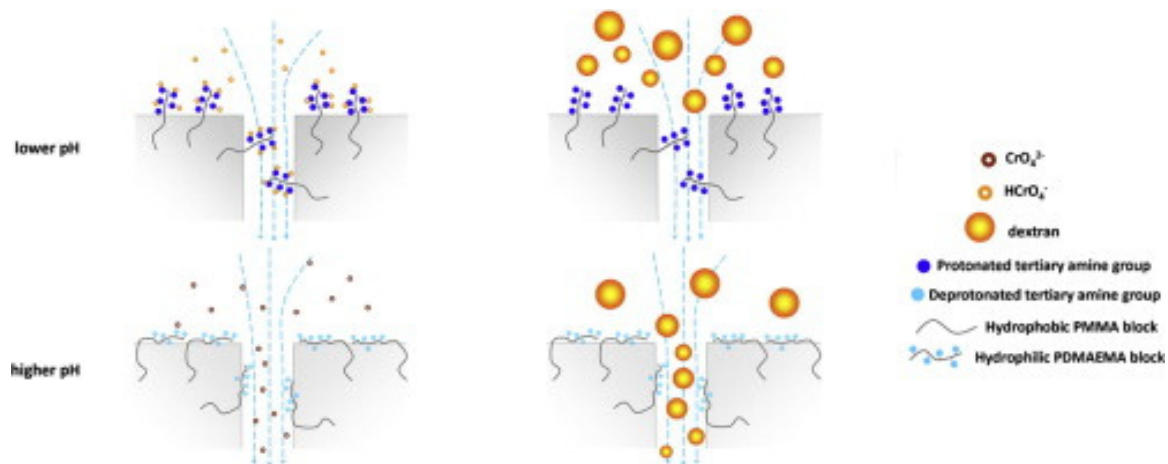


**Figure 13.** Schematization of the mechanism of adsorption of TSA membranes: the membrane sieving ability depends on the pH. At low pH, the amine groups are protonated and therefore able to attract the negative molecular ions of chromium; at high pH, the amine groups are neutral allowing the ion passage through the membrane and then avoiding their adsorption. Reproduced with permission from [166], copyright of Elsevier B.V.

	Increasing pH value			
	2.0	3.5	6.0	9.7
Ionization state of hanging PDMAEMA chains on surface				
Cr(VI) ions existence form in solution	$\text{HCrO}_4^-$ , $\text{H}_2\text{CrO}_4$	$\text{HCrO}_4^-$	$\text{HCrO}_4^-$ , $\text{CrO}_4^{2-}$	$\text{CrO}_4^{2-}$
Electrostatic attraction between Cr(VI) ions and PDMAEMA chains	Strong	Stronger	Middle	Weak
Cr(VI) adsorption	High	Higher	Middle	Low

**Figure 14.** Illustration of ionization state of hanging PDMAEMA chains on membrane surface, and Cr(VI) ion existence forms in solution at various pH values and corresponding electrostatic attraction and adsorption. Reproduced with permission from [166], copyright of Elsevier B.V.

The different protonation degrees of tertiary amine groups of PDMAEMA chains and the various forms of Cr(VI) ions existence are the basis of the pH-dependent adsorption performance of the blend membranes. The adsorption at pH 3.5 is 12.4 times higher than that one at pH 9.7 (Figure 14).

In the study by Kausar [167] the membrane blend is based on two block copolymers: the block copolymer of polyethylene-block-poly(ethylene glycol) (PE-b-PEG) and polycaprolactone (PCL) and the block copolymer of polystyrene and methyl methacrylate (PS-b-MMA). Gold/polystyrene nanoparticles were loaded in the self-assembled membranes to enhance metal ions adsorption. The adsorption efficiency by the self-assembled membrane containing 1 wt% of gold/polystyrene nanoparticles was outstanding for Pb(II) and Hg(II) ions (100% ions removal), even though not enough specifications regarding the test conditions, such as pH, were given.

Zhang et al. [168] fabricated a polysulfone (PSf) block polymer composite membrane template that can be further tailored to enhance binding affinity and expand sorbent functionality. A PAA-lined membrane with a fully interconnected bicontinuous network consisting of pores  $\sim 1 \mu\text{m}$  in diameter was prepared through the use of surface-segregation and vapor-induced phase separation (SVIPS) methodology (Figure 15).

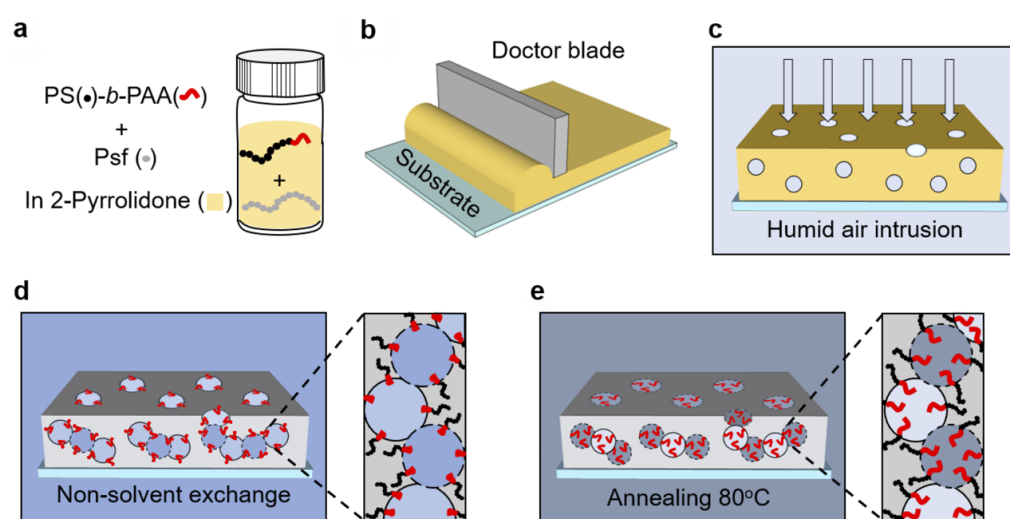


**Figure 15.** Schematic of the surface-segregation and vapor-induced phase separation (SVIPS) membrane fabrication process: (a) The polymer solution was prepared by dissolving the PSf and PS-b-PAA in 2-pyrrolidone. (b) The polymer solution was drawn into a uniform thin film on a glass substrate. (c) The casting solution thin film was exposed in a humid environment (with a relative humidity  $\sim 95\%$ ) for a predetermined amount of time. The intrusion of water vapor from the humid air into the casting solution contributes to the formation of a uniform cross-sectional architecture comprised of spongy cells. (d) The film was subsequently plunged into a nonsolvent water bath that caused the hydrophobic polymers to precipitate and vitrify the membrane nanostructure. Simultaneously, due to their hydrophilic nature, the PAA brushes preferentially segregate toward the surface of the pore wall. (e) The composite membrane was annealed in a bath of DI water at  $80^\circ\text{C}$  to allow the PAA brushes to extend toward the center of the pore. Reproduced from [168], used under CC-BY 4.0.

Then, the pore wall was chemically functionalized to attach binding sites for the adsorption of metal ions. The reaction scheme of Figure 16 outlines the coupling reactions utilized to tailor the chemistry of the PAA-lined PSf template for application as a heavy metal adsorber. The PAA brushes of the parent membrane exhibit modest metal binding capacities as a result of ion-exchange mechanisms. The first reaction attached branched poly-(ethylenimine) (PEI), a chemical linker that expands the number of sites available for further modification and heavy metal capture, to the pore wall. The PEI possesses its own innate metal coordinating capabilities through amine electron donation. PEI was covalently linked to the PAA block through a carbodiimide coupling reaction that was executed by immersing the membrane into an aqueous solution containing branched PEI ( $M_n \approx 60 \text{ kg mol}^{-1}$ ), 1-ethyl-3-(3-(dimethylamino)propyl) carbodiimide hydrochloride (EDC·HCl), and hydroxybenzotriazole (HOBt) at room temperature for 4 days.

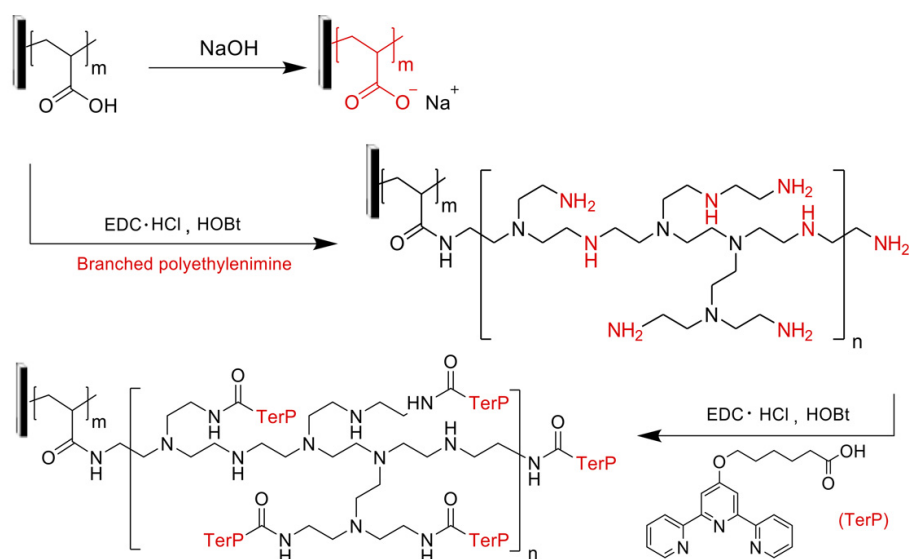


**Figure 16.** The coupling reaction schemes utilized to convert the pore wall chemistry from a parent PAA-lined pore to a terpyridine-lined pore through an intermediate polyethylenimine-lined (PEI-lined) pore. Reproduced from [168], used under CC-BY 4.0.

The second reaction anchors the strong heavy metal coordinating group 6-(2,2':6',2''-terpyridin-4'-yloxy) hexanoic acid (TerP) to the primary amines of the PEI following a similar carbodiimide coupling mechanism as that utilized in the first functionalization step.

The TSA membranes by Zhang et al. [168] are well-suited to capture metal ions from contaminated feed solutions under dynamic flow conditions. Breakthrough curves (Figure 17) were obtained by stacking three membranes in a stirred cell and passing heavy metal contaminated feed solutions through the stack at a volumetric flux (i.e., superficial velocity) of  $\sim 200 \text{ L m}^{-2} \text{ h}^{-1}$ .

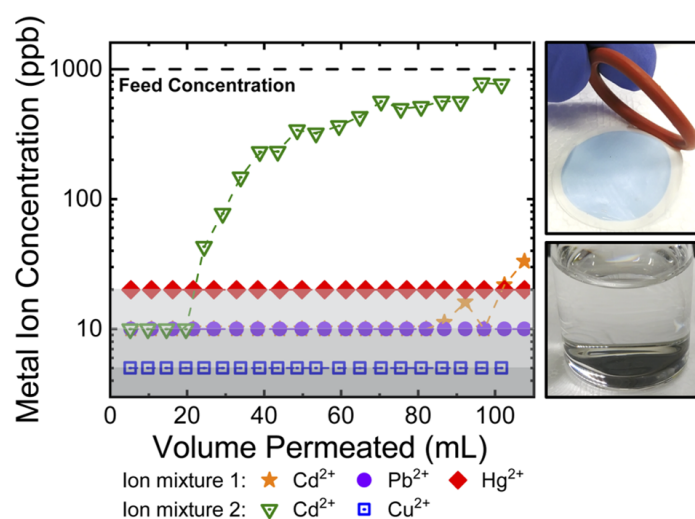


**Figure 17.** Dynamic breakthrough experiments demonstrating metal ion removal in pressure-mediated flow. Reproduced from [168], used under CC-BY 4.0.

Under these conditions, the average residence time of solution within the stack was  $\sim 5$  s. Still, due to the rapid uptake kinetics, this was a sufficient period of time to reduce the concentration of metal ions from 1 ppm in the contaminated feed solutions to the single-digit ppb level in the permeate solutions. Figure 17 shows that no dramatic breakthrough was observed for a ternary feed solution containing a mixture of  $\text{Cd}^{2+}$  (orange star),  $\text{Pb}^{2+}$

(purple circle), and  $\text{Hg}^{2+}$  (red rhombus) metal ions. A binary mixture of 1 ppm of  $\text{Cd}^{2+}$  (green triangle) and 1 ppm of  $\text{Cu}^{2+}$  (blue square) in the feed solution demonstrates a  $\text{Cd}^{2+}$  breakthrough starting at  $\sim 25$  mL, while efficiently removing the incoming  $\text{Cu}^{2+}$ . Photographs of the colorless feed solution from this experiment as well as the surface of the membrane taken after the breakthrough experiment demonstrate the ability of membrane stacks to effectively capture and concentrate metal ions under dynamic flow conditions.

### Inorganic Adsorptive Membranes

In the literature, various examples of inorganic membranes used for the removal of heavy metals, e.g., NaA zeolite [169] MCM-41 [170,171], MCM-48 [171,172], and FAU [173], are reported. However, in such studies, the metal ions, in most cases chromate anions, are rejected on the basis of the solution pH, and therefore the term adsorptive membrane is not quite appropriate. An adsorptive membrane should offer abundant binding sites for the adsorption of heavy metals. In this context, graphene oxide (GO) possesses large quantities of epoxy, hydroxyl, and carboxyl groups on its basal planes and edges that can bind metal ions via the chelation mechanism and/or electrostatic interaction [174–177]. GO membranes used in water need to be stabilized because of electrostatic repulsion between negatively charged GO flakes [178–181]. Several approaches based on the covalent bonding of GO using various cross-linking reagents have been developed in order to synthesize stable GO membranes [178,181–184].

One of such procedures based on cross-linking agents worthy of attention is that by Hu and Mi [178]. A GO membrane was made via layer-by-layer deposition of GO nanosheets, which were cross-linked by 1,3,5-benzenetricarbonyl trichloride (TMC) onto a polydopamine (PDA)-coated PSf support (Figure 18). The cross-linking not only provided the stacked GO nanosheets with the necessary stability to overcome their inherent dispensability in the water environment, but also tuned finely the charges, functionality, and spacing of the GO nanosheets. Water can flow through the nanochannels between GO layers while unwanted solutes are rejected by size exclusion and charge effects.

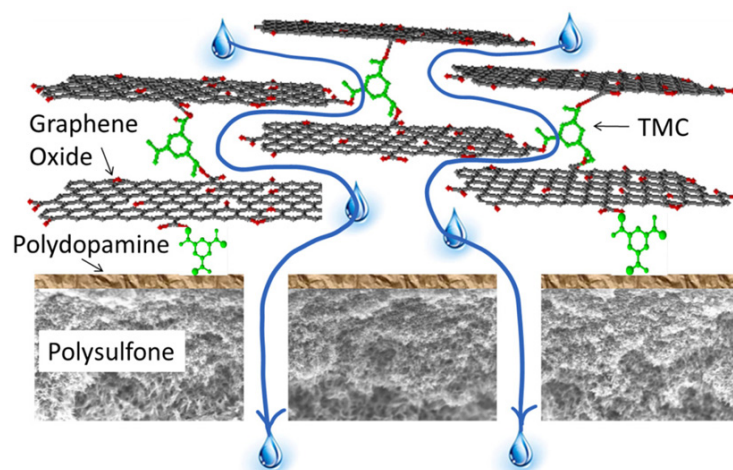


**Figure 18.** Schematic illustration of a step-by-step procedure to synthesize the GO membrane, the mechanism of reactions between PDA and TMC, and the mechanism of reactions between GO and TMC. Reproduced with permission from [178], copyright of American Chemical Society.

Wang et al. [181] and Li et al. [184] used a similar approach to produce adsorptive membranes for heavy metals from aqueous solutions (Table 5, entries 1, 2, respectively). In particular, in [182], a GO-PDA-( $\beta$ -cyclodextrin) (GO-PD- $\beta$ CD) ultrafiltration membrane was fabricated by using the method of drop-coating combined with vacuum filtration. The membrane adsorption capacity was  $101.6 \text{ mg g}^{-1}$  at a solution pH of 6 (Table 6, entry 1). Its performance could almost be completely recovered after a simple clean and regeneration process [182].

**Table 6.** Some examples of GO nanosheets assembled as adsorptive membranes.

Entry #	Cross-Linking Agent/Stabilizer	Heavy Metal Ion	Maximum Adsorption Capacity ( $\text{mg g}^{-1}$ )	Ref.
1	PDA- $\beta$ CD (cross-linking agent)	Pb(II)	102	[181]
2	PDA-PEI (cross-linking agent)	U(VI)	531	[184]
3	PVA (cross-linking agent)	Co(II), Ni(II), Cd(II)	73, 62, 84	[185]
4	Cellulose (cross-linking agent)	Co(II), Ni(II), Cu(II), Zn(II), Cd(II), Pb(II)	16, 14, 27, 17, 27, 108	[186]
5	CNTs (stabilizer)	Co(II), Ni(II), Cu(II), Zn(II), Cd(II), Pb(II)	37, 40, 50, 42, 48, 98	[187]

In [153], PDA induced the grafting of polyethylene imine (PEI) between GO interlayers to form an adsorptive membrane (GO-PDA-PEI) for capturing U(VI). The as-prepared membrane has a hexavalent uranium (U(VI)) adsorption capacity of  $530.6 \text{ mg g}^{-1}$  (Table 6, entry 2), which is 177% higher than that of pristine GO. In the other two studies listed in Table 6 (entries 3, 4), polymers with hydroxyl groups (-OH) such as polyvinyl alcohol (PVA) and cellulose were used to stabilize GO sheets assembled as a membrane.

In particular, Tan et al. [185] noted that if the appropriate amount of PVA attaches to the interlamination of GO membranes, it can effectively prevent their aggregation due to the effective support of PVA, which should enhance the adsorption capacity of the GO membranes. In contrast, if an excessive amount of PVA is used, it could make not available a large number of adsorption sites, therefore reducing the adsorption capacity of GO membranes. Based on these considerations mentioned, highly ordered GO membranes with PVA were prepared by vacuum filtration-induced directional flow for the purpose of removing heavy metal ions from aqueous solutions. In the GO membranes, GO sheets form a lamellar layer, and PVA acts as a physical cross-linking agent and support pillar (Figure 19).

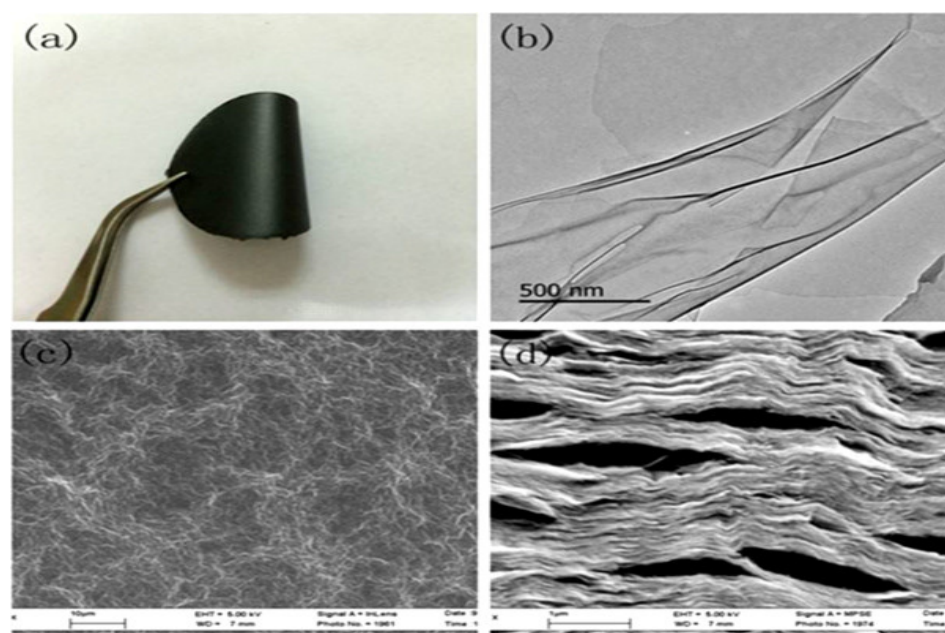


**Figure 19.** (a) Photograph of the GO membrane: (b) TEM image of GO. (c) SEM image of the surface of the GO membrane. (d) SEM image of the cross-section of the GO membrane. Reproduced with permission from [185], copyright of Elsevier.

The maximum adsorption capacities of the GO membranes for  $\text{Cu}^{2+}$ ,  $\text{Cd}^{2+}$ , and  $\text{Ni}^{2+}$  were approximately 72.6, 83.8, and 62.3  $\text{mg g}^{-1}$ , respectively (Table 6, entry 3). The maximum adsorption capacity values of the same heavy metals by using graphene oxide/cellulose membranes in [150] (Table 6, entry 4) are 26.6, 26.8, and 15.5  $\text{mg g}^{-1}$ . In this study, the amount of GO compared to that of cellulose is lower than that used in the work by Tan et al. [185] (Table 6, entry 3), and the adsorption values observed are consequently lower.

Musielak et al. [187] (Table 6, entry 5) used a different strategy to produce stable GO-based membranes. Intercalation of CNTs creates nanochannels, which vastly enhance the permeation of GO by water. CNTs and GO can be covalently bonded using different cross-linking agents [188–190] or stabilized via electrostatic interaction using polyelectrolytes [191]. However, GO membranes can be prepared by noncovalent interaction using oxidized CNTs as reported by Musielak et al. [187]. Excellent durability was observed for GO/CNTs membranes ( $0.44 \text{ mg cm}^{-2}$  GO and  $0.055 \text{ mg cm}^{-2}$  CNTs) at different pH values making them suitable for effective adsorption of metal ions both under flow conditions and vigorous shaking. Although CNTs stabilized the membranes significantly, they strongly influence the adsorption of metal ions on the GO nanosheets. Even a small number of CNTs significantly reduces the adsorption capacities of the GO membranes. This effect can result from the creation of micro- and nanochannels formed from the entangled CNTs. (Figure 20). Thus, the solution flows not only between the GO flakes but also through the micro- and nanochannels. The kinetic data, adsorption isotherms, competitive adsorption experiment, and XPS indicate that adsorption is monolayer coverage and is controlled by chemisorption. The maximum adsorption capacity of the GO/CNT membranes for  $\text{Co}^{2+}$ ,  $\text{Ni}^{2+}$ ,  $\text{Cu}^{2+}$ ,  $\text{Zn}^{2+}$ ,  $\text{Cd}^{2+}$ , and  $\text{Pb}^{2+}$  at pH of 5 are 37, 40, 50, 42, 48, and 98  $\text{mg g}^{-1}$ , respectively (Table 6, entry 5), values, which compared to those of other studies listed in Table 6, can be considered as sufficient.

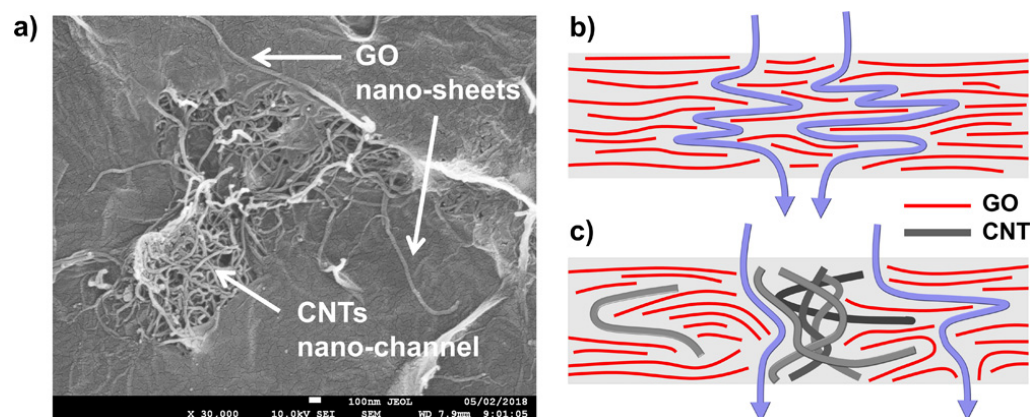


**Figure 20.** SEM image of entangled CNTs forming micro- and nanochannels in GO/CNTs membranes: (a). Flow of the solution through GO (b) and GO/CNTs membranes (c). Reproduced with permission from [187], copyright of American Chemical Society.

#### Functionalized Polymers-Based Adsorptive Membranes

Membrane-based water purification systems are known as effective platforms instead of traditional packed bed adsorption processes to filtrate wastewater, biopharmaceutical by-products, hazardous chemical compounds, and heavy metal ions [191–194]. Furthermore, membranes based on functionalized polymers are great alternatives instead of non-functionalized ones because of their boosted removal rate of pollutants and heavy metal ions from wastewater. These adsorptive membranes contain specific active functional groups on their surfaces that bind with target pollutants or metal ions through either surface complexation or ion exchange process, even by pore sizes larger than the average size of target pollutants or metal ions [117,144,195,196]. Thereby, functionalization of the polymeric part of adsorptive membranes could improve their capability for the

effective removal of metal ions or pollutants from wastewaters by either dynamic or static adsorption processes.

PAN is a promising polymer for the production of UF and MF membranes due to its high mechanical robustness, ideal solvent stability, and cost-effectiveness [197]. The nitrile, i.e., -CN, group of PAN, could be easily modified through the hydrolysis and (3 + 2) cycloaddition reaction at increased temperature toward effectively removing heavy metal ions from wastewaters [197,198]. Likewise, the tetrazole functional groups could be grafted on the resin via the (3 + 2) cycloaddition reaction at 40 °C, which boosts the resin's capability toward adsorption of heavy metal ions in quantities much higher than the non-functionalized resin [199].

Fouling is a severe problem for membrane separation approaches, which can be declined or prevented via employing surface modification techniques, i.e., functionalization. Fouling is known as the accumulation of substances on the surface of the membrane or in the pores of the membrane that could significantly deteriorate the proper performance of membranes. Furthermore, the interaction between the solution's components and the membrane's surface is a governing parameter for extending the fouling of the membrane. For instance, in UF of aquatic media containing proteins, fouling could occur due to the protein's adsorption, aggregation, and denaturation at the membrane-liquid interface. In this case, an increase in the membrane's hydrophilicity could prevent or decline the adsorption of proteins by the membrane due to the adsorption of a higher amount of water by the hydrophilic surface [200,201]. Correspondingly, along with hydrophilicity, the surface modification process also plays a crucial role in membranes' anti-fouling capability. In this regard, both the osmotic effect and steric hindrance of the grafted polymeric branches improves the resistance of the membrane against the fouling [201–204]. Therefore, various kinds of approaches can be considered for preventing fouling, among which grafting diverse types of hydrophilic functional groups of polymers to the surface of the membrane and generating a blend of various polymers to improve the hydrophilicity of the final structure can be mentioned. In addition, a change in the charge density of the polymeric membrane could also be beneficial to improve the performance of the membrane and avoid fouling [205].

Surface functionalization has become a crucial matter for increasing the adsorptive performance of polymeric membranes. The surface functionalization or modification of membranes could minimize undesired reaction/interaction, and also lead to the selective separation of target pollutants and generation of novel purification functions [203]. This beneficial effect could be added to membranes via the introduction of tailored interactions, viz., responsiveness, catalytic properties, and affinity, to the surface of the polymeric membrane via practical approaches. In addition, novel polymeric membranes based on enantiomers, isomers, and specific kinds of biomolecules could provide a selective adsorption process that can be activated through external stimulus [206].

Kumar et al. [207] developed an integrated polymeric platform consisting of PAN and polyvinyltetrazole through the NIPS technique. The process is conducted via a (3 + 2) cycloaddition reaction at 60 °C. A schematic of this process can be seen in Figure 21a. The results showed that the polyvinyltetrazole segments alter the hydrophilic nature and pore sizes of the resulting membrane. In addition, the polyvinyltetrazole site improved the negative charges of the membrane and served as a perfect binding site for the adsorption of chromium in aquatic solutions. The membrane showed static adsorption of 10 ppm at a pH of 5 along with a 44.3 mg g<sup>-1</sup> adsorption rate via the Freundlich isotherm.

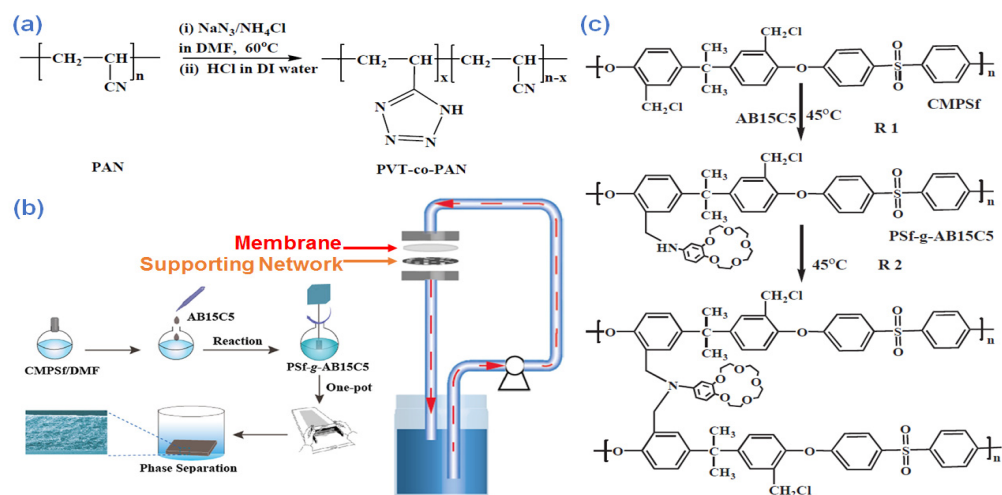


**Figure 21.** (a) Coupling polyvinyltetrazole with PAN via (3 + 2) cycloaddition process at  $60^\circ\text{C}$  [201], (b) preparation of PSf-g-AB15C5 membrane along with a view of the dynamic adsorption process, and (c) the crosslinking and grafting reaction during the formation of PSf-g-AB15C5 [208]. Reproduced with permission from [208], copyright of Elsevier.

In another study, Pei et al. [208] developed a PSf-graft-4-aminobenzo-15-crown-5-ether (PSf-g-AB15C5)-based membrane via a single-pot polymerization process and membrane preparation technique for adsorption of lithium isotope from aquatic media (Figure 21b). A one-pot technique is developed that does not require separation or purification. Correspondingly, the PSf-g-AB15C5 is prepared via grafting with AB15C5 along with chloromethylated Psf (CMPSf) (Figure 21c). The morphology of the as-prepared membrane changed from macrovoid to sponge-like upon a further increase in the viscosity of the reaction, which is mainly a result of the grafting and self-crosslinking process of PSf-g-AB15C5 polymers. Furthermore, the as-developed membrane showed remarkable mechanical robustness (2.12–3.72 MPa) and ideal porosity toward the adsorption of lithium isotope. Moreover, the immobilization of crown ether onto the surface of the membrane ( $0.521\text{ mmol g}^{-1}$ ) could boost the reaction with the  $\text{Li}^+$  ions and lead to a perfect equilibrium separation factor of  $6\text{Li}^+ / 7\text{Li}^+$  up to 1.055. The obtained results showed that such a membrane could be used as an ideal green platform for the separation or adsorption of lithium isotopes from aquatic substrates.

Wu et al. [209] developed a thiol-functionalized mesoporous PVA/ $\text{SiO}_2$  nanofiber via electrospinning. The as-developed membranes contain mercapto groups generated via polycondensation hydrolysis, which exhibited a specific surface area of  $290\text{ m}^2\text{ g}^{-1}$ . The PVA/ $\text{SiO}_2$  membrane showed an absorption rate of  $489.12\text{ mg g}^{-1}$  toward the adsorption of Cu(II) ions from aquatic media at 303 K. The mentioned work further highlighted the potential of polymer functionalization toward improving the adsorption capacity of hybrid polymeric membranes. In Figure 22a, a schematic of the adsorption kinetic of Cu(II) ions by the mesoporous PVA/ $\text{SiO}_2$  membrane is given. In another interesting study, Yao et al. [210] developed a membrane modified with H5(PV2Mo10O40) polyoxometalates (POMs) in order to boost membrane adsorption capacity and catalytic performance. The POM-modified membrane exhibited 100% rejection at the pressure of a 0.5 bar with  $19\text{ L m}^{-2}\text{ h bar}$  water permeability toward removing reactive black 5 (RB5) dye from aqueous media. In Figure 22b, the preparation procedure steps of the POM-modified membrane are reported.

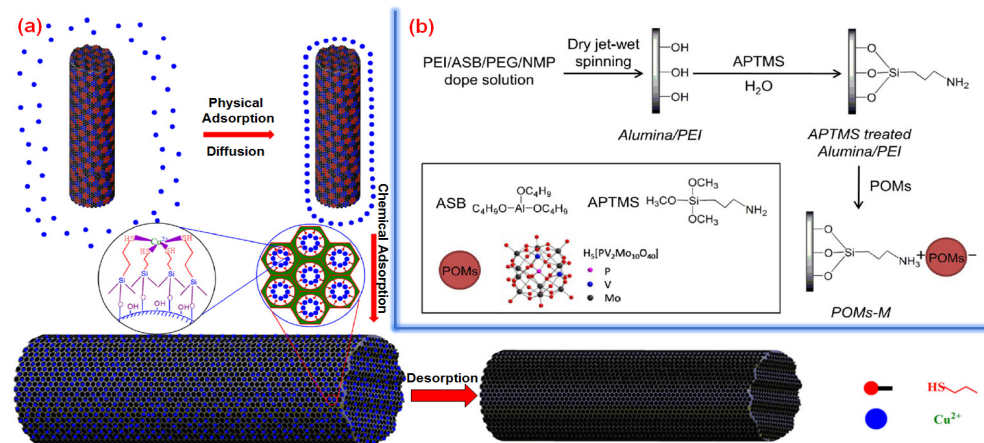


**Figure 22.** (a) Adsorption of Cu(II) via the PVA-SiO<sub>2</sub> nanofiber [202], and (b) production of POM-based membrane [210]. Reproduced with permission from [210], copyright of Elsevier.

The study by Zhang et al. [211] is relevant for the role played by functionalization toward increasing the static binding performance, even though the adsorptive membranes were used for protein separation. The developed membranes are made of cellulose acetate (CA) and prepared by the electrospinning technique. The as-developed nanofibers showed diameters ranging from nanometers to micrometers along with pore sizes ranging from sub-microns to microns. The cellulose nanofibers were hydrolyzed and deacetylated to produce a regenerated cellulose membrane. The surface of the membrane was also functionalized with diethylaminoethyl as an anion exchange ligand. The as-developed membrane could adsorb bovine albumin at the capacity of 40 mg g<sup>-1</sup>, which is much higher than commercially available membranes; a view of these membranes can be seen in Figure 23a–f.

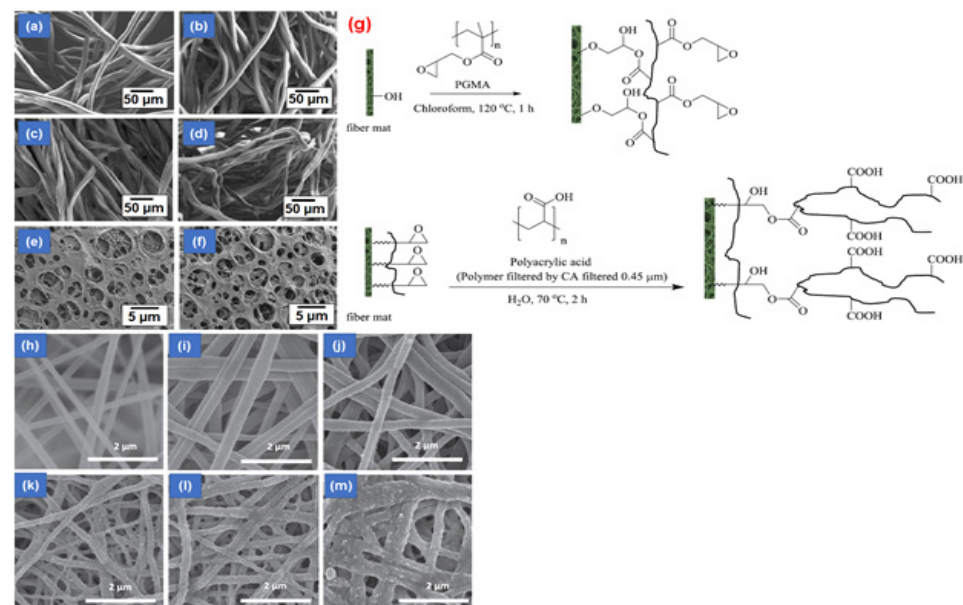


**Figure 23.** SEM images of (a,b) regenerated cellulose micro-fiber, (c,d) bleached cotton fiber, and commercially available cellulose membrane, (e) prior and (f) after surface functionalization with diethylaminoethyl [211]; (g) reaction of the regenerated cellulose membrane with PAA and PGMA; SEM images of the cellulose membrane (h) before and (i) after annealing, (j) after hydrolysis, (k) after immersing in the chloroform, (l) after modification by the poly(glycidyl methacrylate), and (m) after modification with the poly(acrylic acid) [115]. Reproduced with permission from [211] and [115], copyright of Elsevier.

In another study, Chitpong and Husson [115] developed a functionalized cellulose membrane with polyacid to remove heavy metal ions from wastewater. Accordingly, cellulose nanofibers were first developed via the electrospinning approach, stretched via the thermo-mechanical process, and thence transformed into the cellulose nanofiber mat. Afterward, the poly(acrylic acid) is grafted on the surface of the modified cellulose membrane with poly(glycidyl methacrylate) (Figure 23g). Finally, the as-developed functionalized cellulose membranes were used to remove Cd(II) ions from aquatic media. The results showed that the membrane's permeability was highly dependent on the molecular weight of the poly(acrylic acid). The optimum membrane adsorbed about  $160 \text{ mg g}^{-1}$  of Cd(II) ions, much higher than traditional cellulose membranes. A view of the developed membranes and their morphology after functionalization can be seen in Figure 23h–m.

Yang et al. [212] developed a super hydrophilic PAN membrane with an electrospinning approach, functionalized with PDA toward adsorption of Cr(VI) from wastewater (Figure 24a–c). Decoration of the PAN nanofibers with PDA could considerably increase the hydrophilicity of the membrane, avoid fouling and boost its adsorption performance. As a result, the as-developed membrane showed an adsorption capacity of  $61.65 \text{ mg g}^{-1}$  toward the adsorption of Cr(VI) ions. This proper performance is achieved after the functionalization of PAN with PDA due to the generation of active amino and hydroxyl functional groups onto the PAN-based membrane's surface.

These results highlighted the superior role of functionalization toward boosting the capability of polymeric membranes for the separation and adsorption of metal ions. In Table 7, other relevant case studies of adsorptive membranes for heavy metals and metalloids are reported.

**Table 7.** A view of recently developed membranes and their adsorption capacity.

Membrane Materials	Target Pollutant	Adsorption Capacity ( $\text{mg g}^{-1}$ )	Ref.
Chitosan-PVA	Cu(II)	98.65	[213]
	Ni(II)	116.89	
	Cd(II)	124.23	
Chitosan-cellulose	As(V)	39.4	[214]
	Pb(II)	57.3	
	Cu(II)	112.6	
Chitosan-polyethylene oxide	Ni(II)	357.1	[215]
	Cu(II)	310.2	
	Ca(II)	248.1	
	Pb(II)	237.2	
Chitosan-poly (L-lactic acid)	Cu(II)	111.66	[216]
Chitosan-poly(ethylene oxide)	Cu(II)	120	[217]
	Zn(II)	117	
	Pb(II)	108	
Chitosan-PVA	Cu(II)	90.3	[218]
Chitosan-poly(ethylene oxide)	Ni(II)	227.27	[219]
Chitosan-poly(ethylene oxide)	Cr(VI)	208	[220]
Polyacrylic acid-sodium alginate	Cu(II)	591.7	[221]
Chitosan-sodium polyacrylate	Cr(VI)	78.92	[222]
Polyacrylic acid-PVA	Pb(II)	159	[223]
	Cd(II)	102	
Chitosan-CA	Cd(II)	110.48	[224]
Polyacrylic acid-PVA	Pb(II)	288	[225]
Polyethyleneimine-PVA	Cr(VI)	150	[226]
Polyethyleneimine-PDA	Cu(II)	33.59	[227]
Poly(ether sulfones)-poly(ethyleneimine)	Cu(II)	161.29	[228]
	Cd(II)	357.14	
	Pb(II)	94.34	
Polyethyleneimine-PVA	Cu(II)	67.16	[229]
	Cd(II)	116.94	
	Pb(II)	90.03	
Polyaniline-polystyrene	Pb(II)	312	[230]
	Cu(II)	171	
	Hg(II)	148	
	Cd(II)	124	
	Cr(VI)	58	

Table 7. Cont.

Membrane Materials	Target Pollutant	Adsorption Capacity (mg g <sup>-1</sup> )	Ref.
Polyethersulfone-poly (dimethyl amine) ethyl methacrylate	Cu(II)	161.3	[231]
CA-polymethacrylic acid	Pb(II)	146.21	[232]
β-cyclodextrin-polyacrylate	Cu(II) Fe(II)	82 219.5	[233]
Polyindole	Cu(II)	121.95	[234]
PAN—polypyrrole	Cr(VI)	74.91	[235]
Poly(ethylene oxide)	Cu(II)	15.6	[236]
PDA-PVDF-polypyrrole	Cr(VI)	126.7	[237]
Polyindole	Cd(II)	140.36	[238]
PVDF-PDA	Cu(II)	26.7	[239]
PAN-Chitosan-Regenerated cellulose	Pb(II)	500.95	[240]
PAN-polyvinylpyrrolidone	Pb(II)	1520	[241]
Deacetylated cellulose-pyromellitic dianhydride	Pb(II)	326.80	[242]
Chitosan-poly(glycidyl methacrylate)-polyethylenimine	Cr(VI) Cu(II) Co(II)	138.96 69.27 68.31	[243]
CA-polyvinylpyrrolidone	Pb(II) Cu(II) Cd(II)	30.96 19.63 34.70	[244]
Cellulose nanofiber-PAN	Cr(VI) Pb(II)	87.5 137.7	[245]
Chitosan-poly(ethylene oxide)	Cd(II)	232.55	[246]
PAN-CA	Fe(III) Cu(II) Cd(II)	418.32 272.64 126.56	[247]
Polyurethane-phytic acid	Pb(II)	136.52	[248]
Poly(ether sulfone)-poly(3,4-ethylene dioxathiophene)	Pb(II) Cd(II) Cr(VI)	656.42 315.55 418.86	[249]

### Mixed Matrix Adsorptive Membranes

Mixed matrix membranes (MMMs) are obtained by dispersing fillers into polymeric matrices to overcome the limitation of single polymeric and inorganic membranes. MMMs have many advantages, such as high porosity, and thermal and chemical strength, making them an excellent candidate for water purification, especially for removing heavy metals [250]. MMMs with incorporated nanofillers into an inorganic oxide or polymeric matrix, represent an interesting case of adsorptive membranes. Nowadays, the use of MMMs in removing heavy metals from wastewater has received much attention [251–253]. MMMs merge the adsorptive features of the fillers with the processability of the polymers. For example, the use of zeolites as fillers increases the hydrophilicity property of membranes resulting in an increase in water permeability.

Other important fillers are nanosilver, carbon nanotubes, and photocatalytic nanomaterials such as bimetallic nanoparticles and TiO<sub>2</sub> to increase fouling resistance. Metal oxide such as Al<sub>2</sub>O<sub>3</sub> also increases thermal and mechanical stability [254]. Another approach highlights bionanocomposite membranes with surface-immobilized selective proteins [255,256]. GO-based membranes are covalently combined with bovine serum albumin (BSA) for metal ions detection [255]. In this system, BSA acts as a transporter protein in the membrane and endows the membrane with selective recognition of Co<sup>2+</sup>, Cu<sup>2+</sup>, AuCl<sub>4</sub><sup>-</sup>, and Fe<sup>2+</sup>. Combining the metal-binding ability of BSA and the large surface area of GO, the MMM can be used as a water purification strategy to selectively absorb a large amount of AuCl<sub>4</sub><sup>-</sup> from HAuCl<sub>4</sub> solution.

The removal rate of heavy metals by MMMs is related to the binding of adsorbents to adsorbate. The compounds that possess functional groups such as carboxyl, phenolic, lactone, and hydroxyl are very influential in heavy metal removal. Some examples of MMMs are listed in Table 8.

**Table 8.** Characteristics of some adsorptive MMMs for heavy metal and metalloid removal.

MMM (Filler/Polymer Matrix)	Removed Heavy Metal	Reported Removal Efficiency	Membrane Filtration Area (cm <sup>2</sup> )	Ref.
Hydrous ferric oxide NPs <sup>a</sup> /PSf	Pb(II)	13.2 mg g <sup>-1</sup>	-	[257]
Zeolite/PSf	Ni(II)	122 mg g <sup>-1</sup>	13.4	[258]
GO/PSf	Pb(II) Cu(II) Cd(II) Cr(II)	79 mg g <sup>-1</sup> 75 mg g <sup>-1</sup> 68 mg g <sup>-1</sup> 154 mg g <sup>-1</sup>	4	[259–268]
SnNPs <sup>b</sup> /PVDF	Pb(II) Cu(II) Zn(II) Cd(II) Ni(II)	93.9% 92.8% 82.3% 70.7% 63.9%	29.20	[252]
HBE-MMT <sup>c</sup> /PES	Cu(II) Zn(II) Cd(II) Ni(II)	46.8% 66.9% 39.1% 68.8%	-	[260]
HMO <sup>d</sup> /PES	Pb(II)	204.1 mg g <sup>-1</sup>	12.56	[261]
Fe-Mn binary Oxide/PES	As(III)	87.5%	12.56	[262]
Chitosan beads/EVAL	Cu(II)	225 mg g <sup>-1</sup>	-	[263]
α-ZrP <sup>e</sup> /PVDF	Pb(II) Cu(II) Zn(II) Cd(II) Ni(II)	91.2% 93.1% 44.2% 42.8% 44.4%	1	[264]
GMF <sup>f</sup> /PES	As(V)	75.5 mg g <sup>-1</sup>	42	[265]
Zn:Al <sub>2</sub> O <sub>3</sub> <sup>g</sup> /PSf	Pb(II)	98%	-	[266]
Amine modified TiO <sub>2</sub> /CA	Cr(VI)	99.6%	-	[267]
GO/PES	Cu(II) Zn(II)	Cu(II): 72% Zn(II): 87%	3.73	[269]

<sup>a</sup> NPs = nanoparticles; <sup>b</sup> SnNPs = Sn nanoparticles; <sup>c</sup> HBE-MMT = Hyperbranched epoxy-montmorillonite; <sup>d</sup> HMO = hydrous manganese dioxide; <sup>e</sup> α-ZrP = α-zirconium phosphate; <sup>f</sup> GMF = Graphene oxide-manganese ferrite; <sup>g</sup> Zn:Al<sub>2</sub>O<sub>3</sub> = Zinc-doped Aluminium Oxide.

The removal of heavy metals by MMMs is based on some mechanisms such as electrostatic attractions and adsorption, impact of size, and Donnan exclusion. Generally, a high affinity with heavy metal ions is necessary to adsorb the ions by MMMs. A critical point is the pH of the feed, which is effective on the charge of the membrane surface and heavy metal ions, the ion exchange capacity between the MMM and metal ions, and adsorption capacity [253,270–272]. The other influential issue is the stability of MMMs nanomaterials in a different pH range to have a long-term performance during the adsorption [270]. The commonly used polymers for the production of MMMs include CA, PVDF, polyethersulfone (PES), PSf, and PAN. PVDF is an attractive polymer for water treatment applications due to its high mechanical strength and excellent resistance to corrosive chemicals such as bases, acids, and oxidants [273]. Ibrahim et al. [252] investigated the use of SnO<sub>2</sub> entrapped in a PVDF matrix to give MMMs able to remove Pb(II), Cu(II), Zn(II), Cd(II), and Ni(II) (Figure 24a). The maximum removal of Pb(II), Cu(II), Zn(II), Cd(II), and Ni(II) was achieved by the PVDF MMM entrapping 0.25 wt% of SnO<sub>2</sub> with around 93.9 ± 1.7, 92.8 ± 1.3, 82.3 ± 2.0, 70.7 ± 1.1, and 63.9 ± 1.5%, respectively, compared to 93.5 ± 1.3, 92.9 ± 1.7, 68.3 ± 2.1, 50.3 ± 1.8, and 50.3 ± 1.4% in the pristine PVDF membrane. Even though metal ions removal increased compared to neat PVDF membrane for Zn(II), Cd(II), and Ni(II) due to their affinity with SnO<sub>2</sub> [220], the low hydrophilicity of MMMs owing to the intrinsic hydrophobicity of the PVDF host matrix and relatively low loading of the hydrophilic filler (0.25 wt%), necessary to avoid the formation of defects in the membrane films, could explain the insignificant adsorption observed.

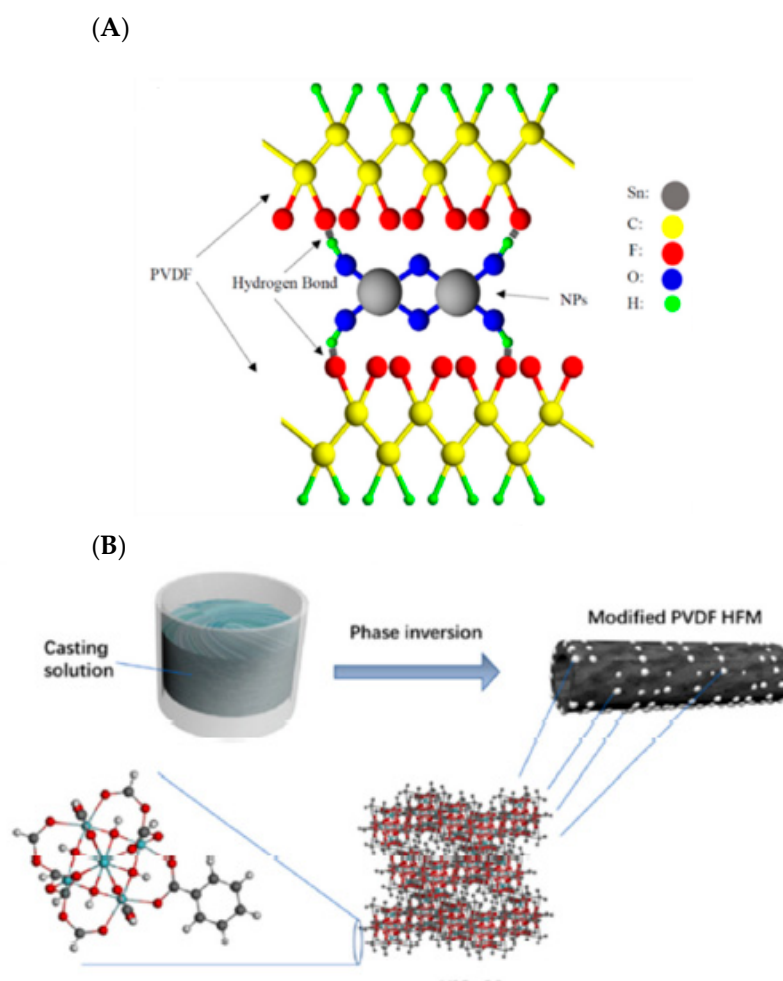


**Figure 24.** (A): Illustration of the interaction between PVDF and SnO<sub>2</sub> filler materials [253]; (B): schematic of fabrication of hollow fiber MMM incorporated with UiO-66 filler materials [273]. Reproduced with permission from [252] and [272], copyright of Elsevier.

Wan et al. [272] prepared PVDF-based MMMs using high valence Zr<sup>4+</sup>-based MOF, i.e., UiO-66, with a loading up to 6 wt%. The measurement of water contact angle showed a significant decrease as more UiO-66 particles were embedded into the PVDF matrix, i.e., from 75° to 46° for pure PVDF membranes and 6 wt% MMM, respectively, indicating a reduction in hydrophobicity of the pristine membrane material. UiO-66 not only improved the hydrophilicity of the PVDF membranes, but also their adsorption capacity due to an extraordinarily high arsenate adsorption capacity of 303 mg g<sup>-1</sup>, ranked among the highest reported in the literature [274]. As shown in Figure 24b, favorable sites for As(III) sorption in the Zr-O-C bond of UiO-66 hollow fiber membranes are oxygen atoms due to binding energy calculations [272].

The high stability of UiO-66 in the presence of a strong acid, e.g., HCl, and a strong base, e.g., NaOH, makes it suitable for applications within a wide pH range of 1 to 10 [275]. Despite the excellent performances of MOF UiO-66 for arsenate sorption, its size, existing as nanoscale powders as for other MOFs, is pretty small, and cannot be readily separated and recycled after the sorption process [276], so its use as filler in adsorptive MMMs can overcome this drawback. At pH 4.7, the maximum arsenate adsorption capacity of PVDF-based MMM prepared by Wan et al. [272] was 267 mg g<sup>-1</sup>.

MOFs represent a very interesting class of fillers for the preparation of MMMs because of the unique features of their nanostructure with high thermal and chemical resistance tunable pores [277], high surface area, and metal binding capacities, which can improve the mass transfer in the sorption process [278,279]. The large surface of MOFs per unit

volume is vital in removing heavy metals in low concentrations [272,274,275,280,281]. In recent years, water-stable MOFs, such as those based on the high valence  $Zr^{4+}$  and  $Fe^{3+}$  metal ions [282], and electrospun nanofibers have been combined to give nanofibrous MOF membranes (NMOMs), with the aim of improving the performance of MOFs for the removal of heavy metals [124,283].

Compared to the conventional method of preparing MMMs, electrospinning has a very low cost and a simple technique is employed in preparing membranes that have relatively high fluxes, porosity, and mechanical strength. This process requires very little polymer and little post treatment of membrane, thus making this a more environmentally friendly technique [284]. NMOMs offer improved molecular transport and easier access to the active sites of MOFs [124]. Since the first study by Efome et al. [285] on NMOMs to separate Pb(II) and Hg(II), the excellent filtration performance and re-generability of the membrane coupled with the choice of an Fe(III)-based hydrostable MOF indicated the potentialities of such new types of adsorptive membranes for the removal of heavy metals.

### 3. Concluding Remarks

Heavy metal pollution of water sources is one of the most important environmental problems that the world has to face. A wide range of technologies has been developed for heavy metal removal. From the literature survey reported in this review, it emerges that adsorptive membrane technology represents an effective and viable method combining the advantages of the adsorption process with those of membrane technology. On the basis of methods used to prepare adsorptive membranes, pre-deposited DM offers many advantages compared to the traditional blend strategy making effective adsorption active sites more available and thus increasing the adsorption performance. Regarding the materials featuring adsorptive membranes, they can be classified into five classes, i.e., bio-based and bio-inspired, inorganic, functionalized, and MMMs. Independently from their differences, each type of these five categories has been designed with the goal to improve the efficiency and selectivity of metal ion removal, which represents the true challenge for this application. Adsorptive membranes featuring coordinative interactions between the heavy metal ions and membrane matrix interactions, i.e., host–guest (bio-inspired membranes) and highly ordered porous structure, which can facilitate the diffusion of metal ions, showed substantial adsorption capacities. Such advanced adsorptive membranes are based on the incorporation of CNTs, MOF, PAFs, and COFs or are chelating membranes.

However, the literature survey on the topic showed that only results at the laboratory level are available suggesting that the technology readiness level (TRL) of adsorptive membranes is still in its early stages. Feasibility studies to approach TRL 3–4 “transformational new membranes” are highly required for the interesting cases of adsorptive membranes such as those functionalized with highly selective groups for metal ions to speed up the commercialization process. How to jump to TRL 3–4 levels?

Chemical stability, long-term stability, and reusability need still to be investigated. Such critical information is missing from many papers.

For conventional adsorptive membranes, i.e., those obtained by a simple mixing of adsorbents and membrane materials and then shaped as membrane, if from one side, a high surface area is necessary for the adsorption, then from the other side, high adsorbent loading results in leaching due to their instability in the membrane matrix. For the design of advanced adsorptive membranes such as bio-inspired membranes, is highly necessary to study the separation performance as well as stability and reusability under various driving forces such as pressure (UF, NF) or the electric potential (ED) gradient.

**Author Contributions:** M.G.B. conceived the original concept and designed the work, made substantial contribution to the reference acquisition, critical analysis/interpretation of data for the work and to the writing, revising the work critically, provide approval for the publication of content. S.M.M., S.A.H. and C.W.L. made substantial contributions to the reference acquisition, analysis or interpretation of data for the sections on functionalized and MMMs adsorptive membranes, revising

the work. The manuscript was written through contribution of all authors. All authors have read and agreed to the published version of the manuscript.

**Funding:** This research received no external funding.

**Institutional Review Board Statement:** Not applicable.

**Informed Consent Statement:** Not applicable.

**Data Availability Statement:** Not applicable.

**Conflicts of Interest:** The authors declare no conflict of interest.

## References

- Kinuthia, G.K.; Ngunjiri, V.; Beti, D.; Lugalia, R.; Wangila, A.; Kamau, L. Levels of heavy metals in wastewater and soil samples from open drainage channels in Nairobi, Kenya: Community health implication. *Sci. Rep.* **2020**, *10*, 8434. [[CrossRef](#)] [[PubMed](#)]
- Ali, H.; Khan, E.; Ilahi, I. Environmental Chemistry and Ecotoxicology of Hazardous Heavy Metals: Environmental Persistence, Toxicity, and Bioaccumulation. *J. Chem.* **2019**, *2019*, 6730305. [[CrossRef](#)]
- Vaseashta, A.; Maftei, C. (Eds.) *Water Safety, Security and Sustainability*; Springer International Publishing: Cham, Switzerland, 2021.
- Zhao, M.; Xu, Y.; Zhang, C.; Rong, H.; Zeng, G. New trends in removing heavy metals from wastewater. *Appl. Microb. Biotechnol.* **2016**, *100*, 6509–6518. [[CrossRef](#)]
- Fu, F.; Wang, Q. Removal of heavy metal ions from wastewaters: A review. *J. Environ. Manag.* **2011**, *92*, 407–418. [[CrossRef](#)] [[PubMed](#)]
- Monier, M.; Abdel-Latif, D. Modification and characterization of PET fibers for fast removal of Hg(II), Cu(II) and Co(II) metal ions from aqueous solutions. *J. Hazard. Mater.* **2013**, *250*, 122–130. [[CrossRef](#)] [[PubMed](#)]
- Takano, J.; Miwa, K.; Fujiwara, T. Boron transport mechanisms: Collaboration of channels and transporters. *Trends Plant Sci.* **2008**, *13*, 451–457. [[CrossRef](#)] [[PubMed](#)]
- Badruk, M.; Kabay, N.; Demircioglu, M.; Mordogan, H.; Ipekoglu, U. Removal of boron from wastewater of geothermal power plant by selective ion-exchange resins. I. Batch sorption–elution studies. *Sep. Sci. Technol.* **1999**, *34*, 2553–2569. [[CrossRef](#)]
- Oki, T.; Kanae, S. Global hydrological cycles and world water resources. *Science* **2006**, *313*, 1068–1072. [[CrossRef](#)]
- Shannon, M.A.; Bohn, P.W.; Elimelech, M.; Georgiadis, J.G.; Marinakos, B.J.; Mayes, A.M. Science and technology for water purification in the coming decades. *Nature* **2008**, *452*, 301–310. [[CrossRef](#)]
- Kabay, N.; Güler, E.; Bryjak, M. Boron in seawater and methods for its separation—A review. *Desalination* **2010**, *261*, 212–217. [[CrossRef](#)]
- Güler, E.; Kaya, C.; Kabay, N.; Arda, M. Boron removal from seawater: State-of-the-art review. *Desalination* **2015**, *356*, 85–93. [[CrossRef](#)]
- Gemici, Ü.; Tarcan, G.; Helvacı, C.; Somay, A.M. High arsenic and boron concentrations in groundwaters related to mining activity in the Bigadiç borate deposits (Western Turkey). *Appl. Geochem.* **2008**, *23*, 2462–2476. [[CrossRef](#)]
- Geneva, S. *Guidelines for Drinking-Water Quality*; World Health Organization: Geneva, Switzerland, 2011.
- Hilal, N.; Kim, G.; Somerfield, C. Boron removal from saline water: A comprehensive review. *Desalination* **2011**, *273*, 23–35. [[CrossRef](#)]
- Eaton, S.V. Effects of boron deficiency and excess on plants. *Plant Physiol.* **1940**, *15*, 95. [[CrossRef](#)]
- Xu, F.; Goldbach, H.E.; Brown, P.H.; Bell, R.W.; Fujiwara, T.; Hunt, C.D.; Goldberg, S.; Shi, L. *Advances in Plant and Animal Boron Nutrition*; Springer: Heidelberg, The Netherlands, 2007.
- Babel, S.; Kurniawan, T.A. Low-cost adsorbents for heavy metals uptake from contaminated water: A review. *J. Hazard. Mater.* **2003**, *97*, 219–243. [[CrossRef](#)]
- Chowdhury, S.; Mazumder, M.J.; Al-Attas, O.; Husain, T. Heavy metals in drinking water: Occurrences, implications, and future needs in developing countries. *Sci. Total Environ.* **2016**, *569*, 476–488. [[CrossRef](#)]
- Tseng, W.-P. Effects and dose-response relationships of skin cancer and blackfoot disease with arsenic. *Environ. Health Perspect.* **1977**, *19*, 109–119. [[CrossRef](#)]
- Nable, R.O.; Bañuelos, G.S.; Paull, J.G. Boron toxicity. *Plant Soil* **1997**, *193*, 181–198. [[CrossRef](#)]
- Guo, Q.; Zhang, Y.; Cao, Y.; Wang, Y.; Yan, W. Boron sorption from aqueous solution by hydrotalcite and its preliminary application in geothermal water deboronation. *Environ. Sci. Pollut. Res.* **2013**, *20*, 8210–8219. [[CrossRef](#)]
- Fu, F.; Zeng, H.; Cai, Q.; Qiu, R.; Yu, J.; Xiong, Y. Effective removal of coordinated copper from wastewater using a new dithiocarbamate-type supramolecular heavy metal precipitant. *Chemosphere* **2007**, *69*, 1783–1789. [[CrossRef](#)]
- Ghosh, P.; Samanta, A.N.; Ray, S. Reduction of COD and removal of Zn<sup>2+</sup> from rayon industry wastewater by combined electro-Fenton treatment and chemical precipitation. *Desalination* **2011**, *266*, 213–217. [[CrossRef](#)]
- Kurniawan, T.A.; Chan, G.Y.; Lo, W.-H.; Babel, S. Physico-chemical treatment techniques for wastewater laden with heavy metals. *Chem. Eng. J.* **2006**, *118*, 83–98. [[CrossRef](#)]
- Barakat, M. New trends in removing heavy metals from industrial wastewater. *Arab. J. Chem.* **2011**, *4*, 361–377. [[CrossRef](#)]

27. Usmana, M.; Zarebanadkouki, M.; Waseem, M.; Katsoyiannis, I.A.; Ernst, M. Mathematical modeling of arsenic(V) adsorption onto iron oxyhydroxides in an adsorption-submerged membrane hybrid system. *J. Hazard. Mater.* **2020**, *400*, 123221. [[CrossRef](#)] [[PubMed](#)]
28. Inglezakis, V.J.; Stylianou, M.A.; Gkantzou, D.; Loizidou, M.D. Removal of Pb(II) from aqueous solutions by using clinoptilolite and bentonite as adsorbents. *Desalination* **2007**, *210*, 248–256. [[CrossRef](#)]
29. Argun, M.E. Use of clinoptilolite for the removal of nickel ions from water: Kinetics and thermodynamics. *J. Hazard. Mater.* **2008**, *150*, 587–595. [[CrossRef](#)]
30. Khelifa, A.; Moulay, S.; Naceur, A. Treatment of metal finishing effluents by the electroflotation technique. *Desalination* **2005**, *181*, 27–33. [[CrossRef](#)]
31. Peter-Varbanets, M.; Zurbrügg, C.; Swartz, C.; Pronk, W. Decentralized systems for potable water and the potential of membrane technology. *Water Res.* **2009**, *43*, 245–265. [[CrossRef](#)]
32. Mohammad, A.W.; Othaman, R.; Hilal, N. Potential use of nanofiltration membranes in treatment of industrial wastewater from Ni-P electroless plating. *Desalination* **2004**, *168*, 241–252. [[CrossRef](#)]
33. Al-Rashdi, B.; Somerfield, C.; Hilal, N. Heavy metals removal using adsorption and nanofiltration techniques. *Sep. Purif. Rev.* **2011**, *40*, 209–259. [[CrossRef](#)]
34. Al-Rashdi, B.; Johnson, D.; Hilal, N. Removal of heavy metal ions by nanofiltration. *Desalination* **2013**, *315*, 2–17. [[CrossRef](#)]
35. Kotrapanavar, N.S.; Hussain, A.; Abashar, M.; Al-Mutaz, I.S.; Aminabhavi, T.M.; Nadagouda, M.N. Prediction of physical properties of nanofiltration membranes for neutral and charged solutes. *Desalination* **2011**, *280*, 174–182. [[CrossRef](#)]
36. Alzahrani, S.; Mohammad, A.W.; Hilal, N.; Abdullah, P.; Jaafar, O. Comparative study of NF and RO membranes in the treatment of produced water—Part I: Assessing water quality. *Desalination* **2013**, *315*, 18–26. [[CrossRef](#)]
37. Cingolani, D.; Fatone, F.; Frison, N.; Spinelli, M.; Eusebi, A.L. Pilot-scale multi-stage reverse osmosis (DT-RO) for water recovery from landfill leachate. *Waste Manag.* **2018**, *76*, 566–574. [[CrossRef](#)] [[PubMed](#)]
38. Oh, J.; Urase, T.; Kitawaki, H.; Rahman, M.; Rhahman, M.; Yamamoto, K. Modeling of arsenic rejection considering affinity and steric hindrance effect in nanofiltration membranes. *Water Sci. Technol.* **2000**, *42*, 173–180. [[CrossRef](#)]
39. Teychene, B.; Collet, G.; Gallard, H.; Croue, J.-P. A comparative study of boron and arsenic (III) rejection from brackish water by reverse osmosis membranes. *Desalination* **2013**, *310*, 109–114. [[CrossRef](#)]
40. Woods, W.G. An introduction to boron: History, sources, uses, and chemistry. *Environ. Health Perspect.* **1994**, *102*, 5–11.
41. Bernstein, R.; Belfer, S.; Freger, V. Toward improved boron removal in RO by membrane modification: Feasibility and challenges. *Environ. Sci. Technol.* **2011**, *45*, 3613–3620. [[CrossRef](#)]
42. Sagiv, A.; Semiat, R. Analysis of parameters affecting boron permeation through reverse osmosis membranes. *J. Membr. Sci.* **2004**, *243*, 79–87. [[CrossRef](#)]
43. Greenlee, L.F.; Lawler, D.F.; Freeman, B.D.; Marrot, B.; Moulin, P. Reverse osmosis desalination: Water sources, technology, and today's challenges. *Water Res.* **2009**, *43*, 2317–2348. [[CrossRef](#)]
44. Garb, Y. *Desalination in Israel: Status, Prospects, and Contexts*, *Water Wisdom*; Rutgers University Press: New Brunswick, NJ, USA, 2010; pp. 238–245.
45. Elimelech, M.; Phillip, W.A. The future of seawater desalination: Energy, technology, and the environment. *Science* **2011**, *333*, 712–717. [[CrossRef](#)]
46. Soo, K.W.; Wong, K.C.; Goh, P.S.; Ismail, A.F.; Othman, N. Efficient heavy metal removal by thin film nanocomposite forward osmosis membrane modified with geometrically different bimetallic oxide. *J. Water Process Eng.* **2020**, *38*, 101591. [[CrossRef](#)]
47. He, M.; Wang, L.; Lv, Y.; Wang, X.; Zhu, J.; Zhang, Y.; Liu, T. Novel polydopamine/metal organic framework thin film nanocomposite forward osmosis membrane for salt rejection and heavy metal removal. *Chem. Eng. J.* **2020**, *389*, 124452. [[CrossRef](#)]
48. Landsman, M.R.; Sujanani, R.; Brodfuehrer, S.H.; Cooper, C.M.; Darr, A.G.; Davis, R.J.; Kim, K.; Kum, S.; Nalley, L.K.; Nomaan, S.M. Water treatment: Are membranes the panacea? *Annu. Rev. Chem. Biomol. Eng.* **2020**, *11*, 559–585. [[CrossRef](#)]
49. Bolisetty, S.; Peydayesh, M.; Mezzenga, R. Sustainable technologies for water purification from heavy metals: Review and analysis. *Chem. Soc. Rev.* **2019**, *48*, 463–487. [[CrossRef](#)]
50. McNair, R.; Szekely, G.; Dryfe, R.A.W. Ion-Exchange Materials for Membrane Capacitive Deionization. *ACS EST Water* **2021**, *1*, 217–239. [[CrossRef](#)]
51. Zhao, R.; Porada, S.; Biesheuvel, P.; Van der Wal, A. Energy consumption in membrane capacitive deionization for different water recoveries and flow rates, and comparison with reverse osmosis. *Desalination* **2013**, *330*, 35–41. [[CrossRef](#)]
52. Mack, C.; Burgess, J.; Duncan, J. Membrane bioreactors for metal recovery from wastewater: A review. *Water SA* **2004**, *30*, 521–532. [[CrossRef](#)]
53. Arican, B.; Gokcay, C.F.; Yetis, U. Mechanistics of nickel sorption by activated sludge. *Process Biochem.* **2002**, *37*, 1307–1315. [[CrossRef](#)]
54. Kelly, C.J.; Tumsaroj, N.; Lajoie, C.A. Assessing wastewater metal toxicity with bacterial bioluminescence in a bench-scale wastewater treatment system. *Water Res.* **2004**, *38*, 423–431. [[CrossRef](#)]
55. Holloway, R.W.; Achilli, A.; Cath, T.Y. The osmotic membrane bioreactor: A critical review. *Environ. Sci. Water Res. Technol.* **2015**, *1*, 581–605. [[CrossRef](#)]
56. Taçi, B.S.; Gashi, S.T. Reverse Osmosis Removal of Heavy Metals from Wastewater Effluents Using Biowaste Materials Pretreatment. *Pol. J. Environ. Stud.* **2019**, *28*, 337–341. [[CrossRef](#)]

57. Chan, B.; Dudeney, A. Reverse osmosis removal of arsenic residues from bioleaching of refractory gold concentrates. *Miner. Eng.* **2008**, *21*, 272–278. [[CrossRef](#)]
58. Ipek, U. Removal of Ni (II) and Zn (II) from an aqueous solution by reverse osmosis. *Desalination* **2005**, *174*, 161–169. [[CrossRef](#)]
59. Rodrigues Pires da Silva, J.; Merçon, F.; Guimarães Costa, C.M.; Radoman Benjo, D. Application of reverse osmosis process associated with EDTA complexation for nickel and copper removal from wastewater. *Desalin. Water Treat.* **2016**, *57*, 19466–19474. [[CrossRef](#)]
60. Xu, P.; Capito, M.; Cath, T.Y. Selective removal of arsenic and monovalent ions from brackish water reverse osmosis concentrate. *J. Hazard. Mater.* **2013**, *260*, 885–891. [[CrossRef](#)] [[PubMed](#)]
61. Petrinic, I.; Korenak, J.; Povodnik, D.; Hélix-Nielsen, C. A feasibility study of ultrafiltration/reverse osmosis (UF/RO)-based wastewater treatment and reuse in the metal finishing industry. *J. Clean. Prod.* **2015**, *101*, 292–300. [[CrossRef](#)]
62. Cséfalvay, E.; Pauer, V.; Mizsey, P. Recovery of copper from process waters by nanofiltration and reverse osmosis. *Desalination* **2009**, *240*, 132–142. [[CrossRef](#)]
63. Chung, S.; Kim, S.; Kim, J.-O.; Chung, J. Feasibility of combining reverse osmosis–ferrite process for reclamation of metal plating wastewater and recovery of heavy metals. *Ind. Eng. Chem. Res.* **2014**, *53*, 15192–15199. [[CrossRef](#)]
64. Mohsen-Nia, M.; Montazeri, P.; Modarress, H. Removal of  $\text{Cu}^{2+}$  and  $\text{Ni}^{2+}$  from wastewater with a chelating agent and reverse osmosis processes. *Desalination* **2007**, *217*, 276–281. [[CrossRef](#)]
65. Qdais, H.A.; Moussa, H. Removal of heavy metals from wastewater by membrane processes: A comparative study. *Desalination* **2004**, *164*, 105–110. [[CrossRef](#)]
66. Malamis, S.; Katsou, E.; Takopoulos, K.; Demetriou, P.; Loizidou, M. Assessment of metal removal, biomass activity and RO concentrate treatment in an MBR–RO system. *J. Hazard. Mater.* **2012**, *209*, 1–8. [[CrossRef](#)]
67. Nanofiltration Membranes to Treat Industrial Wastewater from Heavy Metals. Available online: <https://phys.org/news/2021-04-nanofiltration-membranes-industrial-wastewater-heavy.html> (accessed on 18 April 2022).
68. Gao, J.; Wang, K.Y.; Chung, T.-S. Design of nanofiltration (NF) hollow fiber membranes made from functionalized bore fluids containing polyethyleneimine (PEI) for heavy metal removal. *J. Membr. Sci.* **2020**, *603*, 118022. [[CrossRef](#)]
69. Gherasim, C.-V.; Mikulášek, P. Influence of operating variables on the removal of heavy metal ions from aqueous solutions by nanofiltration. *Desalination* **2014**, *343*, 67–74. [[CrossRef](#)]
70. Cui, Y.; Ge, Q.; Liu, X.-Y.; Chung, T.-S. Novel forward osmosis process to effectively remove heavy metal ions. *J. Membr. Sci.* **2014**, *467*, 188–194. [[CrossRef](#)]
71. Zhao, P.; Gao, B.; Yue, Q.; Liu, S.; Shon, H.K. The performance of forward osmosis in treating high-salinity wastewater containing heavy metal  $\text{Ni}^{2+}$ . *Chem. Eng. J.* **2016**, *288*, 569–576. [[CrossRef](#)]
72. Mahmoud, A.; Hoadley, A.F. An evaluation of a hybrid ion exchange electro dialysis process in the recovery of heavy metals from simulated dilute industrial wastewater. *Water Res.* **2012**, *46*, 3364–3376. [[CrossRef](#)]
73. Hamane, D.; Arous, O.; Kaouah, F.; Trari, M.; Kerdjoudj, H.; Bendjama, Z. Adsorption/photo-electrodialysis combination system for  $\text{Pb}^{2+}$  removal using bentonite/membrane/semiconductor. *J. Environ. Chem. Eng.* **2015**, *3*, 60–69. [[CrossRef](#)]
74. Deghles, A.; Kurt, U. Treatment of tannery wastewater by a hybrid electrocoagulation/electrodialysis process. *Chem. Eng. Process* **2016**, *104*, 43–50. [[CrossRef](#)]
75. Sadyrbaeva, T.Z. Removal of chromium (VI) from aqueous solutions using a novel hybrid liquid membrane—Electrodialysis process. *Chem. Eng. Process* **2016**, *99*, 183–191. [[CrossRef](#)]
76. Dong, Y.; Liu, J.; Sui, M.; Qu, Y.; Ambuchi, J.J.; Wang, H.; Feng, Y. A combined microbial desalination cell and electro dialysis system for copper-containing wastewater treatment and high-salinity-water desalination. *J. Hazard. Mater.* **2017**, *321*, 307–315. [[CrossRef](#)]
77. Su, Y.-N.; Lin, W.-S.; Hou, C.-H.; Den, W. Performance of integrated membrane filtration and electro dialysis processes for copper recovery from wafer polishing wastewater. *J. Water Process Eng.* **2014**, *4*, 149–158. [[CrossRef](#)]
78. Nataraj, S.; Hosamani, K.; Aminabhavi, T. Potential application of an electro dialysis pilot plant containing ion-exchange membranes in chromium removal. *Desalination* **2007**, *217*, 181–190. [[CrossRef](#)]
79. Lambert, J.; Rakib, M.; Durand, G.; Avila-Rodríguez, M. Treatment of solutions containing trivalent chromium by electro dialysis. *Desalination* **2006**, *191*, 100–110. [[CrossRef](#)]
80. Moura, R.C.; Bertuol, D.A.; Ferreira, C.A.; Amado, F.D. Study of chromium removal by the electro dialysis of tannery and metal-finishing effluents. *Int. J. Chem. Eng.* **2012**, *2012*, 179312. [[CrossRef](#)]
81. Kim, D.-H.; Choi, Y.-E.; Park, J.-S.; Kang, M.-S. Capacitive deionization employing pore-filled cation-exchange membranes for energy-efficient removal of multivalent cations. *Electrochim. Acta* **2019**, *295*, 164–172. [[CrossRef](#)]
82. Ali, A.; Quist-Jensen, C.A.; Jørgensen, M.K.; Siekierka, A.; Christensen, M.L.; Bryjak, M.; Hélix-Nielsen, C.; Drioli, E. A review of membrane crystallization, forward osmosis and membrane capacitive deionization for liquid mining. *Resour. Conserv. Recycl.* **2021**, *168*, 105273. [[CrossRef](#)]
83. Huang, Y.; Feng, X. Polymer-enhanced ultrafiltration: Fundamentals, applications and recent developments. *J. Membr. Sci.* **2019**, *586*, 53–83. [[CrossRef](#)]
84. Chakraborty, S.; Dasgupta, J.; Farooq, U.; Sikder, J.; Drioli, E.; Curcio, S. Experimental analysis, modeling and optimization of chromium (VI) removal from aqueous solutions by polymer-enhanced ultrafiltration. *J. Membr. Sci.* **2014**, *456*, 139–154. [[CrossRef](#)]

85. Huang, Y.; Wu, D.; Wang, X.; Huang, W.; Lawless, D.; Feng, X. Removal of heavy metals from water using polyvinylamine by polymer-enhanced ultrafiltration and flocculation. *Sep. Purif. Technol.* **2016**, *158*, 124–136. [[CrossRef](#)]
86. Huang, Y.; Du, J.; Zhang, Y.; Lawless, D.; Feng, X. Batch process of polymer-enhanced ultrafiltration to recover mercury (II) from wastewater. *J. Membr. Sci.* **2016**, *514*, 229–240. [[CrossRef](#)]
87. Ennigrou, D.J.; Gzara, L.; Romdhane, M.R.B.; Dhahbi, M. Cadmium removal from aqueous solutions by polyelectrolyte enhanced ultrafiltration. *Desalination* **2009**, *246*, 363–369. [[CrossRef](#)]
88. Yin, N.; Wang, K.; Wang, L.; Li, Z. Amino-functionalized MOFs combining ceramic membrane ultrafiltration for Pb (II) removal. *Chem. Eng. J.* **2016**, *306*, 619–628. [[CrossRef](#)]
89. Canizares, P.; Pérez, A.; Camarillo, R.; Linares, J. A semi-continuous laboratory-scale polymer enhanced ultrafiltration process for the recovery of cadmium and lead from aqueous effluents. *J. Membr. Sci.* **2004**, *240*, 197–209. [[CrossRef](#)]
90. Oehmen, A.; Vergel, D.; Fradinho, J.; Reis, M.A.; Crespo, J.G.; Velizarov, S. Mercury removal from water streams through the ion exchange membrane bioreactor concept. *J. Hazard. Mater.* **2014**, *264*, 65–70. [[CrossRef](#)] [[PubMed](#)]
91. Katsou, E.; Malamis, S.; Loizidou, M. Performance of a membrane bioreactor used for the treatment of wastewater contaminated with heavy metals. *Bioresour. Technol.* **2011**, *102*, 4325–4332. [[CrossRef](#)]
92. Mahmoudkhani, R.; Torabian, A.; Hassani, A.H.; Mahmoudkhani, R. Copper, cadmium and ferrous removal by membrane bioreactor. *APCBEE Procedia* **2014**, *10*, 79–83. [[CrossRef](#)]
93. Aftab, B.; Khan, S.J.; Maqbool, T.; Hankins, N.P. Heavy metals removal by osmotic membrane bioreactor (OMBR) and their effect on sludge properties. *Desalination* **2017**, *403*, 117–127. [[CrossRef](#)]
94. Marino, T.; Figoli, A. Arsenic removal by liquid membranes. *Membranes* **2015**, *5*, 150–167. [[CrossRef](#)]
95. Ahmad, A.; Kusumastuti, A.; Derek, C.; Ooi, B. Emulsion liquid membrane for heavy metal removal: An overview on emulsion stabilization and destabilization. *Chem. Eng. J.* **2011**, *171*, 870–882. [[CrossRef](#)]
96. Chang, S.H. Types of bulk liquid membrane and its membrane resistance in heavy metal removal and recovery from wastewater. *Desalin. Water Treat.* **2016**, *57*, 19785–19793. [[CrossRef](#)]
97. Bhattacharya, M.; Dutta, S.K.; Sikder, J.; Mandal, M.K. Computational and experimental study of chromium (VI) removal in direct contact membrane distillation. *J. Membr. Sci.* **2014**, *450*, 447–456. [[CrossRef](#)]
98. Manna, A.K.; Sen, M.; Martin, A.R.; Pal, P. Removal of arsenic from contaminated groundwater by solar-driven membrane distillation. *Environ. Pollut.* **2010**, *158*, 805–811. [[CrossRef](#)]
99. Murthy, Z.; Chaudhari, L.B. Application of nanofiltration for the rejection of nickel ions from aqueous solutions and estimation of membrane transport parameters. *J. Hazard. Mater.* **2008**, *160*, 70–77. [[CrossRef](#)]
100. Murthy, Z.; Chaudhari, L.B. Separation of binary heavy metals from aqueous solutions by nanofiltration and characterization of the membrane using Spiegler–Kedem model. *Chem. Eng. J.* **2009**, *150*, 181–187. [[CrossRef](#)]
101. Qasem, N.A.A.; Mohammed, R.H.; Lawal, D.U. Removal of heavy metal ions from wastewater: A comprehensive and critical review. *Npj Clean Water* **2021**, *4*, 36. [[CrossRef](#)]
102. Algieri, C.; Chakraborty, S.; Candamano, S. A Way to Membrane-Based Environmental Remediation for Heavy Metal Removal. *Environments* **2021**, *8*, 52. [[CrossRef](#)]
103. Aijaz, M.O.; Karim, M.R.; Omar, N.M.A.; Othman, M.H.D.; Wahab, M.A.; Akhtar, M.; Uzzaman, M.A.; Alharbi, H.M.; Wazeer, I. Recent Progress, Challenges, and Opportunities of Membrane Distillation for Heavy Metals Removal. *Chem. Rec.* **2022**, *22*, e202100323. [[CrossRef](#)]
104. Khulbe, K.C.; Matsuura, T. Removal of heavy metals and pollutants by membrane adsorption techniques. *Appl. Water Sci.* **2018**, *8*, 19. [[CrossRef](#)]
105. Vo, T.S.; Hossain, M.M.; Jeong, H.M.; Kim, K. Heavy metal removal applications using adsorptive membranes. *Nano Converg.* **2020**, *7*, 36. [[CrossRef](#)]
106. Adam, M.R.; Othman, M.H.D.; Kurniawan, T.A.; Puteh, M.H.; Ismail, A.F.; Khongnakorn, W.; Rahman, M.A.; Jaafar, J. Advances in adsorptive membrane technology for water treatment and resource recovery applications: A critical review. *J. Environ. Chem. Eng.* **2022**, *10*, 107633. [[CrossRef](#)]
107. Kim, S.; Nam, S.-N.; Jang, A.; Jang, M.; Min, C.; Ahjeong, P.; Namguk, S.; Jiyong, H.; Heo, J.; Yoon, Y. Review of adsorption–membrane hybrid systems for water and wastewater treatment. *Chemosphere* **2022**, *286*, 131916. [[CrossRef](#)] [[PubMed](#)]
108. Glass, S.; Mantel, T.; Appold, M.; Sitashree, S.; Usman, M.; Ernst, M.; Filiz, V. Amine-Terminated PAN Membranes as Anion-Adsorber Materials. *Chem. Ing. Tech.* **2021**, *93*, 1396–1400. [[CrossRef](#)]
109. Chand, A.A.K.; Bajer, B.; Schneider, E.S.; Mantel, T.; Ernst, M.; Filiz, V.; Glass, S. Modification of Polyacrylonitrile Ultrafiltration Membranes to Enhance the Adsorption of Cations and Anions. *Membranes* **2022**, *12*, 580. [[CrossRef](#)]
110. Usman, M.; Katsoyiannis, I.; Rodrigues, J.H.; Ernst, M. Arsenate removal from drinking water using by-products from conventional iron oxyhydroxides production as adsorbents coupled with submerged microfiltration unit. *Environ. Sci. Pollut. Res.* **2021**, *28*, 59063–59075. [[CrossRef](#)]
111. Bolisetty, S.; Mezzenga, R. Amyloid–carbon hybrid membranes for universal water purification. *Nat. Nanotechnol.* **2016**, *11*, 365–371. [[CrossRef](#)]
112. Wang, X.; Li, Y.; Li, H.; Yang, C. Chitosan membrane adsorber for low concentration copper ion removal. *Carbohydr. Polym.* **2016**, *146*, 274–281. [[CrossRef](#)]

113. Liang, H.W.; Cao, X.; Zhang, W.J.; Lin, H.T.; Zhou, F.; Chen, L.F.; Yu, S.H. Robust and highly efficient free-standing carbonaceous nanofiber membranes for water purification. *Adv. Funct. Mater.* **2011**, *21*, 3851–3858. [[CrossRef](#)]
114. Chitpong, N.; Husson, S.M. High-capacity, nanofiber-based ion-exchange membranes for the selective recovery of heavy metals from impaired waters. *Sep. Purif. Technol.* **2017**, *179*, 94–103. [[CrossRef](#)]
115. Chitpong, N.; Husson, S.M. Polyacid functionalized cellulose nanofiber membranes for removal of heavy metals from impaired waters. *J. Membr. Sci.* **2017**, *523*, 418–429. [[CrossRef](#)]
116. Weidman, J.L.; Mulvenna, R.A.; Boudouris, B.W.; Phillip, W.A. Nanoporous block polymer thin films functionalized with bio-inspired ligands for the efficient capture of heavy metal ions from water. *ACS Appl. Mater. Interfaces* **2017**, *9*, 19152–19160. [[CrossRef](#)]
117. Weidman, J.L.; Mulvenna, R.A.; Boudouris, B.W.; Phillip, W.A. Nanostructured membranes from triblock polymer precursors as high capacity copper adsorbents. *Langmuir* **2015**, *31*, 11113–11123. [[CrossRef](#)] [[PubMed](#)]
118. Hao, S.; Jia, Z.; Wen, J.; Li, S.; Peng, W.; Huang, R.; Xu, X. Progress in adsorptive membranes for separation—A review. *Sep. Purif. Technol.* **2021**, *255*, 117772. [[CrossRef](#)]
119. Roper, D.K.; Lightfoot, E.N. Separation of biomolecules using adsorptive membranes. *J. Chromatogr. A* **1995**, *702*, 3–26. [[CrossRef](#)]
120. Kubota, N.; Konno, Y.; Miura, S.; Saito, K.; Sugita, K.; Watanabe, K.; Sugo, T. Comparison of two convection-aided protein adsorption methods using porous membranes and perfusion beads. *Biotechnol. Prog.* **1996**, *12*, 869–872. [[CrossRef](#)]
121. Sujanani, R.; Landsman, M.R.; Jiao, S.; Moon, J.D.; Shell, M.S.; Lawler, D.F.; Katz, L.E.; Freeman, B.D. Designing solute-tailored selectivity in membranes: Perspectives for water reuse and resource recovery. *ACS Macro Lett.* **2020**, *9*, 1709–1717. [[CrossRef](#)]
122. Warnock, S.J.; Sujanani, R.; Zofchak, E.S.; Zhao, S.; Dilenschneider, T.J.; Hanson, K.G.; Mukherjee, S.; Ganesan, V.; Freeman, B.D.; Abu-Omar, M.M.; et al. Engineering Li/Na selectivity in 12-Crown-4-functionalized polymer membranes. *Proc. Natl. Acad. Sci. USA* **2021**, *118*, e2022197118. [[CrossRef](#)]
123. Uliana, A.A.; Bui, N.T.; Kamcev, J.; Taylor, M.K.; Urban, J.J.; Long, J.R. Ion-capture electrodialysis using multifunctional adsorptive membranes. *Science* **2021**, *372*, 296–299. [[CrossRef](#)]
124. Adil, H.I.; Thalji, M.R.; Yasin, S.A.; Saeed, I.A.; Assiri, M.A.; Chong, K.F.; Ali, G.A.M. Metal–organic frameworks (MOFs) based nanofiber architectures for the removal of heavy metal ions. *RSC Adv.* **2022**, *12*, 1433. [[CrossRef](#)] [[PubMed](#)]
125. Anantharaman, A.; Chun, Y.; Hua, T.; Chew, J.W.; Wang, R. Pre-deposited dynamic membrane filtration—A review. *Water Res.* **2020**, *173*, 115558. [[CrossRef](#)]
126. Ersahin, M.E.; Oztun, H.; Dereli, R.K.; Ozturk, I.; Roest, K.; Van Lier, J.B. A review on dynamic membrane filtration: Materials, application and future perspectives. *Bioresour. Technol.* **2012**, *122*, 196–206. [[CrossRef](#)] [[PubMed](#)]
127. Johnson, J.S. *Reverse Osmosis Membrane Research: Based on the Symposium on “Polymers for Desalination” Held at the 162nd National Meeting of the American Chemical Society in Washington, D.C., September 1971*; Lonsdale, H.K., Podall, H.E., Eds.; Springer: Boston, MA, USA, 1972; pp. 379–403.
128. Li, L.; Xu, G.; Yu, H. Dynamic Membrane Filtration: Formation, Filtration, Cleaning, and Applications. *Chem. Eng. Technol.* **2018**, *41*, 7–18. [[CrossRef](#)]
129. Tanny, G.B. Dynamic membranes in ultrafiltration and reverse osmosis. *Separ. Purif. Methods* **1978**, *7*, 183–220. [[CrossRef](#)]
130. Hu, Y.; Wang, X.C.; Ngo, H.H.; Sun, Q.; Yang, Y. Anaerobic dynamic membrane bioreactor (AnDMBR) for wastewater treatment: A review. *Bioresour. Technol.* **2018**, *247*, 1107–1118. [[CrossRef](#)]
131. Marcinkowsky, A.E.; Kraus, K.A.; Phillips, H.O.; Johnson, J.S.; Shor, A.J. Hyperfiltration studies. IV. Salt rejection by dynamically formed hydrous oxide Membranes. *J. Am. Chem. Soc.* **1966**, *88*, 5744–5746. [[CrossRef](#)]
132. Usman, M.; Belkasm, A.I.; Kastoyiannis, I.A.; Ernst, M. Pre-deposited dynamic membrane adsorber formed of microscale conventional iron oxide based adsorbents to remove arsenic from water: Application study and mathematical modeling. *J. Chem. Technol. Biotechnol.* **2021**, *96*, 1504–1514. [[CrossRef](#)]
133. Fang, X.; Li, J.; Li, X.; Pan, S.; Zhang, X.; Sun, X.; Shen, J.; Han, W.; Wang, L. Internal pore decoration with polydopamine nanoparticle on polymeric ultrafiltration membrane for enhanced heavy metal removal. *Chem. Eng. J.* **2017**, *314*, 38–49. [[CrossRef](#)]
134. Pan, S.; Jiansheng Li, J.; Noonan, O.; Fang, X.; Wan, G.; Yu, C.; Wang, L. Dual-Functional Ultrafiltration Membrane for Simultaneous Removal of Multiple Pollutants with High Performance. *Environ. Sci. Technol.* **2017**, *51*, 5098–5107. [[CrossRef](#)]
135. Zhang, Y.; Feng, Y.; Xiang, Q.; Liu, F.; Ling, C.; Wang, F.; Li, Y.; Li, A. A high-flux and anti-interference dual-functional membrane for effective removal of Pb(II) from natural water. *J. Hazard. Mater.* **2020**, *384*, 121492. [[CrossRef](#)]
136. Zhang, Y.; Xu, Z.; Yuea, C.; Song, L.; Lva, Y.; Liu, F.; Li, A. Insight into the efficient co-removal of Cr(VI) and Cr(III) by positively charged UiO-66-NH<sub>2</sub> decorated ultrafiltration membrane. *Chem. Eng. J.* **2021**, *404*, 126546. [[CrossRef](#)]
137. Liu, H.; Zuo, K.; Vecitis, C.D. Titanium Dioxide-Coated Carbon Nanotube Network Filter for Rapid and Effective Arsenic Sorption. *Environ. Sci. Technol.* **2014**, *48*, 13871–13879. [[CrossRef](#)]
138. Salehi, E.; Daraei, P.; Shamsabadi, A.A. A review on chitosan-based adsorptive membranes. *Carbohydr. Polym.* **2016**, *152*, 419–432. [[CrossRef](#)]
139. Miretzky, P.; Cirelli, A.F. Cr(VI) and Cr(III) removal from aqueous solution by raw and modified lignocellulosic materials: A review. *J. Hazard. Mater.* **2010**, *180*, 1–19. [[CrossRef](#)]
140. O’Connell, D.W.; Birkinshaw, C.; O’Dwyer, T.F. Heavy metal adsorbents prepared from the modification of cellulose: A review. *Bioresour. Technol.* **2008**, *99*, 6709–6724. [[CrossRef](#)]

141. Wang, R.; Guan, S.; Sato, A.; Wang, X.; Wang, Z.; Yang, R.; Hsiao, B.S.; Chu, B. Nanofibrous microfiltration membranes capable of removing bacteria, viruses and heavy metal ions. *J. Membr. Sci.* **2013**, *446*, 376–382. [[CrossRef](#)]
142. Karim, Z.; Mathew, A.P.; Kokol, V.; Wei, J.; Grahn, M. High-flux affinity membranes based on cellulose nanocomposites for removal of heavy metal ions from industrial effluents. *RSC Adv.* **2016**, *6*, 20644–20653. [[CrossRef](#)]
143. Karim, Z.; Claudpierre, S.; Grahn, M.; Oksman, K.; Mathew, A.P. Nanocellulose based functional membranes for water cleaning: Tailoring of mechanical properties, porosity and metal ion capture. *J. Membr. Sci.* **2016**, *514*, 418–428. [[CrossRef](#)]
144. Jiang, M.; Wang, J.; Li, L.; Pan, K.; Cao, B. Poly(*N,N*-dimethylaminoethyl methacrylate) modification of a regenerated cellulose membrane using ATRP method for copper (II) ion removal. *RSC Adv.* **2013**, *3*, 20625–20632. [[CrossRef](#)]
145. Isogai, A.; Fukuzumi, H. TEMPO-oxidized cellulose nanofibers. *Nanoscale* **2011**, *3*, 71–85. [[CrossRef](#)]
146. Karim, Z.; Mathew, A.P.; Grahn, M.; Mouzon, J.; Oksman, K. Nanoporous membranes with cellulose nanocrystals as functional entity in chitosan: Removal of dyes from water. *Carbohydr. Polym.* **2014**, *112*, 668–676. [[CrossRef](#)]
147. Mathew, A.P.; Oksman, K.; Karim, Z.; Liu, P.; Khan, S.A.; Naseri, N. Process scale-up and characterization of wood cellulose nanocrystals hydrolysed using bioethanol pilot plant. *Ind. Crops Prod.* **2014**, *58*, 212–219. [[CrossRef](#)]
148. Božič, M.; Liu, P.; Mathew, A.P.; Kokol, V. Enzymatic phosphorylation of cellulose nanofibers to new highly-ions adsorbing, flame-retardant and hydroxyapatite-growth induced natural nanoparticles. *Cellulose* **2014**, *21*, 2713–2726. [[CrossRef](#)]
149. Algarra, M.; Vázquez, M.I.; Alonso, B.; Casado, C.M.; Casado, J.; Benavente, J. Characterization of an engineered cellulose based membrane by thiol dendrimer for heavy metals removal. *Chem. Eng. J.* **2014**, *253*, 472–477. [[CrossRef](#)]
150. Giwa, A.; Hasan, S.; Yousuf, A.; Chakraborty, S.; Johnson, D.; Hilal, N. Biomimetic membranes: A critical review of recent progress. *Desalination* **2017**, *420*, 403–424. [[CrossRef](#)]
151. Gouaux, E.; MacKinnon, R. Principles of selective ion transport in channels and pumps. *Science* **2005**, *310*, 1461–1465. [[CrossRef](#)]
152. Kopfer, D.A.; Song, C.; Gruene, T.; Sheldrick, G.M.; Zachariae, U.; De Groot, B.L. Ion permeation in K<sup>+</sup> channels occurs by direct Coulomb knock-on. *Science* **2014**, *346*, 352–355. [[CrossRef](#)] [[PubMed](#)]
153. Mitaa, K.; Sumikama, T.; Iwamoto, M.; Matsuki, Y.; Shigemi, K.; Oiki, S. Conductance selectivity of Na<sup>+</sup> across the K<sup>+</sup> channel via Na<sup>+</sup> trapped in a tortuous trajectory. *Proc. Natl. Acad. Sci. USA* **2021**, *118*, e2017168118. [[CrossRef](#)]
154. Wen, Q.; Yan, D.; Liu, F.; Wang, M.; Ling, Y.; Wang, P.; Kluth, P.; Schauries, D.; Trautmann, C.; Apel, P.; et al. Highly Selective Ionic Transport through Subnanometer Pores in Polymer Films. *Adv. Funct. Mater.* **2016**, *26*, 5796–5803. [[CrossRef](#)]
155. Epsztein, R.; DuChanois, R.M.; Ritt, C.L.; Noy, A.; Elimelech, M. Towards single-species selectivity of membranes with sub-nanometre pores. *Nat. Nanotechnol.* **2020**, *15*, 426–436. [[CrossRef](#)]
156. Zhang, H.; Hou, J.; Hu, Y.; Wang, P.; Ou, R.; Jiang, L.; Liu, J.Z.; Freeman, B.D.; Hill, A.J.; Wang, H. Ultrafast selective transport of alkali metal ions in metal organic frameworks with subnanometer pores. *Sci. Adv.* **2018**, *4*, eaaq0066. [[CrossRef](#)]
157. Pedersen, C.J. Cyclic polyethers and their complexes with metals salts. *J. Am. Chem. Soc.* **1967**, *89*, 7017–7036. [[CrossRef](#)]
158. DuChanois, R.M.; Heiranian, M.; Yang, J.; Porter, C.J.; Li, Q.; Zhang, X.; Verduzco, R.; Elimelech, M. Designing polymeric membranes with coordination chemistry for high-precision ion separations. *Sci. Adv.* **2022**, *8*, eabm9436. [[CrossRef](#)]
159. Nunes, S.P. Block Copolymer Membranes for Aqueous Solution Applications. *Macromolecules* **2016**, *49*, 2905–2916. [[CrossRef](#)]
160. Jha, A.K.; Tsang, S.L.; Ozcam, A.E.; Offeman, R.D.; Balsara, N.P. Master curve captures the effect of domain morphology on ethanol pervaporation through block copolymer membranes. *J. Membr. Sci.* **2012**, *401*, 125–131. [[CrossRef](#)]
161. Buonomenna, M.G.; Tone, C.M.; De Santo, M.P.; Ciuchi, F.; Perrotta, E.; Zappone, B.; Galiano, F.; Figoli, A. Ordering phenomena in nanostructured poly(styrene-*b*-butadiene-*b*-styrene) (SBS) membranes for selective ethanol transport. *J. Membr. Sci.* **2011**, *385*–386, 162–170. [[CrossRef](#)]
162. Jung, A.; Filiz, V.; Rangou, S.; Buhr, K.; Merten, P.; Hahn, J.; Clodt, J.; Abetz, C.; Abetz, V. Formation of integral asymmetric membranes of AB diblock and ABC triblock copolymers by phase inversion. *Macromol. Rapid Commun.* **2013**, *34*, 610–615. [[CrossRef](#)]
163. Pendergast, M.M.; Dorin, R.M.; Phillip, W.A.; Wiesner, U.; Hoek, E.M. Understanding the structure and performance of self-assembled triblock terpolymer membranes. *J. Membr. Sci.* **2013**, *444*, 461–468. [[CrossRef](#)]
164. Peinemann, K.-V.; Abetz, V.; Simon, P.F. Asymmetric superstructure formed in a block copolymer via phase separation. *Nat. Mater.* **2007**, *6*, 992–996. [[CrossRef](#)]
165. Rzaev, J.; Hillmyer, M.A. Nanochannel array plastics with tailored surface chemistry. *J. Am Chem. Soc.* **2005**, *127*, 13373–13379. [[CrossRef](#)]
166. Yao, Z.; Li, Y.; Cui, Y.; Zheng, K.; Zhu, B.; Xu, H.; Zhu, L. Tertiary amine block copolymer containing ultrafiltration membrane with pH-dependent macromolecule sieving and Cr (VI) removal properties. *Desalination* **2015**, *355*, 91–98. [[CrossRef](#)]
167. Kausar, A. Investigation on self-assembled blend membranes of polyethylene-block-poly (ethylene glycol)-block-polycaprolactone and poly (styrene-block-methyl methacrylate) with polymer/gold nanocomposite particles. *Polym.-Plast. Technol. Eng.* **2015**, *54*, 1794–1802. [[CrossRef](#)]
168. Zhang, Y.; Vallin, J.R.; Sahoo, J.K.; Gao, F.; Boudouris, B.W.; Webber, M.J.; Phillip, W.A. High-affinity detection and capture of heavy metal contaminants using block polymer composite membranes. *ACS Cent. Sci.* **2018**, *4*, 1697–1707. [[CrossRef](#)]
169. Liu, H.; Peng, S.; Shu, L.; Chen, T.; Bao, T.; Frost, R.L. Magnetic zeolite NaA: Synthesis, characterization based on metakaolin and its application for the removal of Cu<sup>2+</sup>, Pb<sup>2+</sup>. *Chemosphere* **2013**, *91*, 1539–1546. [[CrossRef](#)] [[PubMed](#)]
170. Zhu, W.; Wang, J.; Wu, D.; Li, X.; Luo, Y.; Han, C.; Ma, W.; He, S. Investigating the heavy metal adsorption of mesoporous silica materials prepared by microwave synthesis. *Nanoscale Res. Lett.* **2017**, *12*, 323. [[CrossRef](#)]

171. Faghihian, H.; Naghavi, M. Synthesis of Amine-Functionalized MCM-41 and MCM-48 for removal of heavy metal ions from aqueous solutions. *Sep. Sci. Technol.* **2014**, *49*, 214–220. [[CrossRef](#)]
172. Taba, P.; Budi, P.; Puspitasari, A. *Adsorption of Heavy Metals on Amine-Functionalized MCM-48*, IOP Conference Series: Materials Science and Engineering; IOP Publishing: Bristol, UK, 2017; p. 012015.
173. Joseph, I.V.; Tosheva, L.; Miller, G.; Doyle, A.M. FAU-Type Zeolite Synthesis from Clays and Its Use for the Simultaneous Adsorption of Five Divalent Metals from Aqueous Solutions. *Materials* **2021**, *14*, 3738. [[CrossRef](#)]
174. Zhao, G.; Ren, X.; Gao, X.; Tan, X.; Li, J.; Chen, C.; Huang, Y.; Wang, X. Removal of Pb(II) ions from aqueous solutions on few-layered graphene oxide nanosheets. *Dalton Trans.* **2011**, *40*, 10945–10952. [[CrossRef](#)]
175. Sitko, R.; Turek, E.; Zawisza, B.; Malicka, E.; Talik, E.; Heimann, J.; Gagor, A.; Feist, B.; Wrzalik, R. Adsorption of divalent metal ions from aqueous solutions using graphene oxide. *Dalton Trans.* **2013**, *42*, 5682–5689. [[CrossRef](#)] [[PubMed](#)]
176. Zhao, G.; Li, J.; Ren, X.; Chen, C.; Wang, X. Few-layered graphene oxide nanosheets as superior sorbents for heavy metal ion pollution management. *Environ. Sci. Technol.* **2011**, *45*, 10454–10462. [[CrossRef](#)] [[PubMed](#)]
177. Wu, W.; Yang, Y.; Zhou, H.; Ye, T.; Huang, Z.; Liu, R.; Kuang, Y. Highly efficient removal of Cu (II) from aqueous solution by using graphene oxide. *Water Air Soil Pollut.* **2013**, *224*, 1372. [[CrossRef](#)]
178. Hu, M.; Mi, B. Enabling graphene oxide nanosheets as water separation membranes. *Environ. Sci. Technol.* **2013**, *47*, 3715–3723. [[CrossRef](#)] [[PubMed](#)]
179. Yu, W.; Graham, N. Development of a stable cation modified graphene oxide membrane for water treatment. *2D Mater.* **2017**, *4*, 045006. [[CrossRef](#)]
180. Yeh, C.-N.; Raidongia, K.; Shao, J.; Yang, Q.-H.; Huang, J. On the origin of the stability of graphene oxide membranes in water. *Nat. Chem.* **2015**, *7*, 166–170. [[CrossRef](#)] [[PubMed](#)]
181. Wang, J.; Huang, T.; Zhang, L.; Yu, Q.J.; Hou, L.A. Dopamine crosslinked graphene oxide membrane for simultaneous removal of organic pollutants and trace heavy metals from aqueous solution. *Environ. Technol.* **2018**, *39*, 3055–3065. [[CrossRef](#)] [[PubMed](#)]
182. Zhang, Y.; Zhang, S.; Chung, T.-S. Nanometric graphene oxide framework membranes with enhanced heavy metal removal via nanofiltration. *Environ. Sci. Technol.* **2015**, *49*, 10235–10242. [[CrossRef](#)] [[PubMed](#)]
183. Jia, Z.; Wang, Y. Covalently crosslinked graphene oxide membranes by esterification reactions for ions separation. *J. Mater. Chem. A* **2015**, *3*, 4405–4412. [[CrossRef](#)]
184. Li, S.; Yang, P.; Liu, X.; Zhang, J.; Xie, W.; Wang, C.; Liu, C.; Guo, Z. Graphene oxidebased dopamine mussel-like cross-linked polyethylene imine nanocomposite coating with enhanced hexavalent uranium adsorption. *J. Mater. Chem. A* **2019**, *7*, 16902–16911. [[CrossRef](#)]
185. Tan, P.; Sun, J.; Hu, Y.; Fang, Z.; Bi, Q.; Chen, Y.; Cheng, J. Adsorption of Cu<sup>2+</sup>, Cd<sup>2+</sup> and Ni<sup>2+</sup> from aqueous single metal solutions on graphene oxide membranes. *J. Hazard. Mater.* **2015**, *297*, 251–260. [[CrossRef](#)]
186. Sitko, R.; Musielak, M.; Zawisza, B.; Talik, E.; Gagor, A. Graphene oxide/cellulose membranes in adsorption of divalent metal ions. *RSC Adv.* **2016**, *6*, 96595–96605. [[CrossRef](#)]
187. Musielak, M.; Gagor, A.; Zawisza, B.; Talik, E.; Sitko, R. Graphene oxide/carbon nanotube membranes for highly efficient removal of metal ions from water. *ACS Appl. Mater. Interfaces* **2019**, *11*, 28582–28590. [[CrossRef](#)]
188. Zhang, L.; Lu, Y.; Liu, Y.-L.; Li, M.; Zhao, H.-Y.; Hou, L.-A. High flux MWCNTs-interlinked GO hybrid membranes survived in cross-flow filtration for the treatment of strontium-containing wastewater. *J. Hazard. Mater.* **2016**, *320*, 187–193. [[CrossRef](#)]
189. Viraka Nellore, B.P.; Kanchanapally, R.; Pedraza, F.; Sinha, S.S.; Pramanik, A.; Hamme, A.T.; Arslan, Z.; Sardar, D.; Ray, P.C. Bio-conjugated CNT-bridged 3D porous graphene oxide membrane for highly efficient disinfection of pathogenic bacteria and removal of toxic metals from water. *ACS Appl. Mater. Interfaces* **2015**, *7*, 19210–19218. [[CrossRef](#)]
190. Kang, H.; Shi, J.; Liu, L.; Shan, M.; Xu, Z.; Li, N.; Li, J.; Lv, H.; Qian, X.; Zhao, L. Sandwich morphology and superior dye-removal performances for nanofiltration membranes self-assembled via graphene oxide and carbon nanotubes. *Appl. Surf. Sci.* **2018**, *428*, 990–999. [[CrossRef](#)]
191. Krogman, K.; Lowery, J.L.; Zacharia, N.S.; Rutledge, G.C.; Hammond, P.T. Spraying asymmetry into functional membranes layer-by-layer. *Nat. Mater.* **2009**, *8*, 512–518. [[CrossRef](#)]
192. Teeters, M.; Conrardy, S.; Thomas, B.; Root, T.; Lightfoot, E. Adsorptive membrane chromatography for purification of plasmid DNA. *J. Chromatogr. A* **2003**, *989*, 165–173. [[CrossRef](#)]
193. Yang, H.; Viera, C.; Fischer, J.; Etzel, M.R. Purification of a large protein using ion-exchange membranes. *Ind. Eng. Chem. Res.* **2002**, *41*, 1597–1602. [[CrossRef](#)]
194. Menkhous, T.J.; Varadaraju, H.; Zhang, L.; Schneiderman, S.; Bjustrom, S.; Liu, L.; Fong, H. Electrospun nanofiber membranes surface functionalized with 3-dimensional nanolayers as an innovative adsorption medium with ultra-high capacity and throughput. *Chem. Commun.* **2010**, *46*, 3720–3722. [[CrossRef](#)]
195. Salehi, E.; Madaeni, S.; Rajabi, L.; Vatanpour, V.; Derakhshan, A.; Zinadini, S.; Ghorabi, S.; Monfared, H.A. Novel chitosan/poly (vinyl) alcohol thin adsorptive membranes modified with amino functionalized multi-walled carbon nanotubes for Cu(II) removal from water: Preparation, characterization, adsorption kinetics and thermodynamics. *Sep. Purif. Technol.* **2012**, *89*, 309–319. [[CrossRef](#)]
196. Farjadian, F.; Schwark, S.; Ulbricht, M. Novel functionalization of porous polypropylene microfiltration membranes: Via grafted poly (aminoethyl methacrylate) anchored Schiff bases toward membrane adsorbers for metal ions. *Polym. Chem.* **2015**, *6*, 1584–1593. [[CrossRef](#)]

197. Scharnagl, N.; Buschatz, H. Polyacrylonitrile (PAN) membranes for ultra- and microfiltration. *Desalination* **2011**, *139*, 191–198. [[CrossRef](#)]
198. Chen, Y.; He, M.; Wang, C.; Wei, Y. A novel polyvinyltetrazole-grafted resin with high capacity for adsorption of Pb(II), Cu(II) and Cr(III) ions from aqueous solutions. *J. Mater. Chem. A* **2014**, *2*, 10444–10453. [[CrossRef](#)]
199. Huang, M.-R.; Li, X.-G.; Li, S.-X.; Zhang, W. Resultful synthesis of polyvinyltetrazole from polyacrylonitrile. *React. Funct. Polym.* **2004**, *59*, 53–61. [[CrossRef](#)]
200. Gölander, C.-G.; Kiss, E. Protein adsorption on functionalized and ESCA-characterized polymer films studied by ellipsometry. *J. Colloid Interface Sci.* **1988**, *21*, 240–253. [[CrossRef](#)]
201. Lundström, I. Surface physics and biological phenomena. *Phys. Scr.* **1983**, *1983*, 5. [[CrossRef](#)]
202. Ulbricht, M. Advanced functional polymer membranes. *Polymer* **2006**, *47*, 2217–2262. [[CrossRef](#)]
203. Minko, S. Grafting on Solid Surfaces: “Grafting to” and “Grafting from” Methods. In *Polymer Surfaces and Interfaces*; Springer: Heidelberg, The Netherlands, 2008; pp. 215–234.
204. Schroen, C.; Stuart, M.C.; Van der Voort Maarschalk, K.; Van der Padt, A.; Van’t Riet, K. Influence of preadsorbed block copolymers on protein adsorption: Surface properties, layer thickness, and surface coverage. *Langmuir* **1995**, *11*, 3068–3074. [[CrossRef](#)]
205. Gopal, R.; Zuwei, M.; Kaur, S.; Ramakrishna, S. Surface Modification and Application of Functionalized Polymer Nanofibers. In *Molecular Building Blocks for Nanotechnology*; Springer: Heidelberg, The Netherlands, 2007; pp. 72–91.
206. Kato, K.; Uchida, E.; Kang, E.-T.; Uyama, Y.; Ikada, Y. Polymer surface with graft chains. *Progr. Polym. Sci.* **2003**, *28*, 209–259. [[CrossRef](#)]
207. Kumar, M.; Shevate, R.; Hilke, R.; Peinemann, K.-V. Novel adsorptive ultrafiltration membranes derived from polyvinyltetrazole-co-polyacrylonitrile for Cu(II) ions removal. *Chem. Eng. J.* **2016**, *301*, 306–314. [[CrossRef](#)]
208. Pei, H.; Yan, F.; Ma, X.; Li, X.; Liu, C.; Li, J.; Cui, Z.; He, B. In situ one-pot formation of crown ether functionalized polysulfone membranes for highly efficient lithium isotope adsorptive separation. *Eur. Polym. J.* **2018**, *109*, 288–296. [[CrossRef](#)]
209. Wu, S.; Li, F.; Wang, H.; Fu, L.; Zhang, B.; Li, G. Effects of poly (vinyl alcohol) (PVA) content on preparation of novel thiol-functionalized mesoporous PVA/SiO<sub>2</sub> composite nanofiber membranes and their application for adsorption of heavy metal ions from aqueous solution. *Polymer* **2010**, *51*, 6203–6211. [[CrossRef](#)]
210. Yao, L.; Zhang, L.; Wang, R.; Chou, S.; Dong, Z. A new integrated approach for dye removal from wastewater by polyoxometalates functionalized membranes. *J. Hazard. Mater.* **2016**, *301*, 462–470. [[CrossRef](#)] [[PubMed](#)]
211. Zhang, L.; Menkhaus, T.J.; Fong, H. Fabrication and bioseparation studies of adsorptive membranes/felts made from electrospun cellulose acetate nanofibers. *J. Membr. Sci.* **2008**, *319*, 176–184. [[CrossRef](#)]
212. Yang, X.; Zhou, Y.; Sun, Z.; Yang, C.; Tang, D. Synthesis and Cr adsorption of a super-hydrophilic polydopamine-functionalized electrospun polyacrylonitrile. *Environ. Chem. Lett.* **2021**, *19*, 743–749. [[CrossRef](#)]
213. Zhang, H.; Ruan, X.; Hu, Y.; Cheng, J.; Tan, P. Adsorptive characteristics of Cu<sup>2+</sup>, Ni<sup>2+</sup> and Cd<sup>2+</sup> on chitosan/poly (vinyl alcohol) nanofiber. *Acta Sci. Circumstantiae* **2015**, *35*, 184–193.
214. Phan, D.-N.; Lee, H.; Huang, B.; Mukai, Y.; Kim, I.-S. Fabrication of electrospun chitosan/cellulose nanofibers having adsorption property with enhanced mechanical property. *Cellulose* **2019**, *26*, 1781–1793. [[CrossRef](#)]
215. Aliabadi, M.; Irani, M.; Ismaeili, J.; Piri, H.; Parnian, M.J. Electrospun nanofiber membrane of PEO/Chitosan for the adsorption of nickel, cadmium, lead and copper ions from aqueous solution. *Chem. Eng. J.* **2013**, *20*, 237–243. [[CrossRef](#)]
216. Zia, Q.; Tabassum, M.; Lu, Z.; Khawar, M.T.; Song, J.; Gong, H.; Meng, J.; Li, Z.; Li, J. Porous poly (L-lactic acid)/chitosan nanofibres for copper ion adsorption. *Carbohydr. Polym.* **2020**, *227*, 115343. [[CrossRef](#)]
217. Shariful, M.I.; Sharif, S.B.; Lee, J.J.L.; Habiba, U.; Ang, B.C.; Amalina, M.A. Adsorption of divalent heavy metal ion by mesoporous-high surface area chitosan/poly (ethylene oxide) nanofibrous membrane. *Carbohydr. Polym.* **2017**, *157*, 57–64. [[CrossRef](#)]
218. Wu, R.-X.; Zheng, G.-F.; Li, W.-W.; Zhong, L.-B.; Zheng, Y.-M. Electrospun chitosan nanofiber membrane for adsorption of Cu (II) from aqueous solution: Fabrication, characterization and performance. *J. Nanosci. Nanotechnol.* **2018**, *18*, 5624–5635. [[CrossRef](#)]
219. Lakhdhar, I.; Belosinschi, D.; Mangin, P.; Chabot, B. Development of a bio-based sorbent media for the removal of nickel ions from aqueous solutions. *J. Environ. Chem. Eng.* **2016**, *4*, 3159–3169. [[CrossRef](#)]
220. Wang, P.; Wang, L.; Dong, S.; Zhang, G.; Shi, X.; Xiang, C.; Li, L. Adsorption of hexavalent chromium by novel chitosan/poly (ethylene oxide)/permutit electrospun nanofibers. *New J. Chem.* **2018**, *42*, 17740–17749. [[CrossRef](#)]
221. Wang, M.; Li, X.; Zhang, T.; Deng, L.; Li, P.; Wang, X.; Hsiao, B.S. Eco-friendly poly (acrylic acid)-sodium alginate nanofibrous hydrogel: A multifunctional platform for superior removal of Cu (II) and sustainable catalytic applications. *Colloids Surf. A* **2018**, *558*, 228–241. [[CrossRef](#)]
222. Jiang, M.; Han, T.; Wang, J.; Shao, L.; Qi, C.; Zhang, X.M.; Liu, C.; Liu, X. Removal of heavy metal chromium using cross-linked chitosan composite nanofiber mats. *Int. J. Biol. Macromol.* **2018**, *120*, 213–221. [[CrossRef](#)]
223. Zhang, S.; Shi, Q.; Christodoulatos, C.; Meng, X. Lead and cadmium adsorption by electrospun PVA/PAA nanofibers: Batch, spectroscopic, and modeling study. *Chemosphere* **2019**, *233*, 405–413. [[CrossRef](#)]
224. Aquino, R.; Tolentino, M.; Amen, S.; Arceo, M.; Dolojan, M.; Basilia, B. Preparation of cellulose acetate blended with chitosan nanostructured membrane via electrospinning for Cd<sup>2+</sup> adsorption in artificial wastewater. In *IOP Conference Series: Earth and Environmental Science*; IOP Publishing: Bristol, UK, 2018; p. 012137.
225. Zhang, S.; Shi, Q.; Christodoulatos, C.; Korfiatis, G.; Meng, X. Adsorptive filtration of lead by electrospun PVA/PAA nanofiber membranes in a fixed-bed column. *Chem. Eng. J.* **2019**, *370*, 1262–1273. [[CrossRef](#)]

226. Zhang, S.; Shi, Q.; Korfiatis, G.; Christodoulatos, C.; Wang, H.; Meng, X. Chromate removal by electrospun PVA/PEI nanofibers: Adsorption, reduction, and effects of co-existing ions. *Chem. Eng. J.* **2020**, *387*, 124179. [[CrossRef](#)]
227. Wu, C.; Wang, H.; Wei, Z.; Li, C.; Luo, Z. Polydopamine-mediated surface functionalization of electrospun nanofibrous membranes: Preparation, characterization and their adsorption properties towards heavy metal ions. *Appl. Surf. Sci.* **2015**, *346*, 207–215. [[CrossRef](#)]
228. Min, M.; Shen, L.; Hong, G.; Zhu, M.; Zhang, Y.; Wang, X.; Chen, Y.; Hsiao, B.S. Micro-nano structure poly (ether sulfones)/poly (ethyleneimine) nanofibrous affinity membranes for adsorption of anionic dyes and heavy metal ions in aqueous solution. *Chem. Eng. J.* **2012**, *197*, 88–100. [[CrossRef](#)]
229. Wang, X.; Min, M.; Liu, Z.; Yang, Y.; Zhou, Z.; Zhu, M.; Chen, Y.; Hsiao, B.S. Poly (ethyleneimine) nanofibrous affinity membrane fabricated via one step wet-electrospinning from poly (vinyl alcohol)-doped poly (ethyleneimine) solution system and its application. *J. Membr. Sci.* **2011**, *379*, 191–199. [[CrossRef](#)]
230. Alcaraz-Espinoza, J.J.; Chávez-Guajardo, A.E.; Medina-Llamas, J.C.; Andrade, C.A.; De Melo, C.P. Hierarchical composite polyaniline–(electrospun polystyrene) fibers applied to heavy metal remediation. *ACS Appl. Mater. Interfaces* **2015**, *7*, 7231–7240. [[CrossRef](#)]
231. Bornillo, K.A.S.; Kim, S.; Choi, H. Cu (II) removal using electrospun dual-responsive polyethersulfone-poly (dimethyl amino) ethyl methacrylate (PES-PDMAEMA) blend nanofibers. *Chemosphere* **2020**, *242*, 125287. [[CrossRef](#)] [[PubMed](#)]
232. Zang, L.; Lin, R.; Dou, T.; Ma, J.; Sun, L. Electrospun superhydrophilic membranes for effective removal of Pb (II) from water. *Nanoscale Adv.* **2019**, *1*, 389–394. [[CrossRef](#)]
233. Zhu, F.; Zheng, Y.-M.; Zhang, B.-G.; Dai, Y.-R. A critical review on the electrospun nanofibrous membranes for the adsorption of heavy metals in water treatment. *J. Hazard. Mater.* **2021**, *401*, 123608. [[CrossRef](#)] [[PubMed](#)]
234. Cai, Z.; Song, X.; Zhang, Q.; Zhai, T. Electrospun polyindole nanofibers as a nano-adsorbent for heavy metal ions adsorption for wastewater treatment. *Fibers Polym.* **2017**, *18*, 502–513. [[CrossRef](#)]
235. Wang, J.; Pan, K.; He, Q.; Cao, B. Polyacrylonitrile/polypyrrole core/shell nanofiber mat for the removal of hexavalent chromium from aqueous solution. *J. Hazard. Mater.* **2013**, *244*, 121–129. [[CrossRef](#)]
236. Mokhena, T.C.; Jacobs, N.V.; Luyt, A. Electrospun alginate nanofibres as potential bio-sorption agent of heavy metals in water treatment. *Express Polym. Lett.* **2017**, *11*, 652–663. [[CrossRef](#)]
237. Ma, F.-F.; Zhang, D.; Zhang, N.; Huang, T.; Wang, Y. Polydopamine-assisted deposition of polypyrrole on electrospun poly (vinylidene fluoride) nanofibers for bidirectional removal of cation and anion dyes. *Chem. Eng. J.* **2018**, *354*, 432–444. [[CrossRef](#)]
238. Cai, Z.-J.; Yang, H.-Z.; Xu, Y.; Wang, C.-K. Preparation of Polyindole Nanofibers and Their Cadmium Ion Adsorption Performance. *Acta Polym. Sin.* **2015**, *5*, 581–588.
239. Ma, F.-F.; Zhang, N.; Wei, X.; Yang, J.-H.; Wang, Y.; Zhou, Z.-W. Blend-electrospun poly (vinylidene fluoride)/polydopamine membranes: Self-polymerization of dopamine and the excellent adsorption/separation abilities. *J. Mater. Chem. A* **2017**, *5*, 14430–14443. [[CrossRef](#)]
240. Huang, M.; Tu, H.; Chen, J.; Liu, R.; Liang, Z.; Jiang, L.; Shi, X.; Du, Y.; Deng, H. Chitosan-rectorite nanospheres embedded aminated polyacrylonitrile nanofibers via shoulder-to-shoulder electrospinning and electrospaying for enhanced heavy metal removal. *Appl. Surf. Sci.* **2018**, *437*, 294–303. [[CrossRef](#)]
241. Hong, G.; Li, X.; Shen, L.; Wang, M.; Wang, C.; Yu, X.; Wang, X. High recovery of lead ions from aminated polyacrylonitrile nanofibrous affinity membranes with micro/nano structure. *J. Hazard. Mater.* **2015**, *295*, 161–169. [[CrossRef](#)]
242. Li, Y.; Wen, Y.; Wang, L.; He, J.; Al-Deyab, S.S.; El-Newehy, M.; Yu, J.; Ding, B. Simultaneous visual detection and removal of lead (II) ions with pyromellitic dianhydride-grafted cellulose nanofibrous membranes. *J. Mater. Chem. A* **2015**, *3*, 18180–18189. [[CrossRef](#)]
243. Yang, D.; Li, L.; Chen, B.; Shi, S.; Nie, J.; Ma, G. Functionalized chitosan electrospun nanofiber membranes for heavy-metal removal. *Polymer* **2019**, *163*, 74–85. [[CrossRef](#)]
244. Xiang, T.; Zhang, Z.; Liu, H.; Yin, Z.; Li, L.; Liu, X. Characterization of cellulose-based electrospun nanofiber membrane and its adsorptive behaviours using Cu (II), Cd (II), Pb (II) as models. *Sci. China Chem.* **2013**, *56*, 567–575. [[CrossRef](#)]
245. Yang, R.; Aubrecht, K.B.; Ma, H.; Wang, R.; Grubbs, R.B.; Hsiao, B.S.; Chu, B. Thiol-modified cellulose nanofibrous composite membranes for chromium (VI) and lead (II) adsorption. *Polymer* **2014**, *55*, 1167–1176. [[CrossRef](#)]
246. Brandes, R.; Belosinschi, D.; Brouillette, F.; Chabot, B. A new electrospun chitosan/phosphorylated nanocellulose biosorbent for the removal of cadmium ions from aqueous solutions. *J. Environ. Chem. Eng.* **2019**, *7*, 103477. [[CrossRef](#)]
247. Feng, Q.; Wu, D.; Zhao, Y.; Wei, A.; Wei, Q.; Fong, H. Electrospun AOPAN/RC blend nanofiber membrane for efficient removal of heavy metal ions from water. *J. Hazard. Mater.* **2018**, *344*, 819–828. [[CrossRef](#)]
248. Fang, Y.; Liu, X.; Wu, X.; Tao, X.; Fei, W. Electrospun polyurethane/phytic acid nanofibrous membrane for high efficient removal of heavy metal ions. *Environ. Technol.* **2021**, *42*, 1053–1060. [[CrossRef](#)]
249. Mohamadi, Z.; Abdolmaleki, A. Heavy metal remediation via poly (3, 4-ethylene dioxothiophene) deposition onto neat and sulfonated nonwoven poly (ether sulfone). *J. Ind. Eng. Chem.* **2017**, *55*, 164–172. [[CrossRef](#)]
250. Casado-Coterillo, C. *Mixed Matrix Membranes*; Multidisciplinary Digital Publishing Institute: Basel, Switzerland, 2019.
251. Lim, Y.J.; Goh, K.; Lai, G.S.; Ng, C.Y.; Torres, J.; Wang, R. Fast water transport through biomimetic reverse osmosis membranes embedded with peptide-attached (pR)-pillar [5] arenes water channels. *J. Membr. Sci.* **2021**, *628*, 119276. [[CrossRef](#)]

252. Ibrahim, Y.; Naddeo, V.; Banat, F.; Hasan, S.W. Preparation of novel polyvinylidene fluoride (PVDF)-Tin (IV) oxide (SnO<sub>2</sub>) ion exchange mixed matrix membranes for the removal of heavy metals from aqueous solutions. *Sep. Purif. Technol.* **2020**, *250*, 117250. [[CrossRef](#)]
253. Marino, T.; Russo, F.; Rezzouk, L.; Bouzid, A.; Figoli, A. PES-kaolin mixed matrix membranes for arsenic removal from water. *Membranes* **2017**, *7*, 57. [[CrossRef](#)]
254. Du, R.; He, L.; Li, P.; Zhao, G. Polydopamine-Modified Al<sub>2</sub>O<sub>3</sub>/Polyurethane Composites with Largely Improved Thermal and Mechanical Properties. *Materials* **2020**, *13*, 1772. [[CrossRef](#)] [[PubMed](#)]
255. Yu, X.; Sun, S.; Zhou, L.; Miao, Z.; Zhang, X.; Su, Z.; Wei, G. Removing Metal Ions from Water with Graphene–Bovine Serum Albumin Hybrid Membrane. *Nanomaterials* **2019**, *9*, 276. [[CrossRef](#)] [[PubMed](#)]
256. Yang, F.; Yang, P. Protein-based Separation Membranes: State of the Art and Future Trends. *Adv. Energy Sustain. Res.* **2021**, *2*, 2100008. [[CrossRef](#)]
257. Abdullah, N.; Gohari, R.; Yusof, N.; Ismail, A.; Juhana, J.; Lau, W.; Matsuura, T. Polysulfone/hydrous ferric oxide ultrafiltration mixed matrix membrane: Preparation, characterization and its adsorptive removal of lead (II) from aqueous solution. *Chem. Eng. J.* **2016**, *289*, 28–37. [[CrossRef](#)]
258. Yurekli, Y. Removal of heavy metals in wastewater by using zeolite nano-particles impregnated polysulfone membranes. *J. Hazard. Mater.* **2016**, *309*, 53–64. [[CrossRef](#)]
259. Mukherjee, R.; Bhunia, P.; De, S. Impact of graphene oxide on removal of heavy metals using mixed matrix membrane. *Chem. Eng. J.* **2016**, *292*, 284–297. [[CrossRef](#)]
260. Balkanloo, P.G.; Mahmoudian, M.; Hosseinzadeh, M.T. A comparative study between MMT-Fe<sub>3</sub>O<sub>4</sub>/PES, MMT-HBE/PES, and MMT-acid activated/PES mixed matrix membranes. *Chem. Eng. J.* **2020**, *396*, 125188. [[CrossRef](#)]
261. Gohari, R.J.; Lau, W.; Matsuura, T.; Halakoo, E.; Ismail, A. Adsorptive removal of Pb (II) from aqueous solution by novel PES/HMO ultrafiltration mixed matrix membrane. *Sep. Purif. Technol.* **2013**, *120*, 59–68. [[CrossRef](#)]
262. Gohari, R.J.; Lau, W.; Matsuura, T.; Ismail, A. Fabrication and characterization of novel PES/Fe–Mn binary oxide UF mixed matrix membrane for adsorptive removal of As (III) from contaminated water solution. *Sep. Purif. Technol.* **2013**, *118*, 64–72. [[CrossRef](#)]
263. Tetala, K.K.; Stamatialis, D.F. Mixed matrix membranes for efficient adsorption of copper ions from aqueous solutions. *Sep. Purif. Technol.* **2013**, *104*, 214–220. [[CrossRef](#)]
264. Abdulkarem, E.; Ibrahim, Y.; Kumar, M.; Arafat, H.A.; Naddeo, V.; Banat, F.; Hasan, S.W. Polyvinylidene fluoride (PVDF)- $\alpha$ -zirconium phosphate ( $\alpha$ -ZrP) nanoparticles based mixed matrix membranes for removal of heavy metal ions. *Chemosphere* **2021**, *267*, 128896. [[CrossRef](#)]
265. Shahrin, S.; Lau, W.-J.; Goh, P.-S.; Ismail, A.F.; Jaafar, J. Adsorptive mixed matrix membrane incorporating graphene oxide-manganese ferrite (GMF) hybrid nanomaterial for efficient As (V) ions removal. *Compos. Part B Eng.* **2019**, *175*, 107150. [[CrossRef](#)]
266. Sherugar, P.; Naik, N.S.; Padaki, M.; Nayak, V.; Gangadharan, A.; Nadig, A.R.; Deon, S. Fabrication of zinc doped aluminium oxide/polysulfone mixed matrix membranes for enhanced antifouling property and heavy metal removal. *Chemosphere* **2021**, *275*, 130024. [[CrossRef](#)]
267. Gebru, K.A.; Das, C. Removal of chromium (VI) ions from aqueous solutions using amine-impregnated TiO<sub>2</sub> nanoparticles modified cellulose acetate membranes. *Chemosphere* **2018**, *191*, 673–684. [[CrossRef](#)]
268. Mukherjee, R.; Bhunia, P.; De, S. Long term filtration modelling and scaling up of mixed matrix ultrafiltration hollow fiber membrane: A case study of chromium (VI) removal. *J. Membr. Sci.* **2019**, *570*, 204–214. [[CrossRef](#)]
269. Marjani, A.; Nakhjiri, A.T.; Adimi, M.; Jirandehi, H.F.; Shirazian, S. Effect of graphene oxide on modifying polyethersulfone membrane performance and its application in wastewater treatment. *Sci. Rep.* **2020**, *10*, 2049. [[CrossRef](#)]
270. Lim, Y.J.; Lee, S.M.; Wang, R.; Lee, J. Emerging materials to prepare mixed matrix membranes for pollutant removal in water. *Membranes* **2021**, *11*, 508. [[CrossRef](#)]
271. Akbari, A.; Sheath, P.; Martin, S.T.; Shinde, D.B.; Shaibani, M.; Banerjee, P.C.; Tkacz, R.; Bhattacharyya, D.; Majumder, M. Large-area graphene-based nanofiltration membranes by shear alignment of discotic nematic liquid crystals of graphene oxide. *Nat. Commun.* **2016**, *7*, 10891. [[CrossRef](#)]
272. Wan, P.; Yuan, M.; Yu, X.; Zhang, Z.; Deng, B. Arsenate removal by reactive mixed matrix PVDF hollow fiber membranes with UiO-66 metal organic frameworks. *Chem. Eng. J.* **2020**, *382*, 122921. [[CrossRef](#)]
273. Warsinger, D.M.; Chakraborty, S.; Tow, E.W.; Plumlee, M.H.; Bellona, C.; Loutatidou, S.; Karimi, L.; Mikelonis, A.M.; Achilli, A.; Ghassemi, A.; et al. A review of polymeric membranes and processes for potable water reuse. *Prog. Polym. Sci.* **2018**, *81*, 209–237. [[CrossRef](#)]
274. Wang, C.; Lee, M.; Liu, X.; Wang, B.; Chen, J.P.; Li, K. A metal-organic framework/ $\alpha$ -alumina composite with a novel geometry for enhanced adsorptive separation. *Chem. Commun.* **2016**, *52*, 8869–8872. [[CrossRef](#)] [[PubMed](#)]
275. Valenzano, L.; Civalieri, B.; Chavan, S.; Bordiga, S.; Nilsen, M.H.; Jakobsen, S.; Lillerud, K.P.; Lamberti, C. Disclosing the complex structure of UiO-66 metal organic framework: A synergic combination of experiment and theory. *Chem. Mater.* **2011**, *23*, 1700–1718. [[CrossRef](#)]
276. Liu, T.Y.; Yuan, H.G.; Liu, Y.Y.; Ren, D.; Su, Y.C.; Wang, X. Metal-organic framework nanocomposite thin films with interfacial bindings and self-standing robustness for high water flux and enhanced ion selectivity. *ACS Nano* **2018**, *12*, 9253–9265. [[CrossRef](#)] [[PubMed](#)]

277. Seoane, B.; Coronas, J.; Gascon, I.; Benavides, M.E.; Karvan, O.; Caro, J.; Kapteijn, F.; Gascon, J. Metal–organic framework based mixed matrix membranes: A solution for highly efficient CO<sub>2</sub> capture? *Chem. Soc. Rev.* **2015**, *44*, 2421–2454. [[CrossRef](#)] [[PubMed](#)]
278. Bruno, R.; Mon, M.; Escamilla, P.; Ferrando-Soria, J.; Esposito, E.; Fuoco, A.; Monteleone, M.; Jansen, J.C.; Elliani, R.; Tagarelli, A. Bioinspired Metal–Organic Frameworks in Mixed Matrix Membranes for Efficient Static/Dynamic Removal of Mercury from Water. *Adv. Funct. Mater.* **2021**, *31*, 2008499. [[CrossRef](#)]
279. Shayegan, H.; Ali, G.A.M.; Safarifard, V. Amide-Functionalized Metal–Organic Framework for High Efficiency and Fast Removal of Pb(II) from Aqueous Solution. *J. Inorg. Organomet. Polym.* **2020**, *30*, 3170–3178. [[CrossRef](#)]
280. Wen, J.; Fang, Y.; Zeng, G. Progress and prospect of adsorptive removal of heavy metal ions from aqueous solution using metal-organic frameworks: A review of studies from the last decade. *Chemosphere* **2018**, *201*, 627–643. [[CrossRef](#)]
281. Shayegan, H.; Ali, G.A.M.; Safarifard, V. Recent Progress in the Removal of Heavy Metal Ions from Water Using Metal–Organic Frameworks. *ChemistrySelect* **2020**, *5*, 124–146. [[CrossRef](#)]
282. Zhou, H.-C.; Kitagawa, S. Metal–Organic Frameworks (MOFs). *Chem. Soc. Rev.* **2014**, *43*, 5415–5418. [[CrossRef](#)]
283. Kobielska, P.A.; Howarth, A.J.; Farha, O.K.; Nayak, S. Metal–organic frameworks for heavy metal removal from water. *Coord. Chem. Rev.* **2018**, *358*, 92–107. [[CrossRef](#)]
284. Li, Z.; Zhou, G.; Dai, H.; Yang, M.; Fu, Y.; Ying, Y.; Li, Y. Biomimetic preparation of hybrid membranes with ultra-high loading of pristine metal–organic frameworks grown on silk nanofibers for hazardous collection in water. *J. Mater. Chem. A* **2018**, *6*, 3402–3413. [[CrossRef](#)]
285. Efome, J.E.; Rana, D.; Matsuura, T.; Lan, C.Q. Metal–organic frameworks supported on nanofibers to remove heavy metals. *J. Mater. Chem. A* **2018**, *6*, 4550–4555. [[CrossRef](#)]